

**Uncovering hidden potential of natural
products**

by

Maria Iacovidou

**A dissertation submitted to the Graduate Faculty in Biochemistry in
partial fulfillment of the requirements for the degree of Doctor of
Philosophy in the City University of New York**

2010

© 2010

MARIA IACOVIDOU

All Rights Reserved

This manuscript has been read and accepted for the Graduate Faculty in Biochemistry in satisfaction of the dissertation requirement for the degree of the Doctor of Philosophy.

Dr. Akira Kawamura

Date

Chair of Examining Committee

Dr. Edward J. Kennelly

Date

Executive Officer

Dr. Edward J. Kennelly

Dr. Laurel A. Eckhardt

Dr. Frida E. Kleiman

Dr. Yasuhiro Itagaki

Supervisory Committee

THE CITY UNIVERSITY OF NEW YORK

Abstract

Uncovering hidden potential of natural products

by

Maria Iacovidou

Advisor: Dr. Akira Kawamura

Herbs and soil bacteria have been arguably the most important sources of therapeutic agents throughout human history. Numerous bioactive compounds have been isolated and characterized from these classical sources of natural products. Because of the long history of research on herbs and soil bacteria, they are sometimes perceived as “exhausted” sources of secondary metabolites. These classical sources of natural products, however, can still include compounds with previously overlooked chemical and biological properties. The unifying theme of this thesis study is to uncover such hidden potential of natural products. To this end, these classical sources of secondary metabolites have been examined from new angles.

The first two chapters of this thesis describe the examination of oriental herbal formulations with biomarker-guided screening, which has been established recently in our group. In this method, natural products are screened based on their ability to modulate the expression of mRNA biomarkers, which are the genes associated with

therapeutic effects of herbal medicine. Importantly, herbal formulations have never been screened in this manner. Thus, biomarker-guided screening can serve as a powerful approach to uncover hidden therapeutic potential of natural products.

Chapter 1 describes the biomarker-guided screening of a “blood cleansing” herbal formulation called Toki-shakuyaku-san (TSS). This formulation has long been used to alleviate various disorders associated with poor blood circulation. Our screening revealed that a simple polyacetylene compound, (6*E*,12*E*)-tetradecadiene-8,10-diyne-1,3-diol diacetate (TDEYA), which has been considered as an “inactive” precursor of other metabolites, regulates the expression of genes associated with blood coagulation, such as COX-2, SerpinB2, and perlecan. Identification of this polyacetylene compound is important because it may open a new paradigm of treating circulation disorders through manipulation of gene expression by small molecules.

Chapter 2 describes the biomarker-guided screening of another herbal formulation, Juzen-taiho-to (JTT), which is widely known as “immune booster” formulation. In fact, JTT is clinically used in Japan to reinvigorate the immune system of cancer patients undergoing chemotherapy and radiation therapy. It is believed that many beneficial effects of JTT are mediated by monocytes and macrophages. Key monocyte-stimulants in JTT have been difficult to identify despite many years of intensive studies by us and others. However, JTT biomarker-guided screening identified β -glucosylceramides (cerebrosides) as the first group of monocyte-stimulants in JTT. This discovery is an important first step to gain mechanistic insights into the clinically tested immunostimulatory effects of JTT.

Finally, chapter 3 describes the screening of secondary metabolites from culturable bacteria from soil samples collected throughout the State of New York. While traditional screenings of secondary metabolites in soil bacteria focus on the search for new antibiotics, our screening looked for a compound with structural complexity which provides us with an access to the pharmacological spaces that are difficult to reach through organic synthesis. This is an important new goal of the screening of bacterial metabolites, because complex molecules of bacterial origin can now be produced from simple carbon sources through metabolic engineering. This study isolated and structurally characterized cyclooctatin B (COB), a new diterpene with a fused 5-8-5 ring system and unique U-shaped conformation. Our preliminary analyses suggest that COB can undergo remarkably elegant cascade reactions when its environment turns mildly acidic. Thus, COB may constitute a new class of pH-sensing bacterial metabolites with a variety of chemical, pharmaceutical, and engineering applications.

Acknowledgments

This thesis could not be brought to completion without the help and the efforts of hardworking and dedicated people. I would like to take this opportunity and especially thank my mentor, Dr. Akira Kawamura for all his guidance, encouragement and support throughout the years of my PhD. Akira helped me in various ways not only related to the research but also in the expansion of my personality. I would also like to sincerely thank all the members of the supervisory committee: Dr. Frida E. Kleiman, Dr. Laurel A. Eckhardt, Dr. Yasuhiro Itagaki and Dr. Edward J. Kennelly for their guidance and advises during my graduate studies. Also, special thanks to Dr. Kleiman's research group for their assistance in certain experiments and for allowing me to use some of their laboratory equipment.

I would also like to thank Dr. Klaus Grohmann for all his help and support these last five years. He was like a father to me, always there to listen to any problems and concerns that might have appeared. Additionally, many thanks to Dr. Grohmann's and Dr. Mootoo's research groups for their help and advises regarding organic chemistry and NMR experiments and data analysis.

As well, I would like to express my gratefulness to our collaborators Dr. Zhitao Li from Binghamton University and Dr. Monica Trujillo from Queensborough Community College and their research groups. Particularly, special thanks to Dr. Trujillo for her useful help on Microbiology and for our good communication and collaboration during the last two years of my PhD.

I would like to extend my thanks to my colleagues (past and present): Dr. Tal H. Hasson for learning me most of the experiments and helping me whenever I needed him,

Emiri Hirokawa and Dorothy Wong who worked with me on the bacteria project and helped me a lot especially with transferring samples from one college to another and performing large scale extractions. Special thanks and gratefulness to Doina M. Mihai and Anna Takaoka: “Girls these last years you were like sisters to me, we had really good time in the lab and I couldn’t have done this without your help!! I love you and I will always have you in a special place in my heard”. Also, many thanks to my friend Murat for being there for me and the girls anytime we needed him.

I would also like to thank my friends Helen, Alex, Tasos, Yiota, Chris, Angela and Stephano for being more like a family to me and my fiancé throughout the years of my PhD. I really cannot thank them enough for everything they have done for us and all their love, support and encouragement.

I would like to express my gratitude, appreciation and thanks to my father, George, my mother, Stella and my brother, Michael for everything that they have done for me throughout these years. Even though we were thousands of miles away they always made me feel that we were just few blocks away and they made me realize even more that family is the most important thing in life.

Finally, I would like to thank my fiancé Spiro for his patience, support, encouragement and love. He was the one encouraging me to come to NY to pursue my PhD and he was there to listen to all my complaints and concerns. Throughout the years of PhD we had some good times as well as difficulties which made us both stronger and more eager to accomplish our goals.

Table of Contents

Chapter I: Search for novel blood cleansing agents in herbal medicine

I. 1.	Introduction	2
I. 2.	Biomarker-guided screening	7
I. 3.	Purification and structural characterization of TDEYA	9
I. 4.	Stereochemical characterization of TDEYA	15
I. 5.	TDEYA is the key mRNA regulatory compound in TSS	16
I. 6.	Discussion	18
I. 7.	Materials and Methods	22
I. 8.	References	29

Chapter II: Uncovering hidden immunostimulants from herbal medicine

II. 1.	Introduction: New cancer immunotherapeutics from old medicine	37
II. 2.	Immunomodulatory activity of phytosteryl glycosides	47
II. 3.	Uncovering “hidden” immunostimulants in JTT	49
II. 4.	Discussion	60
II. 5.	Materials and Methods	64
II. 6.	References	70

Chapter III: Uncovering hidden biosynthetic potential of soil Actinomycetes

III. 1.	Introduction	78
III. 2.	Isolation of metabolite-producing soil bacteria	82
III. 3.	Search for unique metabolites produced by <i>Streptomyces</i>	

<i>griseus</i> MTE4a	84
III. 4. Structural elucidation of cyclooctatin B (COB)	87
III. 5. Acid-sensitivity of COB	92
III. 6. Preliminary biological characterization of COB	94
III. 7. Discussion	95
III. 8. Materials and Methods	103
III. 9. References	106
IV. Appendices	110
V. Bibliography	124

List of Figures

- Figure I.1.** TSS constituents with anti-thrombotic activity in animal models. 6
- Figure I.2.** Overview of the biomarker-guided screening. In this protocol, the herbal medicine of interest is first tested with DNA microarray to identify biomarkers associated with the therapeutic effects of the herbal medicine. qRT-PCR assays are then used to guide the purification of bioactive compounds. 8
- Figure I.3.** (a) qRT-PCR (Serpina1B) guided purification of a gene regulatory compound from TSS. (b) LC/MS positive ion profile of the purified active compound. (c) Serpina1B qRT-PCR assay of the active compound (5 $\mu\text{g/ml}$). GAPDH was used as the endogenous control. $\text{Log}_2(\text{RQ})$ corresponds to the Log Ratio value in the expression profile (Table I.2). RQ stands for relative quantitation (i.e., the fold-change ratio) in real-time PCR analysis. “Reprinted from *Bioorg. Med. Chem. Lett.*, 17, Kawamura et al., ‘A polyacetylene compound from herbal medicine regulates genes associated with thrombosis in endothelial cells’, p. 6879-82, Copyright (2007), with permission from Elsevier.” 12
- Figure I.4.** (a) COSY correlations of the purified active compound. (b) The partial fragment structure deduced based on ^1H NMR, HSQC, and COSY spectra. (c) The identified structure of the active compound. “Reprinted from *Bioorg. Med. Chem. Lett.*, 17, Kawamura et al., ‘A polyacetylene compound from herbal medicine regulates genes associated with thrombosis in endothelial cells’, p. 6879-82, Copyright (2007), with permission from Elsevier.” 13
- Figure I.5.** The ^{13}C -NMR spectrum of purified TDEYA in methanol- d_4 . “Reprinted from *Bioorg. Med. Chem. Lett.*, 17, Kawamura et al., ‘A polyacetylene compound from herbal medicine regulates genes associated with thrombosis in endothelial cells’, p. 6879-82, Supplementary data, Copyright (2007), with permission from Elsevier.” 14
- Figure I.6.** The undetermined chiral center in TDEYA 16
- Figure I.7.** Stereochemical analysis of TDEYA using the CD exciton chirality method. TDEYA and (*R*)-(-)-1,3-Nonanediol (a reference compound) were derivatized to their respective naphthoates, **2** and **3**. The CD spectra of **2** and **3** are 16

shown next to the structures of these compounds.

Figure I.8. qRT-PCR validation of genes differentially regulated by TDEYA: 18
COX2, Perlecan, and TIPARP. **D** (DMSO); **T** (TDEYA). GAPDH was used as
the endogenous control. $\text{Log}_2(\text{RQ})$ corresponds to the Log Ratio value in the
expression profile (Table I.2). “Reprinted from *Bioorg. Med. Chem. Lett.*, 17,
Kawamura et al., ‘A polyacetylene compound from herbal medicine regulates
genes associated with thrombosis in endothelial cells’, p. 6879-82,
Supplementary data, Copyright (2007), with permission from Elsevier.”

Figure II.1. Structures of KRN7000 and agelasphin, its parent compound from 39
marine sponge.

Figure II.2. Structures of putative immunomodulatory components in JTT. The 43
presumed mechanism of each compound is explained in the parentheses.

Figure II.3. Purification scheme to obtain fractions with enriched 44
immunostimulatory activity from JTT. ICAM1 qRT-PCR was used to guide the
purification. The active fraction in each step is shown in red.

Figure II.4. (a) Chromatographic profile of the final C_{18} (ODS) HPLC (100% 45
methanol, isocratic), which resulted in the purification of ELSD-visible fractions
1 and 2. (b) The major components in fraction 1 are in the blue box, whereas the
major component in fraction 2 is in the red box. The UV/ELSD visible peaks
around 4-5 min did not exhibit immunostimulatory activity. (c) ICAM1 qRT-
PCR of fractions 1 and 2 (JTT was used as positive control).

Figure II.5. ICAM1 qRT-PCR analysis of the synthetic PGs: BSSG (**1**), β - 49
sitosteryl β -D-galactoside (**2**) and β -sitosteryl β -D-xyloside (**3**). THP-1 cells were
treated with DMSO (negative control), JTT (100 $\mu\text{g}/\text{ml}$, positive control), **1** (5.5
 $\mu\text{g}/\text{ml}$), **2** (5.5 $\mu\text{g}/\text{ml}$) and **3** (5.5 $\mu\text{g}/\text{ml}$) for 4 h. The structures of the three
synthetic PGs are shown on the right panel.

Figure II.6. Search for immunostimulants in the ELSD “invisible” region. **Left:** 51
HPLC chromatograms obtained with RP-HPLC (C_{18} , 100% MeOH isocratic
elution) equipped with ELSD and PDA detector: ELSD (red); UV220 (blue);
UV254 (green); UV280 (purple); UV350 (pink); UV554 (olive green). **Right:**
ICAM1 qRT-PCR of obtained fractions. C1 and C2 stand for subfraction 1 (4-8

min) and subfraction 2 (8-11.5 min), respectively. F1 and F2 are the PGs fractions.

Figure II.7. Purification of the hidden immunostimulants from JTT. **Left:** HPLC 52 chromatograms obtained with RP-HPLC (C_{18} , 100% MeOH isocratic elution) equipped with ELSD and PDA detector: ELSD (red); UV220 (blue); UV254 (green); UV280 (purple); UV350 (pink); UV554 (olive green). C1 and C2 are the subfractions 1 and 2 respectively, as shown in figure II.6. **Right:** ICAM1 qRT-PCR of fractions A-E. Fraction E represents the PGs fraction.

Figure II.8. Spectroscopic characterization of fraction C. (A) ESI-MS (positive 53 mode). The structure of monostearin is shown in the inset. (B) $^1\text{H-NMR}$ of fraction C (methanol- d_4). (C) $^1\text{H-NMR}$ of monostearin (commercial sample) (methanol- d_4).

Figure II.9. ESI-MS (positive mode) of an acetylation product from fraction C. 54 **Top:** The entire ESI-MS spectrum. **Bottom:** Zoomed spectrum.

Figure II.10. COSY and HMBC analyses of the acetylated product from fraction 55 C. (a) Magnified carbinol/olefin/amide region of COSY spectrum. Observed cross peaks were used to assemble carbons in the sugar moiety and the polar regions of ceramide. (b) Magnified HMBC carbinol/olefin/amide region of HMBC (4Hz). Observed cross peaks were used to verify COSY assignments as well as to determine the linkage site between the sugar and ceramide. (c) Assembled partial structure (planar).

Figure II.11. ESI MS/MS (positive mode) fragmentation analysis of the 58 acetylated sample. **Top:** ESI MS/MS spectrum. **Bottom:** A possible sequence of fragmentations. **In the box:** A fragment structure which accounts for an ion at m/z 331.1028.

Figure II.12. Structures of soya cerebrosides I and II. Soya cerebroside I is the 59 major isomer purified from soy beans.

Figure II.13. ICAM-1 qRT-PCR analysis of Fraction C, soya-cerebroside I (1) 59 and β -galactosylceramides (mixture) (2). DMSO (0.1%, vehicle control); JTT (100 $\mu\text{g/ml}$, positive control); C: Fraction C (5 $\mu\text{g/ml}$); **1:** soya-cerebroside I (5 $\mu\text{g/ml}$); **2:** β -galactosylceramides (5 $\mu\text{g/ml}$). Minimum duplicate experiments

were performed for each condition.

Figure III.1. Clinically important therapeutic agents isolated from the genus of *Streptomyces*. 79

Figure III.2. Structures of known antibiotics isolated from the taxa of actinomycetes. 81

Figure III.3. Metabolites-producing strains isolated from various locations in NY. Pigmentation shown on plates A-F indicates the production of secondary metabolites. Some strains are sporulated (F) with powdery, velvet-like texture and grey/black color, whereas some are non-sporulated (A-E) with rough texture and white or other colors. 83

Figure III.4. Separation of chemical constituents in Fraction D. The CH_2Cl_2 solution of Fraction D was loaded on to a silica gel open column (15 cm \times 1 cm i.d.) and eluted with a step-gradient (0-10% MeOH in CH_2Cl_2 over 20 fractions). (A) TLC profile of the subfractions obtained from Fraction D. TLC was developed with 20% MeOH in CH_2Cl_2 . (B) Comparisons of fractions 16*, 19 and 20 to the background spots (M: The EtOAc extract of the culture medium). Fraction 16* is a combined fraction (Fractions 15-18 in Figure III. 3A). TLC was developed four times with 10% MeOH in CH_2Cl_2 . The unique spot from *Streptomyces griseus* MTE4a is highlighted with a red circle. 87

Figure III.5. Elucidation of the planar structure of a diterpene from *Streptomyces griseus* MTE4a. **Left:** Fragment structures around the three methyl groups were first elucidated with HMBC correlations from the methyl protons (red arrows). The fragments were further extended by COSY correlations (bold blue lines). After this initial analysis, 19 out of 20 carbons were assembled into larger fragments. The ^1H and ^{13}C chemical shifts of three methyl groups as well as the ^{13}C chemical shifts of all other carbons are shown. **Right:** Further analyses of HMBC correlations (red arrows) were used to obtain the planar structure of the diterpene. Bold red lines represent the bonds connected at this stage of the HMBC analysis. 89

Figure III.6. Relative stereochemistry and conformation of the diterpene from *Streptomyces griseus* MTE4a. (a) Relative stereochemistry as determined by 90

NOESY correlations. (b) U-shaped conformation of the central 8-membered ring was suggested by the NOESY correlations of 1-H_β/6-H (β-face; pink line) and 2-H/8-H_α/20-H (α-face; yellow triangle). (c) The NOESY crosspeaks of 1-H_β/6-H and 2-H/8-H_α/20-H. Positive NOESY crosspeaks are shown in dark blue.

Figure III.7. Two different strains of *Streptomyces* produce structurally close diterpenes with a fused 5-8-5 ring system. Two precursors of cyclooctatin have recently been isolated from cytochrome P-450 mutant strains of *S. melanosporofaciens* MI614-43-F2. 91

Figure III.8. (a) ¹H-NMR spectrum of COB in chloroform-*d* shortly after its purification. (b) ¹H-NMR spectrum of COB after the sample was stored in chloroform-*d* for a week. Blue arrows show the conspicuous new peaks emerged during the storage. (c) HMBC crosspeaks of the product formed in chloroform-*d*. A strong HMBC crosspeak was observed from a methyl (*s*) at 1.16 ppm to a carbon at ~95.5 ppm. In addition, a weak crosspeak was also seen from a proton at 3.94 ppm to the same carbon. (d) A possible reaction occurred in chloroform-*d*. The ¹³C-NMR chemical shift for C-10' was estimated on ChemBioDraw. 93

Figure III.9. Antimicrobial activity of COB. The activity indicated by Agar disk method against a lawn culture of *Staphylococcus aureus*. The supernatant of the MTE4a culture was used as positive control and the MTF1 medium as negative control. DMSO was used to dissolve cyclooctatin B (1 mg/ml). 94

Figure III.10. Structures of ophiobolin G, fusicoccin A and ceroplastol II isolated from fungi and insects wax. 96

Figure III.11. The biosynthetic pathway of cyclooctatin in *S. melanosporofaciens* MI614-43F2. It is likely that COB is produced through a similar pathway in *S. griseus* MTE4a, which, however, possess an extra oxidase to hydroxylate the C-17 position. 97

Figure III.12. Possible mechanism of COB transformation in acidic soil. (a) The sites of intramolecular deprotonation which can be anticipated by the unique structure and conformation of COB. (b) A hypothetical transformation pathway in acidic soil. 99

List of Tables and Schemes

Table I.1. The component herbs and botanical origins of TSS.	5
Table I.2. Genes most distinctly regulated by TSS in HUVEC.	10
Table I.3. The ¹³ C-NMR data of TDEYA and the purified material in CDCl ₃ .	14
Table I.4. Endothelial genes most distinctly regulated by the purified active compound (TDEYA; 5 µg/ml; 4h).	17
Table II.1. The component herbs and botanical origin of JTT. Shimotsu-to and Shikunshi-to are related Kampo formulations with the herb composition shown on the table.	41
Table III.1. The ¹³ C-NMR data of COB, cyclooctatin, and biosynthetic precursors. Signals of oxygenated carbons are highlighted by the yellow background.	91
Table III.2. Structure, biological activities and occurrence of A-factor analogues [45].	102
Scheme III.1. Fractionation of the supernatant of <i>S. griseus</i> MTE4a culture. The supernatant of the MTE4a culture was extracted with EtOAc and then fractionated by silica gel chromatography with a step-gradient elution with (A) 100% hexane, (B) hexane/EtOAc (95:5), (C) hexane/EtOAc (90:10) and (D) CH ₂ Cl ₂ /MeOH (90:10). The fractions with antimicrobial activity are highlighted with the red color.	86

List of Abbreviations

ADP	adenosine diphosphate
BSSG	β -sitosterol-D-glucoside
BSS	β -sitosterol
C	carbon
CD	circular dichroism
cDNA	complementary DNA
CDCl ₃	deuterated chloroform
CHCl ₃	chloroform
CH ₂ Cl ₂	methylene chloride
CML	chronic myeloid leukemia
¹³ C-NMR	carbon-13 NMR
COB	cyclooctatin B
COSY	correlation spectroscopy
COX	cyclooxygenase
CVD	cardiovascular disease
DBE	double bond equivalency
DC	dendritic cells
DMADP	dimethylallyl diphosphate
DMSO	dimethyl sulfoxide
$\Delta\Delta$ CT	delta delta CT
EGR1	early growth response factor 1

ELSD	evaporative light scattering detector
ERT	enzyme replacement therapy
ESI-MS	electrospray ionization mass spectrometry
FBS	fetal bovine serum
GalCer	galactosylceramides
GGDP	geranygeranyl diphosphate
H ₂ O	water
HDL	high-density lipoprotein
HER2	human epidermal growth factor receptor 2
HMBC	heteronuclear multiple bond correlation
¹ H-NMR	proton NMR
HPLC	high performance liquid chromatography
HRMS	high resolution mass spectrometry
HSC	hematopoietic stem cells
HSQC	heteronuclear multiple quantum correlation
HUVEC	human umbilical vein endothelial cells
ICAM-1	intercellular adhesion molecule-1
IPP	isopentenyl diphosphate
JTT	Juzen-taiho-to
KBG	Keishi-bukuryo-gan
Kg	kilograms
LAL	limulus amebocyte lysate
LC/MS	liquid chromatography/mass spectroscopy

LDL	low-density lipoprotein
LPS	lipopolysaccharide
Min	minutes
M ⁺	molecular ion
MAS5	Microarray Suite Version 5.0 (Affymetrix GeneChip software)
MeOH	methanol
MgSO ₄	magnesium sulfate
MHz	megahertz
mL	milliliter
mRNA	messenger RNA
MS	mass spectrometry
NaCl	sodium chloride
NMR	nuclear magnetic resonance
NOESY	nuclear Overhauser enhancement spectroscopy
NK	natural killer cells
NKT	natural killer T cells
NRPS	non-ribosomal peptide synthase
QOL	quality of life
PA	plasminogen activator
PAI-2	plasminogen activator inhibitor type 2
PCR	polymerase chain reaction
PDA	photodiode array detector
PGs	phytosteryl glycosides

PGI ₂	prostacyclin
PKS	polyketide synthase
PI	phosphoinositide
qRT-PCR	quantitative reverse-transcriptase polymerase chain reaction
RP-HPLC	reverse phase high performance liquid chromatography
SAR	structure-activity relationship
SerpinB2	serine (or cysteine) proteinase inhibitor, clade B (ovalbumin), member 2
TACAs	tumor-associated carbohydrate antigens
TDEYA	(6 <i>E</i> ,12 <i>E</i>)-tetradecadiene-8,10-diyne-1,3-diol diacetate
TF	tissue factor
Th	T helper cell
TIPARP	TCDD-inducible poly (ADP-ribose) polymerase
TLC	thin layer chromatography
TLR	Toll-like receptor
tPA	tissue-type plasminogen activator
TSS	Toki-shakuyaku-san
TXA ₂	thromboxane A ₂
µg	microgram
µm	micrometer
U	units
uPA	urokinase-type plasminogen activator
UV	ultraviolet spectroscopy

CHAPTER I

Search for novel blood cleansing agents in herbal medicine

I. 1. Introduction

Cardiovascular diseases (CVDs) are the leading killer for both men and women among all racial and ethnic groups in the United States [1]. The most common types of CVDs are stroke, hypertension, congestive heart failure, and coronary heart diseases which include myocardial infarction and chest pain. An estimated 81 million American adults (more than 1 in 3) have 1 or more types of CVDs. Mortality data showed that on average, every 40 seconds, a person has a stroke, and every 4 minutes, a person dies of a stroke in the United States [1].

The common treatments of patients with CVDs include medications that can lower the blood pressure or cholesterol, anti-coagulation agents, and calcium channel blockers. Although these treatments are effective, they are not without adverse side-effects. For example, statins are a class of drugs that lower the blood cholesterol level by blocking HMG-CoA reductase, which catalyzes the rate-determining step of cholesterol biosynthesis. The adverse side-effects of statins are muscle damage (myopathy) and liver failure [2]. Coumadin is an oral anti-coagulant which prevents clots formation by inhibiting vitamin K-dependent coagulation factors. It is known, however, that coumadin can cause fatal bleeding [3]. “Clot busters” or thrombolytics, are a type of heart medication given for blood clots (thrombi) dissolution. These drugs contain tissue plasminogen activator (tPA), streptokinase and urokinase, and dissolve thrombi by activating plasminogen. Known side-effects of this kind of medication are bleeding, allergic reactions, and fever [4]. Calcium channel blockers can induce peripheral vasodilatation and increase the supply of blood and oxygen to the heart, while they also reduce the heart rate. However, they can cause breathing difficulties, irregular or slow

heartbeat, swelling of feet, ankles, and legs and fainting [5]. Thus, various shortcomings of existing therapeutics as well as daunting statistical data call for new class of therapeutics for the treatments of CVDs.

One promising source of anti-coagulation agents with novel mechanisms of action is Japanese Kampo medicine. Kampo medicine originates from Chinese Traditional Medicine, which was introduced to Japan between the fifth and sixth centuries [6]. Kampo medicine utilizes mixtures of various medicinal herbs. Various formulations have been developed and refined over thousands of years of medical practice in East Asia. Since 1976, when the Japanese government approved the use of Kampo in conjunction with Western medicine, Kampo has played a major role in the national health care system in Japan [6]. Now Kampo formulations are used in the treatments of various disorders, such as cancer, hepatitis, menopausal disorders, autonomic imbalances, cold syndrome, digestive disorders, dermatitis, and eczema [6]. They are usually administered in the form of a decoction. Kampo formulations contain a large number of biologically active compounds, such as saponins, glycosides, and flavonoids. However, due to their enormous chemical heterogeneity, characterization of therapeutically relevant compounds has been difficult.

Toki-shakuyaku-san (TSS) is one of many Kampo formulations that have been clinically used in Japan. TSS has long been used for the treatment of blood circulation problems, including gynecological and obstetric disorders [7-10]. The formulation is prescribed to female patients suffering from general weakness with cold hands and feet, edema, fatigue, lower abdominal discomfort, headache, dizziness, shoulder stiffness and ringing in the ears [10]. TSS is made from six different herbs: Hoelen, Cnidii Rhizoma,

Angelicae Radix, Paeoniae Radix, Atractylodis Rhizoma and Alismatis Rhizoma (Table I.1). In the parlance of the Oriental medicine, TSS is a formulation to ‘cleanse stagnated blood,’ thereby nourishing the ‘yang’ of blood. In fact, this somewhat nebulous claim is scientifically supported by the beneficial effects of TSS. It exhibits therapeutic effects for various disorders associated with poor blood circulation, such as hot flashes [10] and preeclampsia [11, 12].

Previous studies suggested that paeoniflorin, sodium ferulate, tetramethylpyrazine and Z-ligustilide may play roles in therapeutic effects of TSS (Figure I.1) [13-16]. Paeoniflorin has been studied as antithrombotic agent [13], antihyperlipidemic agent [17], and as an agent to reduce myocardial damage in animal models [18]. It reduced the plasma cholesterol, triglycerides and low-density lipoprotein (LDL) levels in an experimentally-induced hyperlipidemic rat model [17]. Additionally, paeoniflorin reduced the average weight gain of rats and increased the levels of high-density lipoprotein (HDL) [17]. Sodium ferulate has been shown to inhibit experimental thrombosis in a rat model [19]. In addition, it inhibited *in vitro* platelet aggregation [20]. The *in vivo* action of sodium ferulate was shown to be mediated by the inhibition of cyclooxygenase and thromboxane A₂ (TXA₂) synthase [21]. Moreover, sodium ferulate was shown to inhibit atherosclerosis in a rabbit model [22]. Tetramethylpyrazine has been used for the treatment of coronary atherosclerotic cardiovascular disease and ischemic cerebrocardiac vascular disease [23]. In animal models, tetramethylpyrazine was shown to be an effective antithrombotic agent [24]. In addition, oral administration of Z-ligustilide reduced thrombus formation in rats and prevented platelet aggregation induced by ADP [16].

Table I. 1. The component herbs and botanical origins of TSS.

Ingredients	Botanical origin	Representative compounds	Weigh ratio
Angelicae radix	<i>Angelica acutiloba</i>	Ligustilide, sodium ferulate	3
Paeoniae radix	<i>Paeonia lactiflora</i>	Paeoniflorin, paeonol	4
Cnidii rhizoma	<i>Cnidium officinale</i>	Tetramethylpyrazine, cnidilide	3
Atractylodis Lanceae rhizoma	<i>Atractylodes lancea</i>	Elemol, atractylodin	4
Alismatis Rhizoma	<i>Alisma orientalis</i>	Lecithin, β -sitosterol	4
Hoelen	<i>Sclerotium of Poria Cocos Wolf</i>	Eburicoic acid	4

These four compounds alone, however, do not fully account for the observed therapeutic effects of TSS because of their poor oral availability and/or high dosage requirements. Paeoniflorin [25, 26] and tetramethylpyrazine [27], for example, have notoriously poor bioavailability, which has limited their usages in clinical studies. Sodium ferulate [14] and Z-ligustilide [16], on the other hand, requires very high dosages to exhibit biological activities (~50 mg/kg; ~3 g for a 60 kg adult). Thus, although these compounds may still play some roles in the beneficial effects of TSS, there must be additional compounds responsible for the beneficial effects of this formulation.

It is also noted that these four compounds in TSS have “acute” therapeutic effects by directly modulating biochemical cascades of thrombosis. However, therapeutic effects of Kampo formulations, including TSS, gradually manifest over a period of weeks or even months. For example, in a clinical study that demonstrated the efficacy of TSS for

the treatment of post-stroke patients, TSS was administered over a period of 12 months [28]. Moreover, in another clinical study, a group of patients with anemia associated with menorrhagia has been treated with TSS for a period of 4 to 8 weeks [29]. In order to screen TSS for previously overlooked bioactive compounds, we decided to employ biomarker-guided screening, which had been established in our group [30].

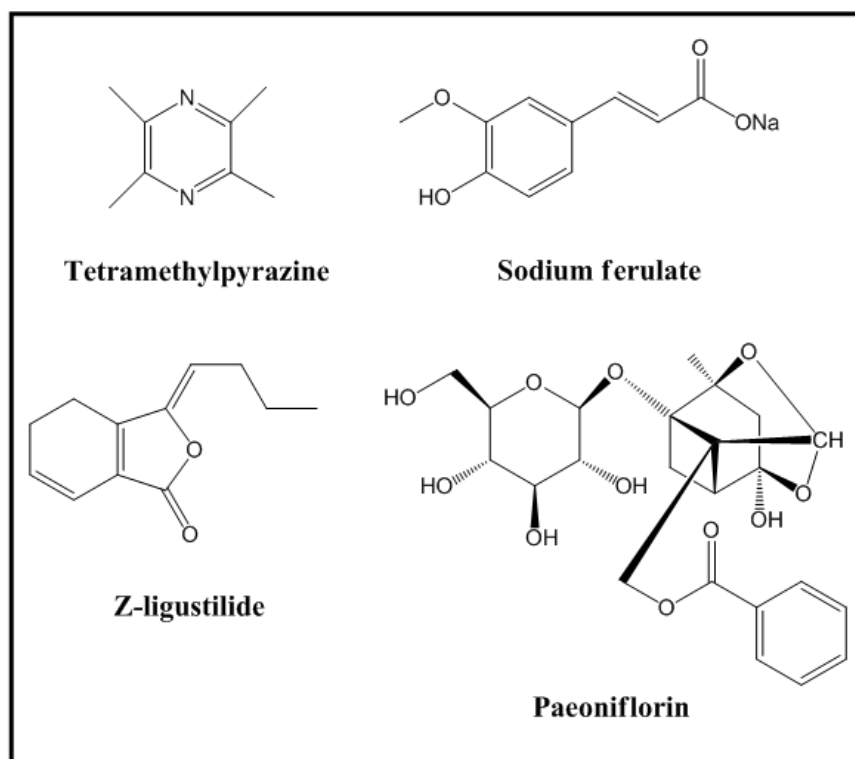


Figure I.1. TSS constituents with anti-thrombotic activity in animal models.

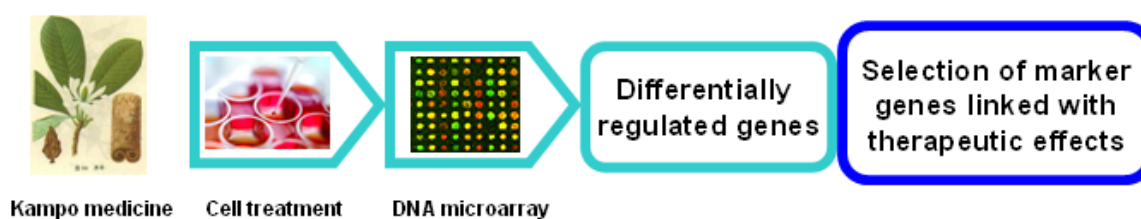
I. 2. Biomarker-guided screening

The National Institute of Health (NIH) has defined the term, biomarker, as “any factor which is objectively measured and evaluated as indicator of normal or pathogenic biological processes and/or as indicators of pharmacological responses to therapeutic intervention” [31]. Biomarkers in the medical field can be used for the diagnosis and prognosis of a disease, for monitoring the development of a disease and guiding the treatment options [31]. Today various forms of biomarkers are available, such as genes [32], microRNA [33], proteins [34] and metabolites [35]. Among the most powerful tools used for the discovery of biomarkers is the DNA microarray technology [36, 37], which can simultaneously quantify tens of thousands of cellular mRNA transcripts. Various mRNA biomarkers are now routinely searched through the use of this technology. DNA microarray has also been used to study herbal medicine [38-40], which demonstrated that a wide variety of mRNA transcripts can be regulated by herbal medicine. In other words, herbal medicine contains a group of compounds that affect biological systems at the transcriptional level. Such herbal compounds, however, have not been systematically searched and characterized.

In order to facilitate the discovery of such gene regulatory compounds in herbal medicine, we developed biomarker-guided screening [30]. Biomarker-guided screening consists of two parts: (1) DNA microarray is used to identify mRNA biomarkers associated with the therapeutic effects of herbal medicine and (2) purification of the bioactive compounds guided by qRT-PCR of mRNA biomarkers (Figure I.2). The first important step of this screening is the selection of a cell line that is relevant to the therapeutic effects of herbal medicine. Once a cell line is selected, cells are treated with

the herbal medicine of interest. Differentially expressed genes are characterized by DNA microarray. Genes that have been previously associated with the therapeutic effects of the herbal medicine are selected as candidate mRNA biomarkers. At this stage, quantitative reverse-transcriptase polymerase chain reaction (qRT-PCR), a highly sensitive and reproducible method to quantify mRNA transcripts [41], is employed to verify the regulation of candidate biomarkers by the herbal medicine. Genes verified by qRT-PCR are then used to guide the purification of transcriptional regulators in herbal medicine.

1. Expression profiling of herb of interest



2. qRT-PCR guided fractionation

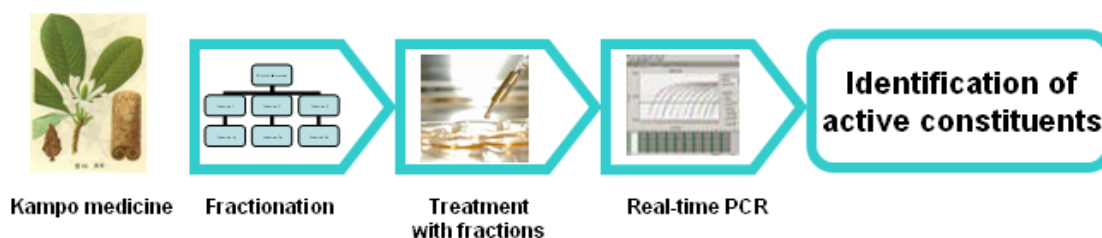


Figure I.2. Overview of the biomarker-guided screening. In this protocol, the herbal medicine of interest is first tested with DNA microarray to identify biomarkers associated with the therapeutic effects of the herbal medicine. qRT-PCR assays are then used to guide the purification of bioactive compounds.

I. 3. Purification and structural characterization of TDEYA

As the first step of biomarker-guided screening, we chose human umbilical vein endothelial cells (HUVEC) as the cell line for our study because beneficial effects of TSS are all related to improved blood circulation. For the gene profiling analysis, HUVEC were treated with 100 µg/ml of TSS for 4 h, a dosage that roughly corresponds to the therapeutic dosage of this formulation (7.5 g/kg/day). At this concentration, TSS did not affect the growth of the cells (data not shown). Expression profiling with Affymetrix GeneChip™ Human Genome U133 Plus 2.0 array revealed that, out of over 47,000 transcripts on the array, 92 genes were differentially regulated by TSS. Table I.2 summarizes the most distinctly regulated genes. Among these genes was SerpinB2 (serine (or cysteine) proteinase inhibitor, clade B (ovalbumin) member 2), which is also known as plasminogen activator inhibitor type 2 (PAI-2). Since SerpinB2 is a well-characterized gene in terms of its roles in blood coagulation and circulation disorders [42-44], we decided to use this gene as a biomarker for the screening of TSS.

The qRT-PCR of SerpinB2 was used to guide the purification of gene regulatory compounds in TSS. Fractionation of TSS was carried out as outlined in Figure I.3a. Individual fractions were submitted to the qRT-PCR assay to examine their ability to induce SerpinB2. Activity was observed in the fractions indicated by the red arrows in Figure I.3.a. After several steps of fractionation, the active compound was isolated by reversed phase HPLC (RP-HPLC). The purified compound gave a single LC/MS peak (Figure I.3.b). At the concentration of 5 µg/ml, the purified compound caused approximately 2-fold induction ($\log_2\text{RQ} \sim 1$) of SerpinB2 in HUVEC (Figure I.3.c).

Table I. 2. Genes most distinctly regulated by TSS in HUVEC.

UniGene ID	Gene	Log Ratio ^a	Fold Change	Change p-value ^b
Hs.12813	TCDD-inducible poly (ADP-ribose) polymerase	0.7	1.6	0.00002
Hs.196384	Prostaglandin-endoperoxide synthase 2 (COX2)	1.0	2.0	0.00002
Hs.594481	Serpin peptidase inhibitor, clade B, member 2 (SerpinB2)	1.0	2.0	0.00002
Hs.433791	Transmembrane protein 46	0.9	1.9	0.00002
Hs.326035	Early growth response 1	0.8	1.7	0.00002
Hs.651231	Heparan sulfate proteoglycan (perlecan)	-0.7	-1.6	0.99904
Hs.594486	Unknown	-1.9	-3.7	0.99944
Hs.29055	Guanine nucleotide binding protein-like 3	-0.8	-1.7	0.99955
Hs.557980	Unknown	-0.7	-1.6	0.99996
Hs.355753	1-Acylglycerol-3-phosphate O-acyltransferase 6	-1.2	-2.3	0.99998

^aLog₂(signal in TSS-treated HUVEC/signal in control HUVEC).

^bLog p-values are calculated using the Wilcoxon signed rank test and Tukey Biweight on MAS5. MAS5 calls a gene ‘decreased (D)’ when its p-value between control- and drug-treated group is between 1 and 0.997, whereas a gene is considered ‘increased (I)’ when its p-value is between 0 and 0.003. Shown are the top five up- (light blue boxes) and down-regulated genes (yellow boxes) based on the Change p-values.

The identity of the active compound was determined by spectroscopic analyses using high resolution mass spectrometry (HRMS) and NMR (in methanol-*d*₄). Briefly, the molecular formula of the active compound was determined to be C₁₈H₂₂O₄ based on HRMS. A partial structure was deduced by ¹H-NMR, HSQC, and COSY (Figures I.4.a,b).

Database (SciFinder) search identified one compound with a matching molecular formula ($C_{18}H_{22}O_4$) and the partial structure (Figure I.4.b). This compound, (6*E*,12*E*)-tetradecadiene-8,10-diyne-1,3-diol diacetate (TDEYA), is a known component in *Atractylodis Rhizoma* (Figure I.4c) [45].

The ^{13}C -NMR spectrum also suggested that the purified compound was TDEYA (Figure I.5), although the published ^{13}C -NMR data of TDEYA had been measured in $CDCl_3$ [45]. Subsequent measurement of the purified sample in chloroform-*d* unequivocally confirmed the identity of the active compound as TDEYA (Table I.3).

Little is known about the biological properties of TDEYA, except for a modest inhibitory activity against xanthine oxidase ($IC_{50} = 1.0 \times 10^{-4}$ M) [46, 47]. Because of its simple chemical structure with multiple unsaturated bonds, TDEYA has also been considered as a precursor of more structurally complex secondary metabolites.

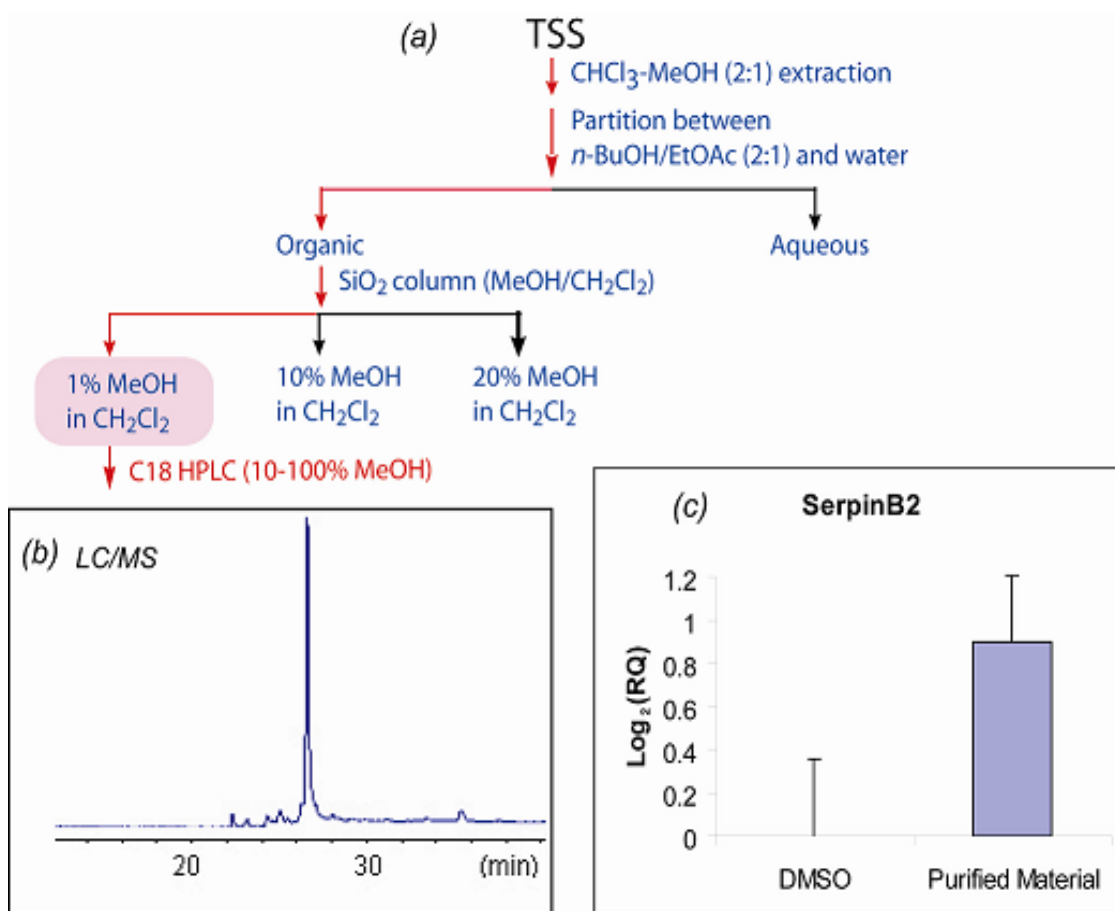


Figure I.3. (a) qRT-PCR (SerpinB2) guided purification of a gene regulatory compound from TSS. (b) LC/MS positive ion profile of the purified active compound. (c) SerpinB2 qRT-PCR assay of the active compound (5 $\mu\text{g/ml}$). GAPDH was used as the endogenous control. $\text{Log}_2(\text{RQ})$ corresponds to the Log Ratio value in the expression profile (Table I.2). RQ stands for relative quantitation (i.e., the fold-change ratio) in qRT-PCR analysis. “Reprinted from *Bioorg. Med. Chem. Lett.*, 17, Kawamura et al., ‘A polyacetylene compound from herbal medicine regulates genes associated with thrombosis in endothelial cells’, p. 6879-82, Copyright (2007), with permission from Elsevier.”

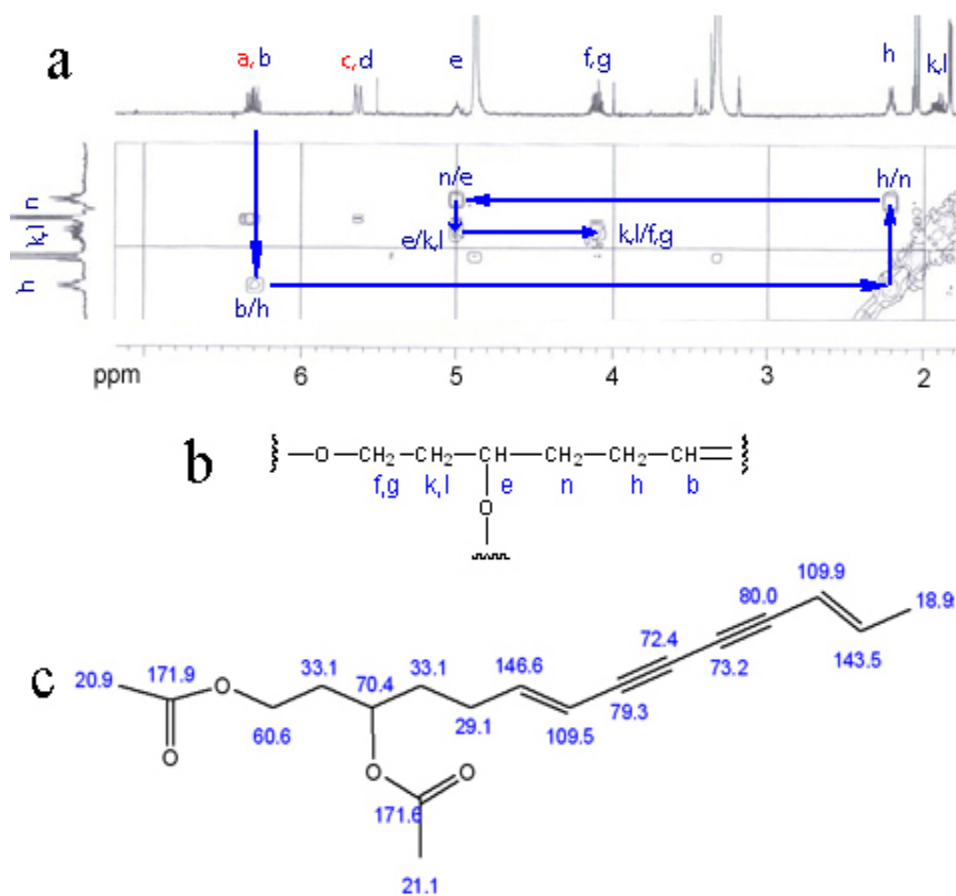


Figure I.4. (a) COSY correlations of the purified active compound. (b) The partial fragment structure deduced based on ¹H-NMR, HSQC, and COSY spectra. (c) The identified structure of the active compound. “Reprinted from *Bioorg. Med. Chem. Lett.*, 17, Kawamura et al., ‘A polyacetylene compound from herbal medicine regulates genes associated with thrombosis in endothelial cells’, p. 6879-82, Copyright (2007), with permission from Elsevier.”

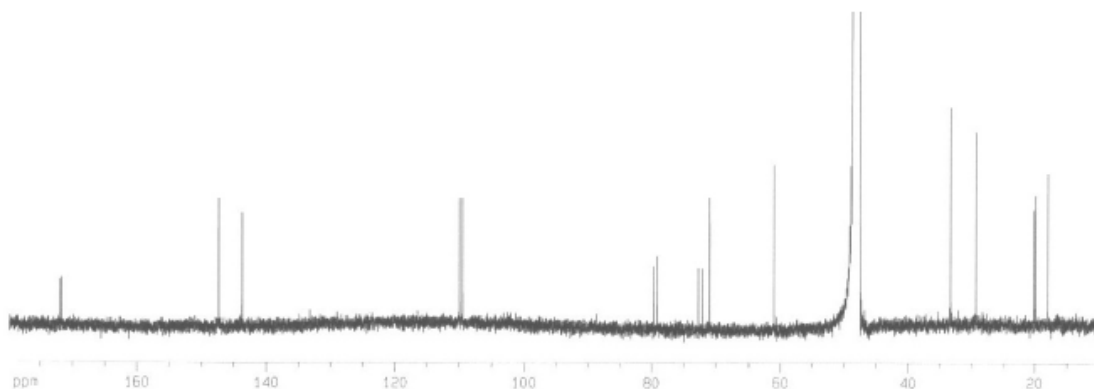


Figure I.5. The ^{13}C -NMR spectrum of purified TDEYA in methanol- d_4 . “Reprinted from *Bioorg. Med. Chem. Lett.*, 17, Kawamura et al., ‘A polyacetylene compound from herbal medicine regulates genes associated with thrombosis in endothelial cells’, p. 6879-82, Supplementary data, Copyright (2007), with permission from Elsevier.”

Table I.3. The ^{13}C -NMR data of TDEYA and the purified material in CDCl_3 .

Carbon	TDEYA (published)	Purified TDEYA from TSS
1	60.6	60.636
2	33.1	33.092
3	70.4	70.370
4	33.1	33.089
5	29.1	29.148
6	146.6	146.524
7	109.5	109.560
8	79.3	79.298
9	72.4	72.305
10	73.2	73.156
11	80.0	80.049
12	109.9	109.919
13	143.5	143.508
14	18.9	18.916
CH_3	21.1	21.115
CH_3	20.9	20.941
$\text{O}=\text{C}-\text{O}$	170.9	171.010
$\text{O}=\text{C}-\text{O}$	170.6	170.617

I. 4. Stereochemical characterization of TDEYA

The absolute configuration of TDEYA has not been characterized (Figure I.6). To address this issue, CD exciton chirality method was employed [48-50]. Exciton chirality method is a simple and highly sensitive method to determine the stereochemistry of organic molecules. To apply this method, the compound of interest has to be first derivatized with UV-absorbing chromophores. If the compound is a single enantiomer, the chromophoric derivative exhibits a distinct bisignate CD curve which reflects its absolute stereochemistry.

In our study, a commercially available (*R*)-(-)-1,3,-nonanediol was used as a reference to examine the stereochemistry of TDEYA. The reference compound was naphthoylated with a standard method [50]. On the other hand TDEYA was first converted to a saturated diol, which was then naphthoylated using the same procedure (Figure I.7). Since only a minute quantity of naphthoylated TDEYA was obtained, the amount of this derivative was quantified based on the UV absorption. As expected for an enantiomerically pure compound, 1, 3-dinaphthoate of (*R*)-(-)-1,3,-nonanediol (reference) exhibited a distinct CD cotton effect (bisignate curve) (Figure I.7, compound **3**). On the other hand, the naphthoate derivative of TDEYA, did not show clear signals (Figure I.7, compound **2**). Thus, this CD study suggested that the purified TDEYA might be a racemic mixture. Further attempts to separate the mixture with chiral HPLC (Chiralcel OD) [51], however, have not been successful.

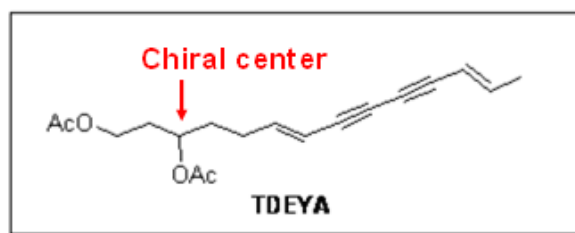


Figure I.6. The undetermined chiral center in TDEYA.

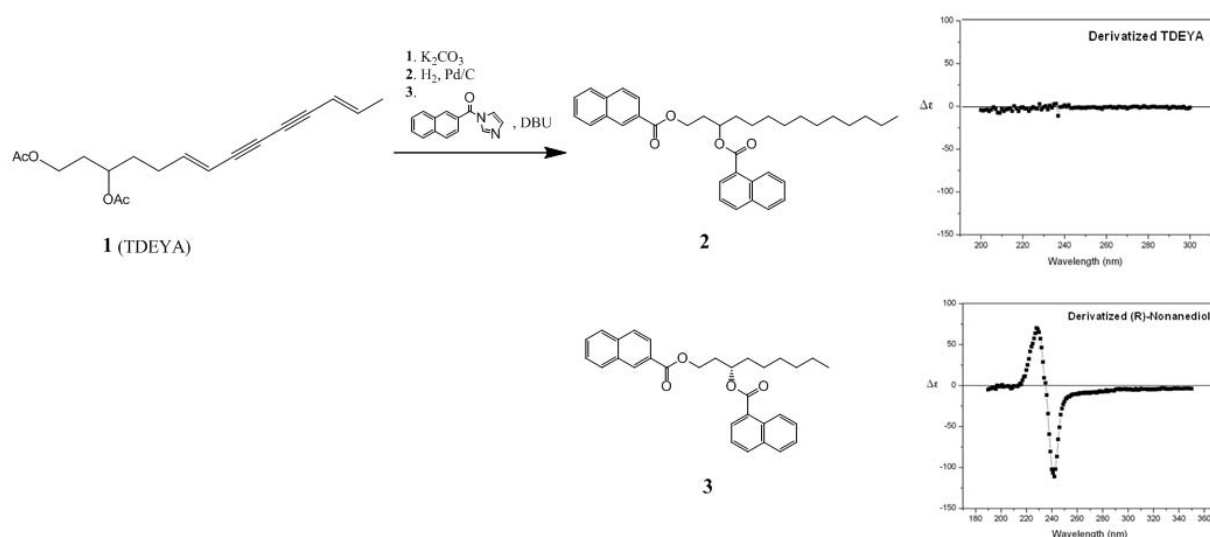


Figure I.7. Stereochemical analysis of TDEYA using the CD exciton chirality method. TDEYA and (*R*)-(-)-1,3-Nonanediol (a reference compound) were derivatized to their respective naphthoates, **2** and **3**. The CD spectra of **2** and **3** are shown next to the structures of these compounds.

I. 5. TDEYA is the key mRNA regulatory compound in TSS

The identification of TDEYA as the regulator of SerpinB2 made us wonder whether TDEYA regulates additional genes, especially those observed in the original expression profile of TSS (Table I.2). To address this issue, we conducted mRNA

expression profiling of TDEYA. Table I.4 summarizes the most distinctly regulated genes by TDEYA in HUVEC. It turned out that many genes overlapped between the TSS and TDEYA profiles (e.g., the genes highlighted in *Italic* in Table I.4), indicating that TDEYA is a key gene regulatory compound in TSS. Among the overlapped genes, differential regulation of perlecan, COX2, and TI-PARP by TDEYA was further validated by qRT-PCR (Figure I. 8).

Table I.4. Endothelial genes most distinctly regulated by the purified active compound (TDEYA; 5 µg/ml; 4 h)

UniGene ID	Gene	Log Ratio ^a	Fold change	Change p-value ^b
<i>Hs. 12813</i>	<i>TCDD-inducible poly(ADP-ribose) polymerase (TI-PARP)</i>	1.2	2.3	0.00002
<i>Hs. 196384</i>	<i>Prostaglandin-endoperoxide synthase 2 (COX2)</i>	1.0	2.0	0.00002
<i>Hs. 594481</i>	<i>Serpin peptidase inhibitor, clade B, member 2 (SerpinB2)</i>	1.0	2.0	0.00002
Hs. 154654	Cytochrome P450, family 1, subfamily B, polypeptide 1	2.7	6.5	0.00002
<i>Hs. 390594</i>	<i>EGR1: early growth response 1</i>	1.2	2.3	0.00056
Hs. 591945	Zinc finger and BTB domain containing 16	-1.0	-2.0	0.99992
Hs. 124649	ATP-binding cassette, sub-family G, member 1	-0.9	-1.9	0.99995
<i>Hs. 651231</i>	<i>Heparan sulfate proteoglycan 2 (perlecan)</i>	-0.8	-1.7	0.99996
Hs. 170355	Mesenchyme homeobox 2	-1.1	-2.1	0.99997
Hs. 468972	AT rich interactive domain 1A (SWI-like)	-0.9	-1.9	0.99998

Italic: These genes were also seen in the list of the most distinctly regulated genes by TSS (Table I.2).

^aLog Ratio and ^bChange p-value were explained under Table I.1. The top five up- (blue boxes) and down-regulated (yellow boxes) genes are shown (based on the Change p-value).

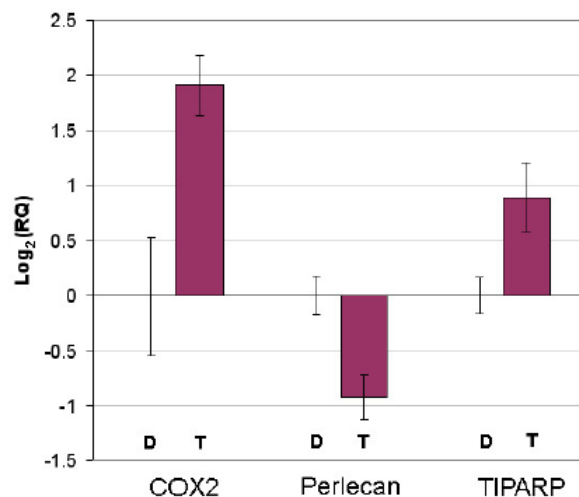


Figure I.8. qRT-PCR validation of genes differentially regulated by TDEYA: COX-2, Perlecan, and TIPARP. **D** (DMSO); **T** (TDEYA). GAPDH was used as the endogenous control. Log₂(RQ) corresponds to the Log Ratio value in the expression profile (Table I.2). “Reprinted from *Bioorg. Med. Chem. Lett.*, 17, Kawamura et al., ‘A polyacetylene compound from herbal medicine regulates genes associated with thrombosis in endothelial cells’, p. 6879-82, Supplementary data, Copyright (2007), with permission from Elsevier.”

I. 6. Discussion

Biomarker-guided screening of TSS, a “blood cleansing” herbal formulation, identified TDEYA as a key gene regulatory compound, which differentially regulates several genes associated with blood coagulation, including, SerpinB2, Perlecan, and COX-2. Known functions of these genes are in accordance with the therapeutic effects of TSS.

SerpinB2 is sometimes considered as a 'coagulation factor' because of its ability to inhibit plasminogen activator (PA); a protein serves as a thrombolytic agent [52]. However, insufficient SerpinB2 has been linked to disorders associated with poor blood circulation. For example, low plasma level of SerpinB2 in pregnant women is a well-known prognostic marker for decreased placental function and intrauterine growth retardation [44, 53-55]. The up-regulation of SerpinB2 by TDEYA as well as TSS is, therefore, in accordance with the therapeutic effects of TSS, although its biological and medical implications have to be further studied.

Perlecan is an extracellular matrix protein which belongs to the heparan sulfate proteoglycans family and has been found to be involved in various vascular processes, such as angiogenesis and wound healing [56]. A recent study illustrated that perlecan is down-regulated in endothelial cells treated by antithrombin, which inactivates several enzymes of the coagulation system [57]. While some studies suggested that heparan sulfate proteoglycans decrease atherosclerosis [58, 59], a recent study showed that perlecan actually promotes atherosclerosis in a mouse model [60]. In our study, TSS and TDEYA down-regulated perlecan in endothelial cells. Taken together, these results collectively suggest that reduction of perlecan in endothelial cells may be beneficial for blood circulation.

COX-2 is another interesting gene identified in our current study. COX-2 is widely known as a pro-inflammatory gene involved in the biosynthesis of prostaglandins. However, the antithrombotic function of COX-2 was revealed recently through the increased risk of thrombotic cardiovascular events (heart attacks) among the patients treated with COX-2 inhibitors, also known as coxibs [61]. A possible mechanism of this

unfavorable effects of coxibs was suggested based on the prostanoid imbalance [62, 63]. Since arterial thrombosis is monitored by a balance between COX-1-dependent generation of thromboxane A₂ (TXA₂) by platelets and COX-2-dependent generation of prostacyclin (PGI₂) in the vascular layer of endothelial cells, the use of coxibs will inhibit the production of PGI₂, which acts as a vasodilator and inhibitor of platelet aggregation. On the other hand, coxibs do not affect the COX-1-dependent production of TXA₂, which is a platelet aggregator and a blood clotting promoter. As a result, coxibs can tilt the balance between TXA₂ and PGI₂ and cause thrombotic cardiovascular events. The modest induction of COX-2 by TSS and TDEYA suggests a possibility that small molecules could be used to adjust this balance between TXA₂ and PGI₂.

While many of the observed genes appear to be in line with the therapeutic effects of TSS, there are some exceptions. For example, our study found the induction of early growth response 1 (EGR1) by TSS and TDEYA. EGR1 is a transcription factor involved in responses to growth factors and stresses [64]. Particularly, EGR1 was found to induce tissue factor (TF), a molecule known for its pro-thrombotic activity and initiation of the intravascular coagulation cascade [65]. It was recently shown that the expressions of EGR1 and TF were significantly up-regulated in the thrombus-covered wall of human abdominal aortic aneurysm and that over-expression of EGR1 in endothelial cells promoted the intravascular thrombus formation *in vivo* using a mouse model [66]. In any event, the strong association of these genes to blood coagulation and cardiovascular diseases suggests that the putative ‘blood cleansing’ activity of TSS is mediated, in part, by these genes.

The identification of TDEYA as a key gene regulator of TSS is important, because the molecule can serve as a potential new pharmacophore for the treatment of CVDs through manipulation of gene expression. TDEYA is, by no means, a classical pharmacophore for anti-coagulation activity; as described earlier, classical anti-coagulation agents include, paeoniflorin, sodium ferulate, tetramethylpyrazine and Z-ligustilide [13-16]. Polyacetylene natural products have been known to possess cytotoxicity [67, 68], anti-microbial activity [69], anti-diabetic activity [70], anti-malaria and anti-bacterial activity [71] and anti-angiogenic activity [72]. TDEYA, on the other hand, did not exhibit any cytotoxicity against endothelial cells. Thus, it is important to further characterize the structural elements that confer the unique biological activity of TDEYA.

Another important issue to be addressed is the stereochemistry of TDEYA. Our current CD study suggested that TDEYA from TSS is a racemic mixture. It is, however, not clear if both enantiomers are needed for the observed gene regulatory activity. It is possible that only one of the two isomers possesses the observed activity. Alternatively, synergism between the two enantiomers may be important for the activity. Separation of the two isomers from natural samples or synthesis of individual enantiomers has to be carried out to address this question.

In conclusion, biomarker-guided screening identified TDEYA, as a key gene regulatory compound in TSS. TDEYA regulates the expression of genes associated with blood coagulation. Identification of TDEYA is important because it opens a new possibility to treat circulation disorders through the regulation of gene expression by small organic molecules.

I. 7 Material and Methods

Materials: All solvents for purification were in the HPLC grade and were purchased from Fisher Scientific. TSS formulation was purchased from Honso Pharmaceutical Co. (Nagoya, Japan). The TSS formulation (lot number: 05I120) was standardized by ferulic acid (test result 0.024%; specification 0.019-0.033%) and paeoniflorin (test result 1.53%; specification 1.24-1.94%). Unless specified otherwise, all other chemicals and reagents were obtained through Fisher Scientific or VWR Scientific, and used without further purification.

Cell Culture: Primary Human Umbilical Vein Endothelial Cells (HUVEC) were purchased from BioWhittaker. Cells were propagated in Endothelium Growth Medium-2 (EGM-2, BioWhittaker) in a 37 °C humidified 5% CO₂ incubator, and subcultured at 70-80% confluency. Cells at the passages 2 - 4 were used for the experiments.

Gene expression profiling: Cells were treated with TSS (100 µg/ml) or DMSO vehicle controls for 4h in a 37 °C humidified 5% CO₂ incubator. 100 µg/ml is a sub-toxic concentration of TSS as determined by MTS cell proliferation assay (Promega);[73] IC₅₀ of TSS was above 500 µg/ml (data not shown). Total RNA was purified with Qiagen RNeasy mini kit. Expression profiling was carried out by following Affymetrix GeneChip Expression Profiling Manual. Briefly, synthesis of biotinylated cRNA via double strand cDNA with T7 promoter was carried out with Affymetrix One-Cycle Target Labeling and Control Reagent kit. Biotinylated cRNA samples were fragmented. Fragmented samples were submitted to Rockefeller University Genomics Center for

hybridization to Human Genome U133 Plus 2.0 array, staining, washing, and scanning. The resulting data were analyzed with Affymetrix GeneChip® Microarray Suite Software Version 5.0 (MAS5). Two independent experiments were carried out for each treatment condition: TSS treated and DMSO (control) treated HUVEC (total 4 chips). This enabled four comparisons between TSS-treated and control groups. In the gene expression profiling of TDEYA, i.e., the purified active compound, cells were treated with TDEYA (5 µg/ml) or DMSO vehicle control for 4 h in a 37 °C humidified 5% CO₂ incubator. The rest of the procedure is same as one described for the profiling of TSS.

qRT-PCR assay: HUVEC were plated onto each well of 6-well plate at ~20% confluency in 2 ml EGM/well and incubated for 24 hours to allow them to recover from passage. Cells were treated with 20 µl of TSS fractions for 4 hours. RNeasy mini kit (Qiagen) was used to purify the total RNA. RNA samples were quantified using UV absorbance at 260 nm. Samples with the 260nm/280nm ratio ~1.8 or higher were used for the subsequent study. The first strand cDNA samples were synthesized with Gibco BRL Superscript Choice system and oligo (dT) 12-18 primer. TaqMan® Gene Expression Assays (Applied Biosystems) were carried out on Applied Biosystems 7500 Real-Time PCR system using pre-optimized assays for SerpinB2, COX-2, Perlecan, TIPARP, and GAPDH (endogenous control). The $\Delta\Delta\text{CT}$ method was employed to quantify differential gene regulation. The raw data were first normalized by the endogenous control (GAPDH) for individual samples. Then the relative quantification (RQ) values, i.e., the fold-change ratios, were obtained by comparing the normalized data against the DMSO vehicle control. At least duplicate experiments were carried out for each sample during the

fractionation. Minimum triplicate experiments were carried out for the final data presented in Figure I.3c and Figure I.8. Student's paired t-Test, with a two-tailed distribution, was used to assess the statistical significance of the difference between control and drug treated samples. qRT-PCR results of all tested genes (SerpB2, COX2, perlecan, and TI-PARP) were consistent with the DNA microarray profile (Figure I.3c and Figure I.8), although there were minor differences in terms of the magnitude of changes in expression.

qRT-PCR guided fractionation of TSS: Fractionation was carried out with 500 g of TSS. Five different solvent systems (hexane, ethyl acetate, chloroform, methanol, and 2:1 mixture of chloroform-methanol) were tested for the initial extraction. Both extracts and insoluble materials were tested by the real-time RT-PCR of SerpinB2 as described above. It was found that the chloroform-methanol (2:1) mixture extracts the SerpinB2 regulatory activity most efficiently. This chloroform-methanol extract was partitioned between 1-butanol/EtOAc (2:1) and water. The activity was then found in the organic layer. Further fractionation of this organic layer was carried out with silica gel chromatography. Three fractions, namely, 1%, 10% and 20% methanol/CH₂Cl₂ fractions, were obtained. The activity was found in the 1% methanol/ CH₂Cl₂ fraction (2 g of crude mixture). Peaks in this 1% MeOH/CH₂Cl₂ fraction were isolated with semi-preparative C18 column with a linear gradient (10-100% MeOH in water, 0.1% trifluoroacetic acid, 3 ml/min). The presence of trifluoroacetic acid in the solvent system did not affect the gene regulatory activity; the activity was acid stable. The activity was found in a peak eluted at 18 min in our HPLC condition.

High resolution LC/MS: LC/MS spectra were acquired on an Agilent Technologies 6210 Time-of-Flight mass spectrometer equipped with an Agilent Technologies 1200 capillary HPLC system. Chromatography was performed on a Zorbax 0.5mm × 150mm SB-C18 column (#5064-8256) using water containing 0.1% formic acid and 50µM ammonium formate (Solvent A) and methanol containing 0.1% formic acid and 50µM ammonium formate (Solvent B) at a flow rate of 12 µl/minute. The gradient program was as follows: 10% B (0-2min), 10-100% B (2-20 min), 100% B (20-50 min). Total run time was 50 min. The temperature of the column was held at 40°C for the entire run. Sample ionization was accomplished using an Agilent Technologies electrospray source with data collection in the positive ion mode. Ionization source parameters were the following: nebulizer pressure of 20psi, drying gas temperature of 300°C, drying gas flow rate of 8.0 L/min, and capillary voltage was set to 3500V. The mass spectrometer was set to acquire data with a fragmentor voltage of 165V. A mass range of 100 to 3200 m/z was scanned using 10,000 transients per scan. The length of transients was 104992. The reference masses used were triethylamine with $[M+H]^+$ at 102.12827 and HP 922 with $[M+H]^+$ at m/z 922.009798. The instrument was controlled with Agilent Mass Hunter Workstation A.02.02 and the data was processed using Applied Biosystems Analyst QS 1.1 software. The molecular formula of the purified compound was determined to be $C_{18}H_{22}O_4$, based on the following ions: ammonium adduct ion $[M+NH_4]^+$, m/z 320.1863 (calcd 320.1856), sodium adduct ion $[M+Na]^+$, m/z 325.1413 (calcd 325.1410) and the protonated adduct ion $[M+H]^+$, m/z 303.1594 (calcd 303.1590).

NMR: For the initial structural characterization, the purified material was dissolved in methanol-*d*₄. NMR spectra were measured by Brüker Avance 500MHz NMR Spectrometer equipped with a dual [¹³C, ¹H] CryoProbe. The dual [¹³C, ¹H] CryoProbe, in which the receiver and transmitter coils are cooled to approximately 20K to reduce contributions to noise in the signal obtained [74], allowed rapid measurement of ¹H, HSQC, and COSY (total less than two hours) with ~0.1 mg of the purified material. ¹³C-NMR was measured by overnight experiment. Data were acquired and processed with the Brüker XWIN-NMR software package. In order to make a direct comparison with the published ¹³C-NMR data of TDEYA, which had been measured in CDCl₃ [45], we re-purified 1 mg of the active compound and measured ¹³C-NMR in CDCl₃.

Preparation of 1-(2-naphthoyl) imidazole: 1,1-Carbonyldiimidazole (0.843 g, 5.2 mmol) was added in one portion to a stirred solution of 2-naphthoic acid (1 g, 2.6 mmol) in anhydrous THF (40 mL). The mixture was stirred at 25 °C for 30 min and the solvent was then evaporated under reduced pressure. The crude product was purified by small column filtration (silica gel, hexanes/EtOAc, 6:4) to afford 1-(2-naphthoyl) imidazole as a white solid (554.2 mg, 82.7%). *R*_f = 0.50 (hexanes/EtOAc, 7:3).

Hydrolysis and hydrogenolysis of TDEYA: TDEYA (10 mg) was hydrolyzed for 1h at 60°C using MeOH (0.5 ml) and K₂CO₃ as catalyst (10 mg) (monitored by TLC). From the resulting product, the solvent was removed under reduced pressure and the hydrogenolysis was performed using formic acid (0.1 ml) and Pd/C as catalyst (10 mg). The reaction took place at room temperature and for 24 hours.

Derivatization of (*R*)-(-)-1, 3-Nonanediol: (*R*)-(-)-1, 3-Nonanediol (10 mg, 62.4 μ moles) was placed in a dried 10ml-round bottomed flask, dissolved in anhydrous acetonitrile (1 ml), 1-(2-naphthoyl) imidazole (100 mg, in excess) was added and DBU was used (1 drop) as a catalyst. The mixture was stirred at room temperature for 24 hours. The solvent was evaporated and the final product is purified by preparative TLC. Hexane-Ethyl acetate (1:1) gives R_f values of 0.3. The product spot is scraped and extracted by MeOH. The purified 1,3-bisnaphthoate derivative was then submitted to the CD measurements in acetonitrile.

Derivatization of 1,3-tetradecanediol (saturated diol of TDEYA): 1,3-tetradecanediol (23 mg, 99.8 μ moles) was placed in a dried 10 ml-round bottomed flask, dissolved in anhydrous acetonitrile (1ml), 1-(2-naphthoyl) imidazole (100mg, in excess) was added and DBU was used (1 drop) as a catalyst. The mixture was stirred at room temperature for 24 hours (monitored by TLC). The solvent was evaporated and the final product is purified by preparative TLC. Hexane-Ethyl acetate (1:1) gives R_f values of 0.3. The product spot is scraped and extracted by MeOH. The purified 1,3-bisnaphthoate derivative was then submitted to the CD measurements in acetonitrile.

CD measurements: Circular dichroism (CD) spectra were recorded using an AVIV 200 CD spectrometer equipped with a Peltier thermal controller with 1-mm optical length and 1-nm bandwidth. Baseline correction was done using the solvent and the same cuvette. Other parameters for CD measurements were: Slit width 0.187mm, Sensitivity -0.64 mdeg, Start wavelength 350nm, end wavelength 290nm. The concentration of the

samples was calibrated using UV absorbance at 230nm with the extinction coefficient of 58,000.

I. 8. References

1. Lloyd-Jones, D., Adams, R. J., Brown, T. M., Carnethon, M., Dai, S., Simone, G. D., Ferguson, T. B., Ford, E., Furie, K., Gillespie, C., Go, A., Greenlund, K., Haase, N., Hailpern, S., Ho, P. M., Howard, V., Kissela, B., Kittner, S., Lackland, D., Lisabeth, L., Marelli, A., McDermott, M. M., Meigs, J., Mozaffarian, D., Mussolino, M., Nichol, G., Roger, V., Rosamond, W., Sacco, R., Sorlie, P., Stafford, R., Thom, T., Wasserthiel-Smoller, S., Nathan, D., Heart Disease and Stroke Statistics 2010 Update. A Report From the American Heart Association. *Circulation*, 2009: p. 1-171.
2. Sørensen, H.T., Lash, T. L., Statins and amyotrophic lateral sclerosis – the level of evidence for an association. *J. Intern. Med.*, 2009. **266**(6): p. 520-6.
3. Palareti, G., Cosmi, B., Bleeding with anticoagulation therapy - who is at risk, and how best to identify such patients. *Thromb. Haemost.*, 2009. **102**(2): p. 268-78.
4. Longstaff, C., Thelwell, C., Understanding the enzymology of fibrinolysis and improving thrombolytic therapy. *FEBS Lett.*, 2005. **579**(15): p. 3303-9.
5. Bramlage, P., Hasford, J., Blood pressure reduction, persistence and costs in the evaluation of antihypertensive drug treatment – a review. *Cardiovascular Diabetol.*, 2009. **8**(18): p. 1-13.
6. Yamada, H., Saiki, I., *Juzen-taiho-to (Shi-Quan-Da-Bu-Tang): Scientific Evaluation and Clinical Applications*. 2005, FL: CRC, Boca Raton. 256.
7. Koyama, T., Role of Kampo (herbal) medicine for management in postmenopausal women in Japan. *J. Jpn. Menopause Soc.*, 1993. **1**: p. 75-9.
8. Kano, T., Ito, C., Kasamatsu, H., Miyawaki, Y., Clinical study of prognosis of 200 deliveries after Kampo-treatment for ovarian dysfunctional infertilities and tocolysis. *Jpn. J. Fertil. Steril.*, 1991. **36**: p. 612-20.
9. Kotani, N., Oyama, T., Sakai, I., Hashimoto, H., Muraoka, M., Ogawa, Y., Matsuki, A., Analgesic Effect of a Herbal Medicine for Treatment of Primary Dysmenorrhea - A Double-blind Study. *Am. J. Chin. Med.*, 1997. **25**(2): p. 205-12.
10. Tanaka, T., Effects of herbal medicines on menopausal symptoms induced by gonadotropin-releasing hormone agonist therapy. *Clin. Exp. Obstet. Gynecol.*, 2001. **28**(1): p. 20-23.
11. Takei, H., Yamamoto, M., Kase, Y., Takeda, S., The Effect of Herbal Medicine Toki-shakuyaku-san on Blood Pressure in an N⁰-Nitro-L-Arginine Methyl Ester-Induced Pre-eclampsia Rat Model During Pregnancy and the Postpartum Period. *J. Pharmacol. Sci.*, 2005. **98**(3): p. 255-62.

12. Takei, H., Nakai, Y., Hattori, N., Yamamoto, M., Kurauchi, K., Sasaki, H., Aburada, M., The herbal medicine Toki-shakuyaku-san improves the hypertension and intrauterine growth retardation in preeclampsia rats induced by Nomega-nitro-L-arginine methyl ester. *Phytomedicine*, 2004. **11**(1): p. 43-50.
13. Ye, J., Duan, H., Yang, X., Yan, W., Zheng, X., Anti-thrombosis effect of paeoniflorin: evaluated in a photochemical reaction thrombosis model in vivo. *Planta Med.*, 2001. **67**(8): p. 766-767.
14. Wang, B.H., Ou-Yang, J. P., Pharmacological actions of sodium ferulate in cardiovascular system. *Cardiovasc. Drug Rev.*, 2005. **23**(2): p. 161-72.
15. Li, M., Handa, S., Ikeda, Y., Goto, S., Specific Inhibiting Characteristics of Tetramethylpyrazine, One of the Active Ingredients of the Chinese Herbal Medicine 'Chuanxiong,' on Platelet Thrombus Formation Under High Shear Rates. *Thrombosis Research*, 2001. **104**: p. 15-28.
16. Zhang, L., Du, J. R., Wang, J., Yu, D. K., Chen, Y. S., He, Y., Wang, C. Y., Z-ligustilide extracted from Radix Angelica Sinensis decreased platelet aggregation induced by ADP Ex Vivo and arterio-venous Shunt Thrombosis in Vivo in rats. *Yakugaku Zasshi*, 2009. **129**(7): p. 855-859.
17. Yang, H.O., Ko, W. K., Kim, J. Y., Ro, H. S., Paeoniflorin: an antihyperlipidemic agent from Paeonia lactiflora. *Fitoterapia*, 2004. **75**: p. 45-49.
18. Nizamutdinova, I.T., Jin, Y. C., Kim, J. S., Yean, M. H., Kang, S. S., Kim, Y. S., Lee, J. H., Seo, H. G., Kim, H. J., Chang, K. C., Paeonol and paeoniflorin, the main active principles of Paeonia albiflora, protect the heart from myocardial ischemia/reperfusion injury in rats. *Planta Med.*, 2008. **74**(1): p. 14-18.
19. Xu, L.N., Ouyang, R., Antithrombotic effect of sodium ferulate in rats. *Zhongguo Yao Li Xue Bao*, 1981. **2**(1): p. 35-7.
20. Yin, Z.Z., Zhang, L.Y., Xu, L. N., The effect of danggui (Angelica sinensis) and its ingredient ferulic acid on rat platelet aggregation and release of 5-HT. *Yao Xue Xue Bao*, 1980. **15**: p. 321.
21. Wang, Z., Gao, Y. H., Huang, R. S., Zhu, G. Q., Sodium ferulate is an inhibitor of thromboxane A₂ synthetase. *Zhongguo Yao Li Xue Bao*, 1988. **9**: p. 430-33.
22. Wang, B., Ouyang, J., Liu, Y., Yang, J., Wei, L., Li, K., Yang, H., Sodium Ferulate Inhibits Atherosclerogenesis in Hyperlipidemia Rabbits. *J. Cardiovasc. Pharmacol.*, 2004. **43**(4): p. 549-54.
23. Xu, H., Shi, D. Z., Guan, C. Y., Clinical application and pharmacological actions of ligustrazine. *Chin. J. Integr. Tradit. West. Med.*, 2003. **23**(5): p. 376-9.

24. Sheu, J.R., Kan, Y. C., Hung, W. C., Ko, W. C., Yen, M. H., Mechanisms Involved in the Antiplatelet Activity of Tetramethylpyrazine in Human Platelets. *Thrombosis Research*, 1997. **88**: p. 259-70.
25. Takeda, S., Isono, T., Wakui, Y., Matsuzaki, Y., Sasaki, H., Amagaya, S., Maruno, M., Absorption and excretion of paeoniflorin in rats. *J. Pharm. Pharmacol.*, 1995. **47**(12A): p. 1036-40.
26. Takeda, S., Isono, T., Wakui, Y., Mizuhara, Y., Amagaya, S., Maruno, M., Hattori, M., In-vivo assessment of extrahepatic metabolism of paeoniflorin in rats: relevance to intestinal floral metabolism. *J. Pharm. Pharmacol.*, 1997. **49**(1): p. 35-39.
27. Xu, R., Li, Y., Huang, X., Recent advances in pharmacokinetics of ligustrazine. *J. Anhui. TCM. Coll.*, 2002. **21**(1): p. 58-61.
28. Goto, H., Satoh, N., Hayashi, Y., Hikiami, H., Nagata, Y., Obi, R., Shimada, Y., A Chinese Herbal Medicine, Tokishakuyakusan, Reduces the Worsening of Impairments and Independence After Stroke: A 1-year Randomized, Controlled Trial. *Evid Based Complement Alternat Med.*, 2009: p. 1-6.
29. Akase, T., Akase, T., Onodera, S., Jobo, T., Matsusita, R., Kaneko, M., Tashiro, S., A Comparative Study of the Usefulness of Toki-shakuyaku-san and An Oral Iron Preparation in the Treatment of Hypochromic Anemia in Cases of Uterine Myoma. *Yakuyaku Zasshi*, 2003. **123**(9): p. 817-24.
30. Kawamura, A., Brekman, A., Grigoryev, Y., Hasson, T. H., Takaoka, A., Wolfe, S., Soll, C. E., Rediscovery of natural products using genomic tools. *Bioorg. Med. Chem. Lett.*, 2006. **16**(11): p. 2846-9.
31. Wright, C.F., Hall, A. , Matthews, F. E., Brayne, C., Biomarkers, Dementia, and Public Health. *Ann. N. Y. Acad. Sci.*, 2009. **1180**: p. 11-19.
32. Yerushalmi, R., Woods, R., Ravdin, P. M., Hayes, M. M., Gelmon, K. A., Ki67 in breast cancer: prognostic and predictive potential. *Lancet Oncol.*, 2010. **11**(2): p. 174-83.
33. Sethupathy, P., Collins, F. S., MicroRNA target site polymorphisms and human disease. *Trends Genet.*, 2008. **24**(10): p. 489-97.
34. Hwang, H.J., Quinn, T., Zhang, J., Identification of glycoproteins in human cerebrospinal fluid. *Methods Mol. Biol.*, 2009. **566**: p. 263-76.
35. Rutella, S., Bonanno, G., De Cristofaro, R., Targeting indoleamine 2,3-dioxygenase (IDO) to counteract tumour-induced immune dysfunction: from biochemistry to clinical development. *Endocr. Metab. Immune Disord. Drug Targets*, 2009. **9**(2): p. 151-77.

36. Lockhart, D.J., Winzeler, E.A., Genomics, gene expression and DNA arrays. *Nature*, 2000. **405**: p. 827-36.
37. Brown, P.O., Botstein, D., Exploring the new world of the genome with DNA microarrays. *Nat. Genet.*, 1999. **21**: p. 33-7.
38. Watanabe, C.M., Wolfram, S., Ader, P., Rimbach, G., Packer, L., Maguire, J.J., Schultz, P.G., Gohil, K., The in vivo neuromodulatory effects of the herbal medicine ginkgo biloba. *Proc. Natl. Acad. Sci. USA*, 2001. **98**(12): p. 6577-80.
39. Yang, S.H., Kim, J.S., Oh, T.J., Kim, M.S., Lee, S.W., Woo, S.K., Cho, H.S., Choi, Y.H., Kim, Y.H., Rha, S.Y., Chung, H.C., An, S.W., Genome-scale analysis of resveratrol-induced gene expression profile in human ovarian cancer cells using a cDNA microarray. *Int. J. Oncol.*, 2003. **22**(4): p. 741-50.
40. Gohil, K., Moy, R.K., Farzin, S., Maguire, J.J., Packer, L., mRNA expression profile of a human cancer cell line in response to Ginkgo biloba extract: induction of antioxidant response and the Golgi system. *Free Radic. Res.*, 2000. **33**(6): p. 831-49.
41. Sambrook, J., and Russell, D., *Molecular cloning, A laboratory manual*. 2001, Cold Spring Harbor, New York: Cold Spring Harbor Laboratory Press
42. Kruithof, E.K.B., M. S.; Bunn, C. L., Biological and clinical aspects of plasminogen activator inhibitor type 2. *Blood*, 1995. **86**(11): p. 4007-24.
43. Medcalf, R.L.S., S. J., The undecided serpin. The ins and outs of plasminogen activator inhibitor type 2. *FEBS J.*, 2005. **272**(19): p. 4858-67.
44. Astedt, B., Lindoff, C., Lecander, I., Significance of the plasminogen activator inhibitor of placental type (PAI-2) in pregnancy. *Semin. Thromb. Hemost.*, 1998. **24**(5): p. 431-5.
45. Kano, Y., Komatsu, K., Saito, K., Bando, H., Sakurai, T., A new polyacetylene compound from *Atractylodes* rhizome. *Chem. Pharm. Bull.*, 1989. **37**(1): p. 193-94.
46. Sakurai, T., Yamada, H., Saito, K., Kano, Y., Enzyme inhibitory activities of acetylene and sesquiterpene compounds in *atractylodes* rhizome. *Biol. Pharm. Bull.*, 1993. **16**(2): p. 142-5.
47. Sakurai, T., Sugawara, H., Saito, K., Kano, Y., Effects of the acetylene compound from *Atractylodes* rhizome on experimental gastric ulcers induced by active oxygen species. *Biol. Pharm. Bull.*, 1994. **17**(10): p. 1364-8.
48. Kawamura, A., Berova, N., Nakanishi, K., Voigt, B. and Adam, G., Configurational assignment of brassinosteroid sidechain by exciton coupled circular dichroic spectroscopy. *Tetrahedron*, 1997. **53**: p. 11961-70.

49. Kawamura, A., Berova, N., Nakanishi, K., Use of circular dichroism for assigning stereochemistry of sphingosine and other long chain bases. *Methods Enzymol.*, 2000. **312**: p. 217-27.
50. Kawamura, A., Berova, N., Dirsch, V., Mangoni, A., Nakanishi, K., Schwartz, G., Bielawska, A., Hannun, Y., Kitagawa, I., Picomole scale stereochemical analysis of sphingosines and dihydrosphingosines. *Bioorg. Med. Chem.*, 1996. **4**(7): p. 1035-43.
51. Davankov, V.A., Analytical chiral separation methods. *Pure & Appl. Chem.*, 1997. **69**(7): p. 1469-74.
52. Humphries, J., Gossage, J. A., Modarai, B., Burnand, K. G., Sisson, T. H., Murdoch, C., Smith, A., Monocyte urokinase-type plasminogen activator up-regulation reduces thrombus size in a model of venous thrombosis. *J. Vasc. Surg.*, 2009. **50**(5): p. 1127-34.
53. Estelles, A., Gilabert, J., Espana, F., Aznar, J., Galbis, M., Fibrinolytic parameters in normotensive pregnancy with intrauterine fetal growth retardation and in severe preeclampsia. *Am. J. Obstet. Gynecol.*, 1991. **165**: p. 138-42.
54. Gilabert, J., Estelles, A., Ayuso, M. J., Espana, F., Chirivella, M., Grancha, S., Mico, J. M., Aznar, J., Evaluation of plasminogen activators and plasminogen activator inhibitors in plasma and amniotic fluid in pregnancies complicated with intrauterine fetal growth retardation. *Gynecol. Obstet. Invest.*, 1994. **38**(3): p. 157-62.
55. Grancha, S., Estelles, A., Gilabert, J., Chirivella, M., Espana, F., Aznar, J., Decreased expression of PAI-2 mRNA and protein in pregnancies complicated with intrauterine fetal growth retardation. *Thromb. Haemost.*, 1996. **76**(5): p. 761-7.
56. Knox, S.M., Whitelock, J. M., Perlecan: how does one molecule do so many things? *Cell. Mol. Life Sci.*, 2006. **63**: p. 2435-45.
57. Zhang, W., Chuang, Y. J., Swanson, R., Li, J., Seo, K., Leung, L., Lau, L. F., Olson, S. T., Antiangiogenic antithrombin down-regulates the expression of the proangiogenic heparan sulfate proteoglycan, perlecan, in endothelial cells. *Blood*, 2004. **103**: p. 1185-91.
58. Engelberg, H., Endogenous heparin activity deficiency: the 'missing link' in atherogenesis? *Atherosclerosis*, 2001. **159**: p. 253-60.
59. Pillarisetti, S., Lipoprotein modulation of sub-endothelial heparan sulfate proteoglycans (perlecan) and atherogenicity. *Trends Cardiovasc Med.*, 2000. **10**: p. 60-65.

60. Tran-Lundmark, K., Tran, P. K., Paulsson-Berne, G., Friden, V., Soininen, R., Tryggvason, K., Wight, T. N., Kinsella, M. G., Boren, J., Hedin, U., Heparan Sulfate in Perlecan Promotes Mouse Atherosclerosis: Roles in Lipid Permeability, Lipid Retention, and Smooth Muscle Cell Proliferation. *Circ. Res.*, 2008. **103**: p. 43-52.
61. Iezzi, A., Ferri, C., Mezzetti, A., Cipollone, F., COX-2: Friend or Foe? *Curr. Pharm. Des.*, 2007. **13**: p. 1715-21.
62. FitzGerald, G.A., Nonsteroidal anti-inflammatory drugs, coxibs, and cardio-renal physiology: a mechanism-based approach. *Am. J. Cardiol.*, 2002. **89**: p. 1D-2D.
63. Grosser, T., Fries, S., FitzGerald, G. A., Biological basis for the cardiovascular consequences of COX-2 inhibition: therapeutic challenges and opportunities. *J. Clin. Invest.*, 2006. **116**: p. 4-15.
64. Lucerna, M., Pomyje, J., Mechtcheriakova, D., Kadl, A., Gruber, F., Bilban, M., Sobanov, Y., Schabbauer, G., Breuss, J., Wagner, O., Bischoff, M., Clauss, M., Binder, B. R., Hofer, E., Sustained Expression of Early Growth Response Protein-1 Blocks Angiogenesis and Tumor Growth. *Cancer Res.*, 2006. **66**(13): p. 6708-13.
65. Day, S.M., Reeve, J. L., Pedersen, B., Farris, D. M., Myers, D. D., Im, M., Wakefield, T. W., Mackman, N., Fay, W. P., Macrovascular thrombosis is driven by tissue factor derived primarily from the blood vessel wall. *Blood*, 2005. **105**: p. 192-8.
66. Shin, I.S., Kim, J. M., Kim, K. L., Jang, S.Y., Jeon, E. S., Choi, S. H., Kim, D. K., Suh, W., Kim, Y. W., Early Growth Response Factor-1 Is Associated With Intraluminal Thrombus Formation in Human Abdominal Aortic Aneurysm. *J. Am. Coll. Cardiol.*, 2009. **53**(9): p. 792-9.
67. Chicca, A., Pellati, F., Adinolfi, B., Matthias, A., Massarelli, I., Benvenuti, S., Martinotti, E., Bianucci, A. M., Bone, K., Lehmann, R., Nieri, P., Cytotoxic activity of polyacetylenes and polyenes isolated from roots of *Echinacea pallida*. *British Journal of Pharmacology*, 2008. **153**: p. 879-85.
68. Huang, H., Q., Zhang, X., Shen, Y. H., Su, J., Liu, X. H., Tian, J. M., Lin, S., Shan, L., Zhang, W. D., Polyacetylenes from *Bupleurum longiradiatum*. *J. Nat. Prod.*, 2009. **72**: p. 2153-57.
69. Lechner, D., Stavri, M., Oluwatuyi, M., Pereda-Miranda, R., Gibbons, S., The anti-staphylococcal activity of *Angelica dahurica* (Bai Zhi). *Phytochemistry*, 2004. **65**: p. 331-5.
70. Chien, S.C., Young, P. H., Hsu, Y. J., Chen, C. H., Tien, Y. J., Shiu, S. Y., Li, T. H., Yang, C. W., Marimuthu, P., Tsai, L. F., Yang, W. C., Anti-diabetic properties

- of three common *Bidens pilosa* variants in Taiwan. *Phytochemistry*, 2009. **70**: p. 1246-54.
71. Tobinaga, S., Sharma, M. K., Aalbersberg, W. G., Watanabe, K., Iguchi, K., Narui, K., Sasatsu, M., Waki, S., Isolation and identification of a potent antimalarial and antibacterial polyacetylene from *Bidens pilosa*. *Planta Med.*, 2009. **75**(6): p. 624-8.
 72. Wu, L.W., Chiang, Y. M., Chuang, H. C., Wang, S. Y., Yang, G. W., Chen, Y. H., Lai, L. Y., Shyur, L. F., Polyacetylenes Function as Anti-angiogenic Agents. *Pharm. Res.*, 2004. **21**(11): p. 2112-19.
 73. Malich, G., Marcovic, B., Winder, C., The sensitivity and specificity of MTS tetrazolium assay for detecting the in vitro cytotoxicity of 20 chemicals using human cell lines. *Toxicology*, 1997. **124**: p. 179-92.
 74. Styles, P., Soffe, N. F., Scott, C. A., Cragg, D. A., Row, F., White, D. J., White, P. C. J., A high-resolution NMR probe in which the coil and the preamplifier are cooled with liquid nitrogen. *J. Magn. Reson.*, 1984. **60**: p. 397-404.

CHAPTER II

Uncovering hidden immunostimulants from herbal medicine

II.1. Introduction: New cancer immunotherapeutics from old medicine

Cancer remains to be among the top causes of death worldwide with mortality rate of 1,500 deaths per day in the United States [1]. Although several new agents, such as imatinib (Gleevec[®]; for chronic myeloid leukemia (CML)) and trastuzumab (Herceptin[®]; for her2 positive breast cancer), have shown new directions in cancer therapy [2-5], classical cytotoxic agents, such as carboplatin [6, 7] and paclitaxel [6, 8], remain to be the first-line therapies for many common cancers. The very low response rate (10-30%) to these cytotoxic agents continues to be a major problem in cancer chemotherapy. Because of the obvious need for new drugs, major research efforts are directed toward the development of therapeutic agents with new targets, such as kinases [9, 10], angiogenesis [11, 12], metabolic pathways [13, 14] and the immune system (cancer immunotherapy) [15, 16].

Among these new directions of cancer therapy, immunotherapy is unique because it does not directly target cancer growth or metastasis. Instead, cancer immunotherapy is based on the notion that the immune system can be “manipulated” to fight tumors similarly as prophylactic vaccines fight infections [15]. Immunotherapeutic agents can also be useful to improve the quality of life (QOL) of cancer patients whose immune systems are often damaged by chemotherapy or radiation therapy. Compounds that can revive the immune system, if identified, would improve QOL of patients by facilitating the recovery from surgery and reducing the chance of infection [17].

Development of safe and effective immunotherapeutics, however, is a much harder task than originally anticipated. Bacterial and fungal membrane components, such as lipopolysaccharides (LPS), peptidoglycans, and lipoteichoic acids, which are potent

Toll-like receptor (TLR) agonists, have been tested as immunoadjuvants for cancer therapy with mixed results [18-21]. In addition, these bacterial and fungal lipids are potentially dangerous because they can elicit uncontrolled immune responses (septic shock) [22]. Tumor-associated carbohydrate antigens (TACAs) are another group of compounds that have been studied intensively for cancer immunotherapy [23-25]. Cancer vaccine development based on TACAs, however, has shown limited success [26, 27]. As a result, the focus of TACAs research has shifted to other applications, such as biomarker development for cancer diagnosis and prognosis [28, 29].

Another group of immunostimulants that garnered attention recently is galactosylceramides (GalCer), such as agelashin, which were originally found from marine sponge (Figure II.1) [30-32]. KRN7000, a synthetic derivative of agelasphin, exhibited a promising anti-cancer activity mediated by natural killer T (NKT)-cells, eradicating various tumors in experimental animal models [33-35]. Phase I/II clinical trials of KRN7000, however, turned out to be not quite as remarkable as the animal studies [36, 37]. These results underscore the difficulty of predicting how the human immune system might respond to new immunotherapeutics. An ideal source of new immunotherapeutics might be old folk remedies whose safety and efficacy have been refined throughout human history.

The biomarker-guided screening of herbal medicine, as exemplified in the preceding chapter, can uncover previously overlooked immunotherapeutics from long-tested folk remedies. A promising but as-yet unapprised source of cancer immunotherapeutics is Juzen-taiho-to (JTT), which has been used to boost immune functions for thousands of years in oriental medicine [38]. JTT (Shi-Quan-Da-Bu-Tang in

Chinese), is composed of ten different crude drugs namely, Astragali Radix, Cinnamoni Cortex, Rehmanniae Radix, Paeoniae Radix, Cnidii Rhizoma, Atractylodis Rhizoma, Angelicae Radix, Ginseng Radix, Hohen and Glycyrrhizae Radix (Table II.1) [38]. In Japan, clinical use of JTT was approved by the Japanese government in 1976. Since then, it has been used in conjunction with chemotherapy and radiation therapy to improve the QOL of cancer patients [39-41]. More than three decades of clinical use has shown that JTT is effective in alleviating leukopenia as well as anemia and nausea [42]. In addition, preclinical studies have shown that JTT inhibits tumor progression and metastasis through activation of monocytes and macrophages [38, 43, 44]. Thus, JTT is a great source of potential immunotherapeutics to improve QOL of cancer patients and possibly to prevent cancer progression and metastasis.

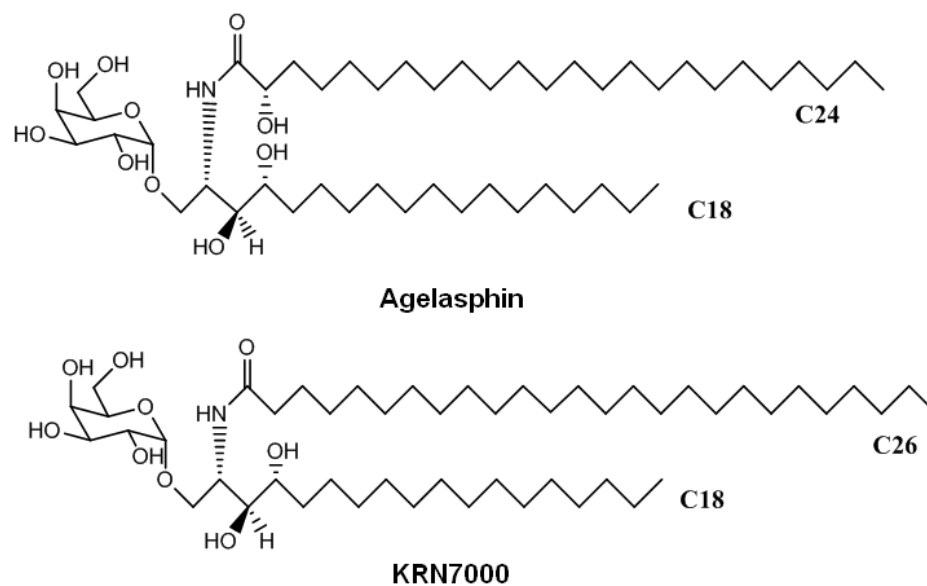


Figure II. 1. Structures of KRN7000 and agelasphin, its parent compound isolated from marine sponge.

Chemical characterization of JTT, however, is lagging far behind the characterization of clinical utility. Although several groups of compounds, including terpenoids, fatty acids, and oligosaccharides (Figure II.2), have been suggested as potential immunomodulatory components, these compounds alone cannot explain the variety and potency of the beneficial effects of JTT. For example, none of these compounds explain the potent activation of monocytes and macrophages, which are believed to mediate, at least in part, the therapeutic effects of JTT, including anti-cancer and anti-metastatic activity [38, 43, 44]. In addition, high dosages required for the activities of these compounds are discordant with their bioavailability. For example, paeoniflorin exhibits various biological activities at 10 $\mu\text{g/ml}$ or higher [45-47], which, in a very crude estimate, is translated to the dosage of 10 mg/kg or 600 mg for an adult (60 kg). JTT, however, contains only ~50 mg of paeoniflorin in a daily dosage. As mentioned in the last chapter, paeoniflorin has very poor (3-4%) bioavailability when administered orally [48, 49]. Taken together, it is unlikely that paeoniflorin plays a meaningful role in the immunomodulatory effects of JTT.

The establishment of biomarker-guided screening [50, 51], as described in the previous chapter, put us in a unique position to uncover previously overlooked immunostimulants in JTT. Our screening of JTT was initiated in 2004 by Dr. Tal H. Hasson (currently at Teva Pharmaceutical, Israel), who was a graduate student at that time [52]. The mRNA biomarkers of monocyte stimulation were searched with gene expression profiling of a monocytic leukemia cell line (THP1 cells) treated with JTT [52]. Many of the observed genes have been associated with monocyte stimulation, such as cytokines, chemokines and cell adhesion molecule. Intercellular adhesion molecule 1

(ICAM1), a well known target of NF- κ B, was then selected as a biomarker of monocyte-stimulation because the induction of this gene was verified in the most reproducible manner in the subsequent real-time PCR analyses [52].

Table II.1. The component herbs and botanical origin of JTT. Shimotsu-to and Shikunshi-to are related Kampo formulations with the herb composition shown on the table.

	Ingredients	Botanical origin	Representative compounds	Weigh ratio
Shimotsu-to	Angelicae Radix	<i>Angelica acutiloba</i>	Ligustilide	3
	Cnidii Rhizoma	<i>Cnidium officinale</i>	Cnidilide, Ligustilide	3
	Paeoniae Radix	<i>Paeonia lactiflora</i>	Paeoniflorin, paeonol	3
	Rehmanniae Radix	<i>Rehmannia glutinosa</i>	Acteoside	3
Shikunshi-to	Ginseng Radix	<i>Panax ginseng</i>	Ginsenoside Ro	3
	Atractylodis Rhizoma	<i>Atractylodes japonica</i>	Atractylon	3
	Holen	<i>Sclerotium of Poria</i> <i>Cocos Wolf</i>	Eruricoic acid	3
	Glycyrrizae Radix	<i>Glycyrrizae uralensis</i>	Glycyrrhizin, formononetin	3
Others	Astragali radix	<i>Astragalus membranaceus</i>	Formononetin	3
	Cinnamoni Cortex	<i>Cinnamomum cassia</i>	Cinnamic acid, cinnamic aldehyde	3

Fractionation of JTT guided by ICAM1 (qRT-PCR) revealed that the monocyte stimulatory activity resided in hydrophobic fractions containing various lipids and steroids. A purification scheme was then established to reproducibly enrich immunostimulatory activity from JTT (Figure II.3) [52]. The study also identified

phytosteryl glycosides as main components in the purified fractions, although it remained to be determined whether these steroids were responsible for the observed activity (Figure II.4).

Although the established purification scheme could reproducibly enrich the monocyte-stimulatory activity from JTT, there remained a possibility that the observed activity was due to endotoxin contamination. To test this possibility, the fractions enriched with monocyte-stimulatory activity were subjected to limulus amoebocyte lysate (LAL) endotoxin test [52]. The test revealed that endotoxin in our fractions was below the detection level of the LAL assay and the observed activity could not be explained by accidental endotoxin contamination [52].

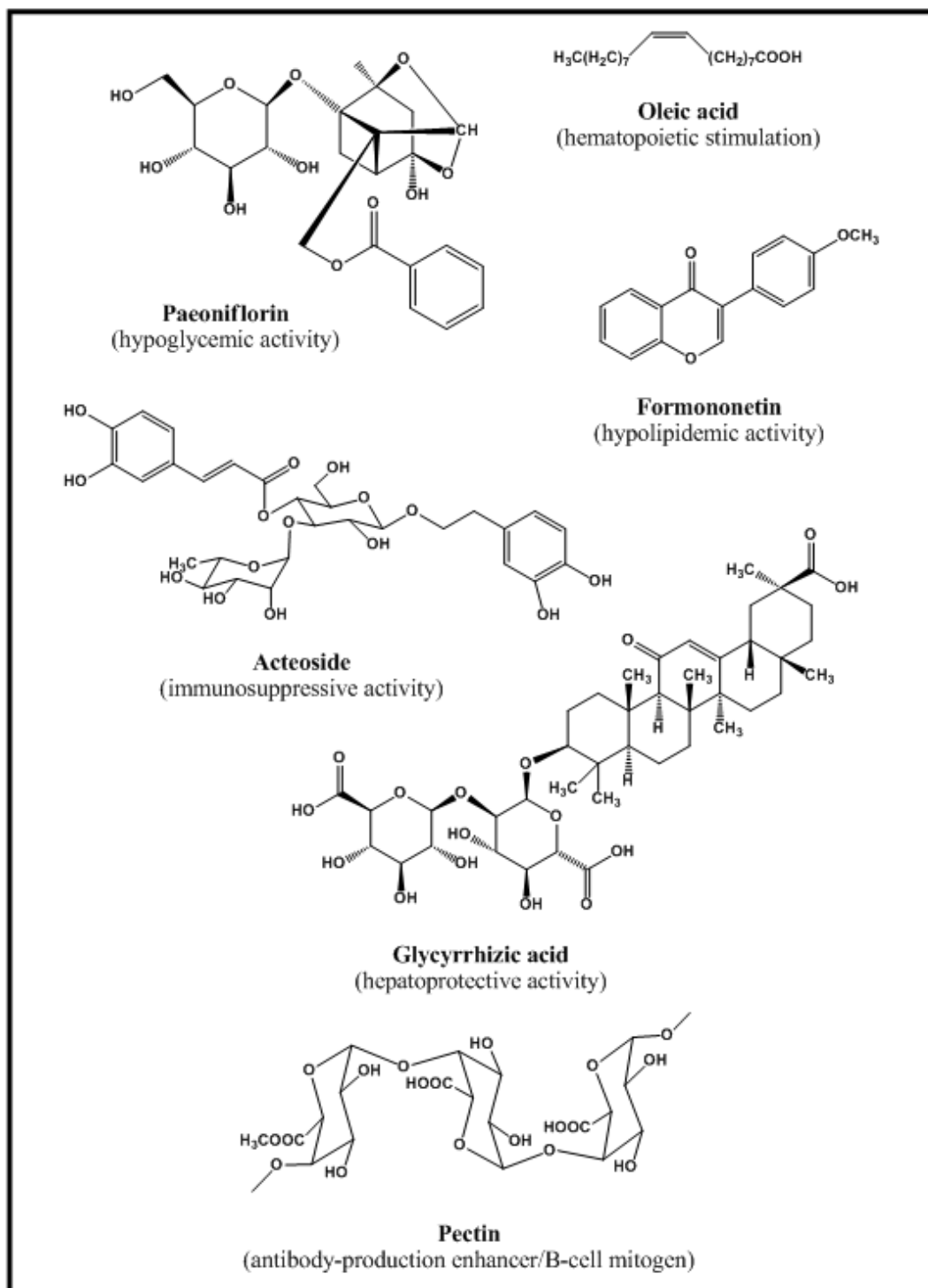


Figure II.2. Structures of putative immunomodulatory components in JTT. The presumed mechanism of each compound is explained in the parentheses.

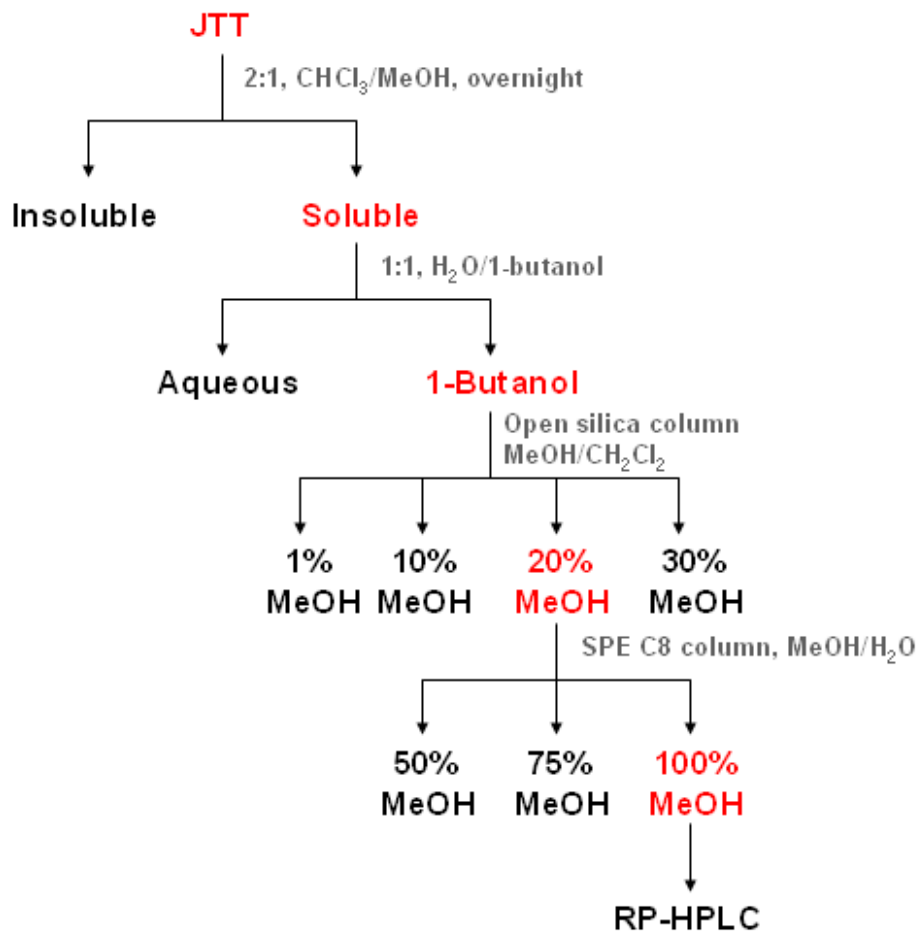


Figure II.3. Purification scheme to obtain fractions with enriched immunostimulatory activity from JTT. ICAM1 qRT-PCR was used to guide the purification. The active fraction in each step is shown in red.

Behind these progresses, however, our screening of JTT has been stymied by many technical challenges. After all, there are reasons why JTT is an “as-yet unapprised” source of immunotherapeutics. A major challenge was the immense heterogeneity of this herbal formulation. JTT is a mixture of ten different herbs (Table II.1), each of which can contain thousands of chemical components. Another challenge was the disappearance of activity during purification. While the ICAM1-guided fractionation was successful, screening with other genes, including SerpinB2, had to be terminated because of the loss of activity at an early stage of fractionation (data not shown). This may have been caused by decomposition of active compounds or separation of synergistic mixtures. The disappearance of activity may also have been caused by poor solubility of active compounds in aqueous solutions. In fact, our previous study revealed that a purified fraction (fraction 2 in Figure II.4) could lose activity through the formation of large nanoparticles (aggregates) in aqueous solutions [52].

These technical problems were further compounded by another challenge which became clear during the establishment of the purification protocol. It turned out that immunostimulatory activity did not correlate with any of the HPLC peaks observed by the photodiode array (PDA) detector. This indicated that the active compounds did not possess strong UV-absorbing chromophores. To overcome this problem, evaporative light scattering detector (ELSD), which was widely considered as the “universal detector” of non-volatile molecules [53-55], was employed in our JTT screening. ELSD indeed enabled the visualization of peaks that could not be detected by PDA (The fractions 1 and 2 in Figure II.4.a), and the purified peaks exhibited the immunostimulatory activity (Figure II.4.c). Since then, our screening had relied on ELSD to isolate the active

compounds. In retrospect, however, this overreliance on ELSD misled the final stage of our screening (*vide infra*).

Additionally, the screening of JTT suffered from low purification yield. From 1 kg of dried JTT powder, only a few hundred micrograms of immunostimulatory fraction, which is still a mixture, can be obtained after RP-HPLC. Although it could be argued that the active compounds are very potent, this low yield seriously stunted the progress of this project.

II. 2. Immunomodulatory activity of phytosteryl glycosides

Our previous studies revealed phytosteryl glycosides (PGs) as the main components of ELSD visible HPLC peaks (The fractions 1 and 2 in Figure II.4). PGs have been suggested to possess immunomodulatory activities, including T-cell stimulation, cytokine induction in NK-cells, and restoration of Th1/Th2 balance [56, 57], although PGs used in those studies were crude lipid mixtures from plant sources. The observed activities, therefore, could be due to PGs or lipids. It was, therefore, important to determine immunomodulatory activities of synthetic PGs devoid of lipid contaminants.

Thus, synthetic β -sitosteryl β -D-glucoside (BSSG) and its structural analogs (Figure II.5) were subjected to the qRT-PCR assay of ICAM1 using THP1 cells. As shown in Figure II.5 (left panel), these compounds did not exhibit significant immunostimulatory activity. The observed results were clearly different from the activities of the materials purified from JTT (Figure II.4.c). As pointed out earlier, however, the apparent lack of activity could have been caused by poor solubility of these

synthetic samples in aqueous buffers. Thus, various attempts, such as sonication, heating, and drug formulation agents (e.g., Cremophor EL), were made to solubilize synthetic PGs prior to the qRT-PCR assay. However, none of these samples reproduced the activities of natural samples (data not shown).

These results, therefore, suggested that PGs were not the immunostimulants of JTT. In retrospect, the results were in agreement with our failed attempts to isolate immunostimulants from the fractions 1 and 2 in Figure II.4, in which these fractions were further separated by reversed phase HPLC and all ELSD visible peaks were subjected to the qRT-PCR assay as well as structural characterization. While the ELSD visible peaks were confirmed to be PGs, none of the isolated steroids exhibited the immunostimulatory activity [52].

Although our results show that PGs are devoid of immunostimulatory activity, it is premature to disregard them completely as inactive components in JTT. It is still remarkable that the immunostimulatory activity was inseparable from PGs even after a long series of purification scheme as depicted in Figure II.3. At the very least, PGs are great chemical markers of immunostimulatory activity, which can be used as surrogate markers during the purification. Moreover, they might be important formulation agents to regulate the delivery and uptake of active compounds. The nanoparticle formation described earlier may be an indication of how PGs modulate biological properties of JTT [52]. Further characterization of such nanoparticles can provide mechanistic insights into the therapeutic actions and potential synergism of JTT. Such studies, however, have to be put on hold until the true immunostimulants are identified.

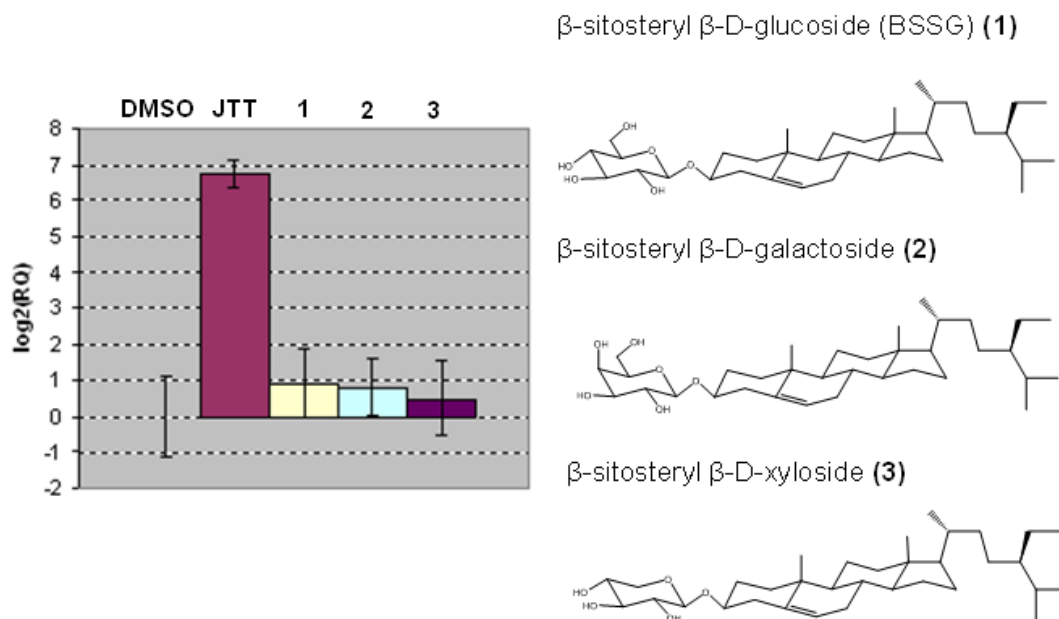


Figure II.5. ICAM1 qRT-PCR analysis of the synthetic PGs: BSSG (1), β -sitosteryl β -D-galactoside (2) and β -sitosteryl β -D-xyloside (3). THP-1 cells were treated with DMSO (negative control), JTT (100 μ g/ml, positive control), 1 (5.5 μ g/ml), 2 (5.5 μ g/ml) and 3 (5.5 μ g/ml) for 4 h. The structures of the three synthetic PGs are shown on the right panel.

II. 3. Uncovering “hidden” immunostimulants in JTT

At this point, our overreliance on the ELSD was called into question. There was a possibility that the immunostimulants in JTT were not readily detected by ELSD because of their small quantities. Ms. Anna Takaoka in our group and I, therefore, conducted a large scale preparation with 3 kg of dried JTT powder and obtained the 100% methanol fraction from the solid phase extraction (SPE) C₈ column (Figure II.3). This fraction was then subjected to RP-HPLC (C₁₈, 100% methanol isocratic). Of our particular interest was the chromatographic region between 4 and 11.5 min that were devoid of ELSD peaks

in our previous studies. Probably because of the large scale preparation, ELSD detected several small peaks between 4 and 11.5 min, although they were still much smaller than the phytosteryl glycoside peak at 13 min. Two large fractions, namely, subfraction 1 (4-8 minutes) and subfraction 2 (8-11.5 minutes) were first obtained to narrow down the region where the activity was eluted (Figure II.6). The ICAM-1 qRT-PCR assay of these collections revealed that subfraction 2 retained significant immunostimulatory activity.

Therefore, the region between 8 and 11.5 min was further divided into four smaller fractions, namely, fractions A-D, which roughly corresponded to the small ELSD peaks in this region (Figure II.7). ICAM1 qRT-PCR revealed that the activity was eluted as a broad peak corresponding to fractions B-D (Figure II.7). Preliminary analyses of these fractions by ¹H-NMR and ESI-MS indicated that all of these fractions were still mixtures of several compounds (data not shown). Among the three, however, fraction C exhibited the simplest ESI-MS profile (Figure II.8). In addition, the sample quantity (~1.5 mg) appeared sufficient to conduct comprehensive structural characterization. We, therefore, focused our effort on the identification of molecular species in fraction C.

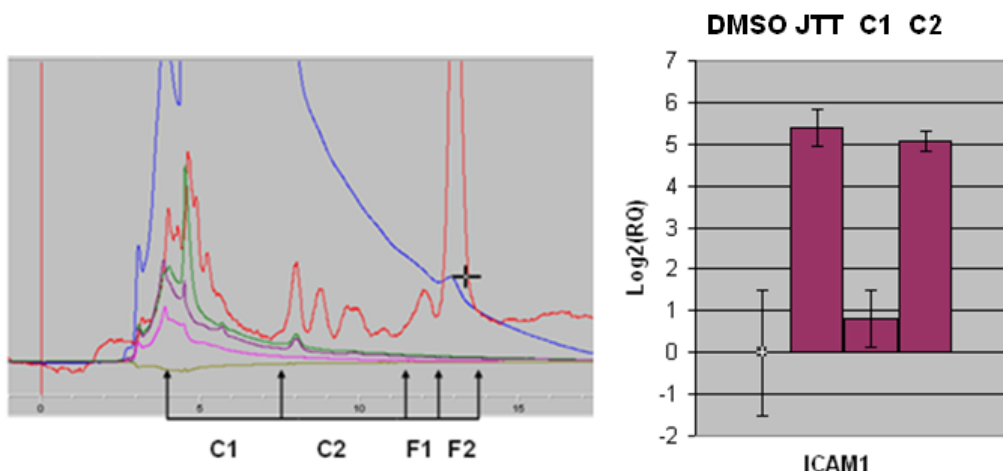


Figure II.6. Search for immunostimulants in the ELSD “invisible” region. **Left:** HPLC chromatograms obtained with RP-HPLC (C_{18} , 100% MeOH isocratic elution) equipped with ELSD and PDA detector: ELSD (red); UV220 (blue); UV254 (green); UV280 (purple); UV350 (pink); UV554 (olive green). **Right:** ICAM1 qRT-PCR of obtained fractions. C1 and C2 stand for subfraction 1 (4-8 min) and subfraction 2 (8-11.5 min), respectively. F1 and F2 are the PGs fractions.

ESI-MS analysis revealed a compound with a molecular formula of $C_{21}H_{42}O_4$ (Exact mass 358.3053) as indicated by the most conspicuous ion at m/z 381.2972 $[M+Na]^+$ (calcd 381.2975) and an accompanying ion at m/z 359.3151 $[M+H]^+$ (calcd 359.3156) (Figure II.8.A). This formula coincided with monostearin, a simple glycerolipid with one acyl chain (see the inset of Figure II.8.A). 1H -NMR also suggested that the major component of this fraction was a lipid with a simple framework like monostearin (Figure II.8.B). Since monostearin was commercially available, we obtained the commercial sample and examined its 1H -NMR (Figure II.8.C). The 1H -NMR comparison showed clear match between the signals of monostearin and those of the major component of fraction C. Thus, these results indicated that the two were indeed the

same compounds. However, ICAM1 qRT-PCR assay did not detect immunostimulatory activity of monostearin (data not shown).

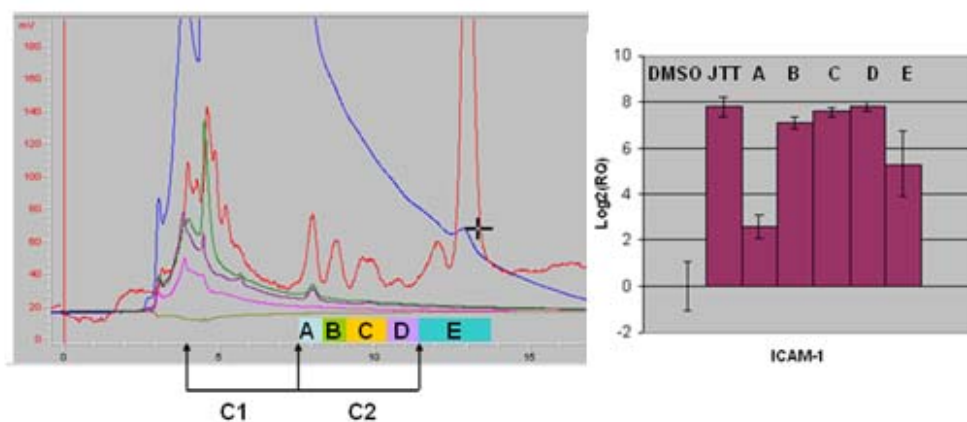


Figure II.7. Purification of the hidden immunostimulants from JTT. **Left:** HPLC chromatograms obtained with RP-HPLC (C₁₈, 100% MeOH isocratic elution) equipped with ELSD and PDA detector: ELSD (red); UV220 (blue); UV254 (green); UV280 (purple); UV350 (pink); UV554 (olive green). C1 and C2 are the subfractions 1 and 2 respectively as shown in figure II.6. **Right:** ICAM1 qRT-PCR of fractions A-E. Fraction E represents the PGs fraction.

Our attention was then turned to the minor components in fraction C. ESI-MS suggested the presence of a minor component that gave an ion at m/z 736.5328 (Figure II.8.A). This compound, however, was not clearly visible on ¹H-NMR (Figure II.8.B). Since it was difficult to conduct spectroscopic analysis in the presence of the major component (monostearin), fraction C was subjected to microscale acetylation reaction, which alters chromatographic profiles of individual components. Acetylated compounds were then separated by silica gel column chromatography. One product that did not appear to be the diacetate of monostearin (based on TLC) was then purified and subjected to spectroscopic analyses.

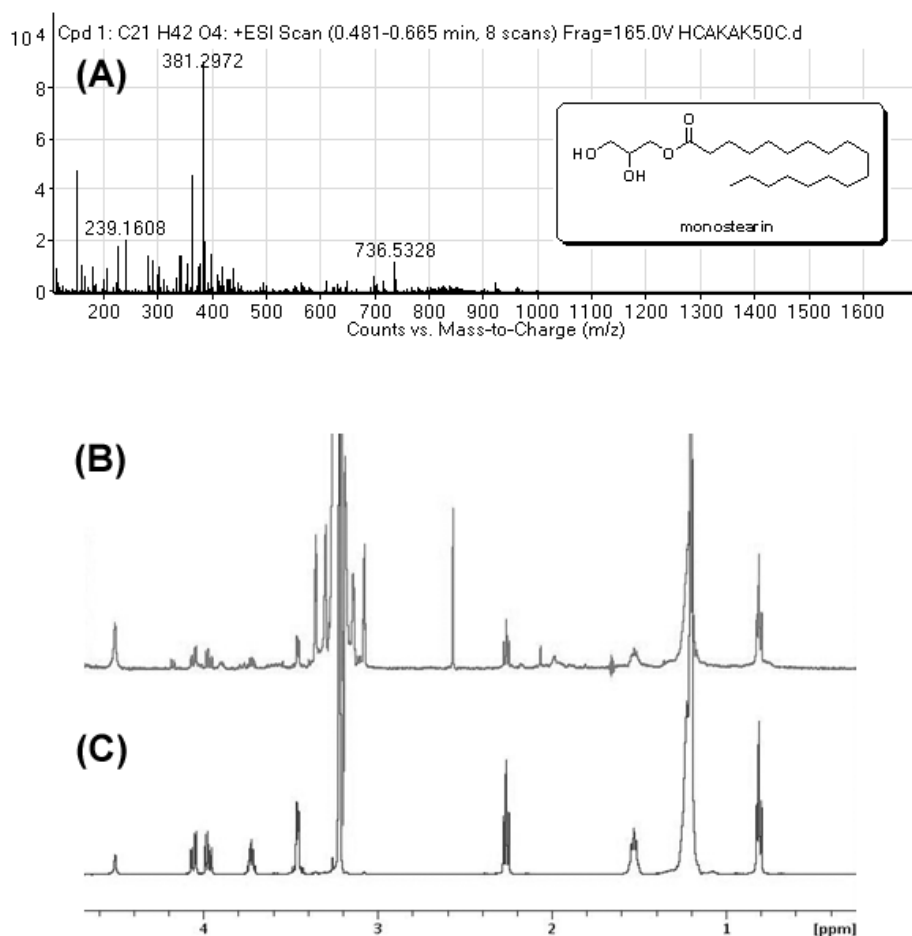


Figure II.8. Spectroscopic characterization of fraction C. (A) ESI-MS (positive mode). The structure of monostearin is shown in the inset. (B) ¹H-NMR of fraction C (methanol-*d*₄). (C) ¹H-NMR of monostearin (commercial sample) (methanol-*d*₄).

The molecular formula of this acetylated sample was determined to be C₅₂H₈₇NO₁₅ (Exact mass: 965.6076) based on the observed ESI-MS ions at *m/z* 966.6145 [M+H]⁺ (calcd 966.6148) and 983.6413 [M+NH₄]⁺ (calcd 983.6414) (Figure II.9). Analyses of ¹H, ¹³C, DEPT, and HSQC (Appendices A-D) suggested the presence of one sugar, double bonds, six acetates, and a ceramide framework. Subsequent COSY and HMBC analyses indeed led to the framework of monoglycosylceramide (cerebroside)

(Figure II.10 and Appendices E and F). The COSY and HMBC analyses also revealed two olefinic fragments, two propyl fragments (Figure II.10.c), and a number of methylenes, many of which are indistinguishable on NMR.

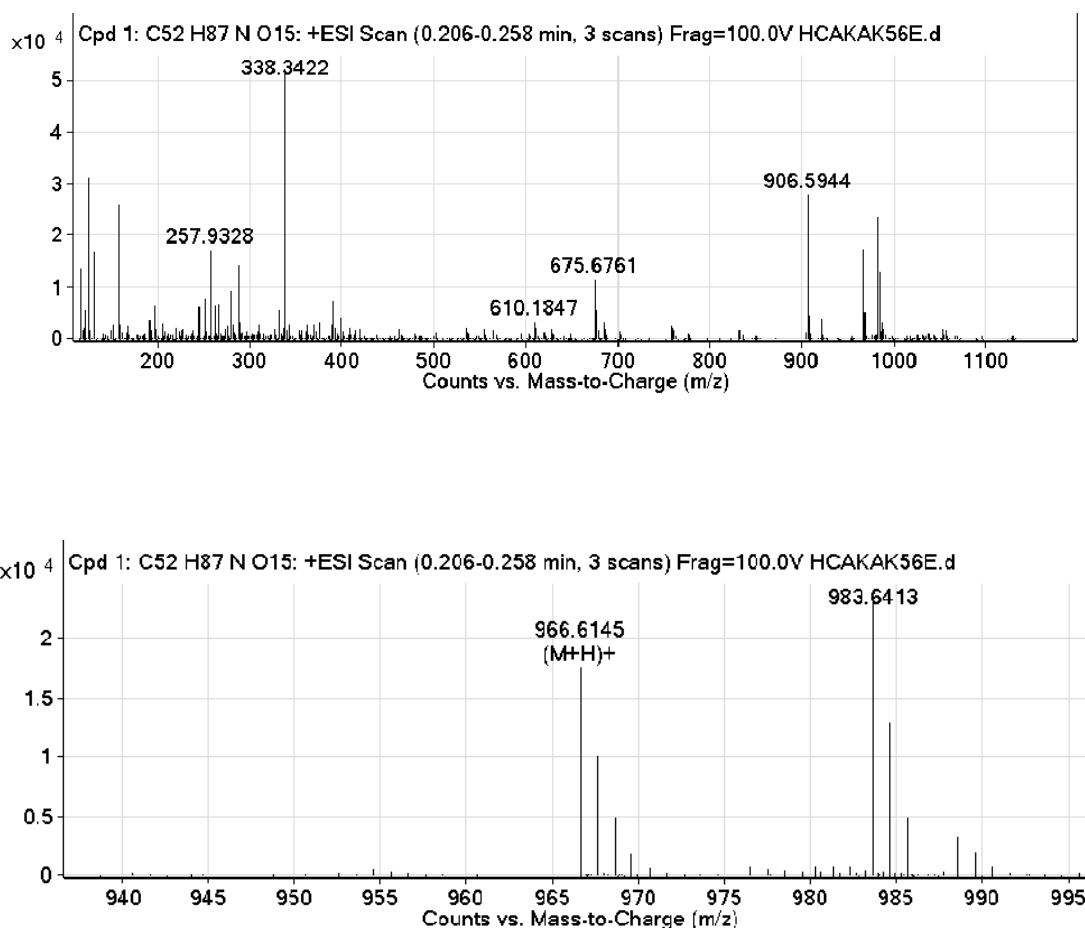


Figure II.9. ESI-MS (positive mode) of an acetylation product from fraction C. **Top:** The entire ESI-MS spectrum. **Bottom:** Zoomed spectrum.

The structure of the sugar was deduced to be a 2'',3'',4'',6''-tetraacetate of β -glucoside based on the proton and carbon chemical shifts [58] as well as the large coupling constants (\sim 8-10 Hz) of protons on the pyranose ring moiety, namely, 1''-H (anomeric, *d*, 8.0 Hz), 2''-H (*dd*, 9.5, 8.0Hz), 3''-H (*dd*, 9.5, 9.6 Hz), 4''-H (*dd*, 9.8, 9.5

Hz), and 5''-H (*ddd*, 9.8, 4.5, 3.8 Hz). In addition, the *trans* configuration of the C-4/C-5 double bond was confirmed based on the characteristic large coupling constant between 4-H and 5-H (15.4 Hz) as well as the ^{13}C chemical shift of C-6 (32.6 ppm): It is well known that the carbons adjacent to a *trans*-double bond appear at ~ 32 ppm, whereas those next to a *cis*-double bond are observed at ~ 27 ppm [59].

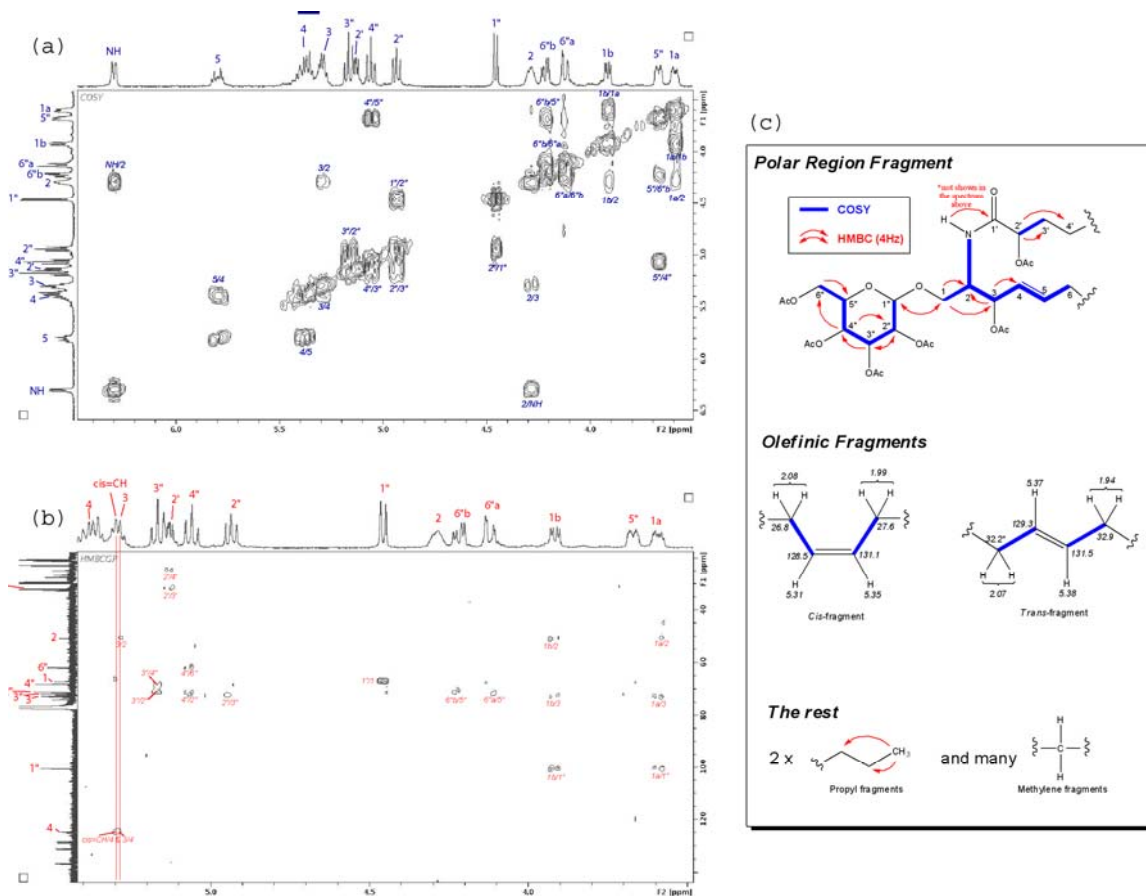


Figure II.10. COSY and HMBC analyses of the acetylated product from fraction C. (a) Magnified carbinol/olefin/amide region of COSY spectrum. Observed cross peaks were used to assemble carbons in the sugar moiety and the polar regions of ceramide. (b) Magnified HMBC carbinol/olefin/amide region of HMBC (4Hz). Observed cross peaks were used to verify COSY assignments as well as to determine the linkage site between the sugar and ceramide. (c) Assembled partial structure (planar).

At this point, it became clear that the acetate sample was a mixture of two *cis/trans* configurational isomers for the following reasons. The double bond equivalency (DBE) of this acetate was calculated to be ten (molecular formula $C_{52}H_{87}NO_{15}$). Nine of them were accounted for by six acetate carbonyls, one amide bond, one pyranose ring (glucose) and the C-4/C-5 double bond. There remained, however, two fragments with double bonds (*cis* and *trans*) (Figure II.10.C). In fact, the NMR signals associated with these two fragments were consistently weaker than the signals of other parts. Taken together, the acetate sample appeared to be a mixture of two configurational isomers. The positions of the double bonds could also be different. Attempts to separate the two isomers, however, have not been successful so far, although numerous conditions have been examined.

In order to gain further structural information, the acetate sample was further characterized with ESI MS/MS fragmentation. The $[M+H]^+$ ion at m/z 966.6145 was fragmented to give major ions at m/z 906.5922, 558.4872, 331.1028, and 262.2533. The observation of a fragment ion at m/z 262.2533 indicated the formation of $C_{18}H_{32}N^+$ (Exact mass 262.2529). This ion could be explained if the remaining one double bond was located in the sphingosine backbone instead of the 2'-hydroxylated acyl chain. Figure II.11 shows a sequence of fragmentations consistent with the observed ions.

Taken together, spectroscopic data of the acetylated sample suggest that the minor components in fraction C are a mixture of soya cerebroside I and II [60, 61] or their close structural isomers with respect to the double bond position and the configuration of 2'-OH (Figure II.12). In fact, the ESI spectrum of fraction C contains an ion at m/z

736.5328 (Figure II.8.A), which is consistent with the sodium adducts (m/z 736.5334 calcd for $C_{40}H_{75}NNaO_9^+$) of these isomeric compounds.

Further structural characterization of these cerebroside from JTT as well as comparison with authentic soya cerebroside is currently underway in our group. These studies are expected to conclusively determine the structures of these compounds.

Meanwhile, immunostimulatory activities of commercially available monoglycosylceramide isomers (Figure II.13; soya cerebroside I, **1**, and β -galactosylceramides (mixture), **2**) have been characterized with the qRT-PCR of ICAM1 using THP1 cells. Soya cerebroside I exhibited a modest induction of ICAM1 in THP1 cells. Although the activity of soya cerebroside I was much weaker than the activity of fraction C, the observation of this activity was notable because, after a series of disappointments with synthetic PGs and commercial monostearin, it was the first time to observe monocyte-stimulatory activity of a purified compound in our assay. On the other hand, β -galactosylceramides (mixture) did not exhibit any activity, although they are structurally very close to soya cerebroside I (Figure II. 13). Collectively, these results indicated that the mixture of cerebroside in fraction C contributed to the immunostimulatory activity of JTT.

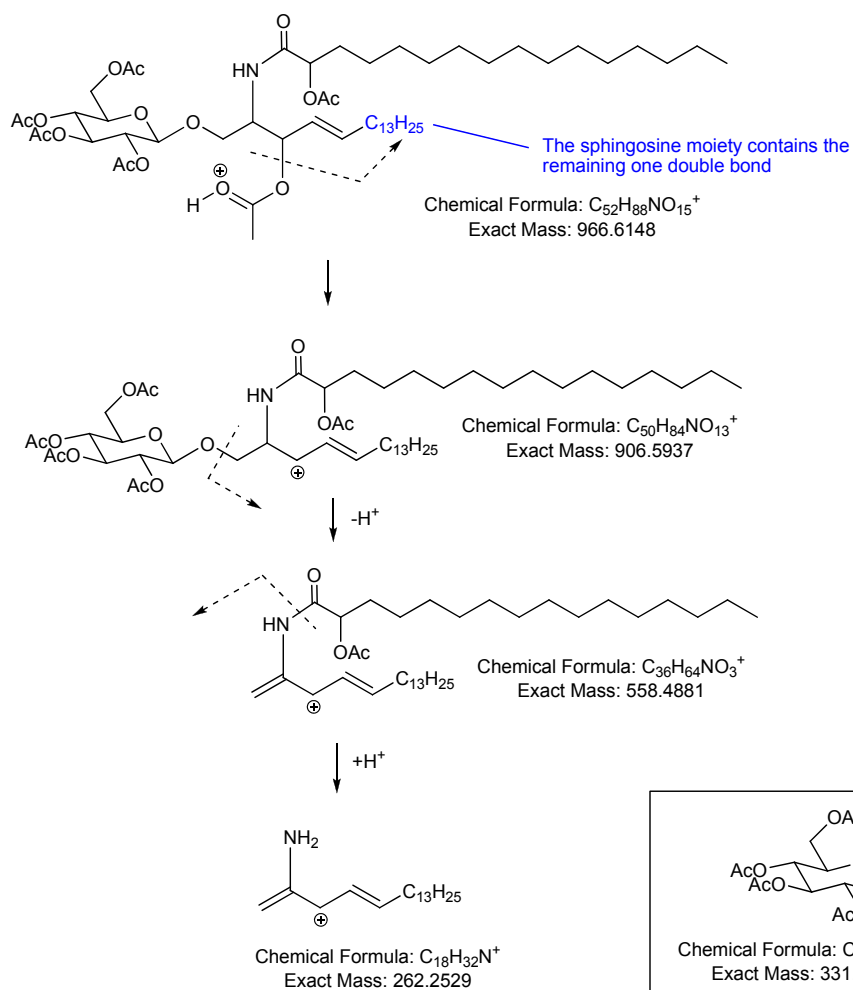
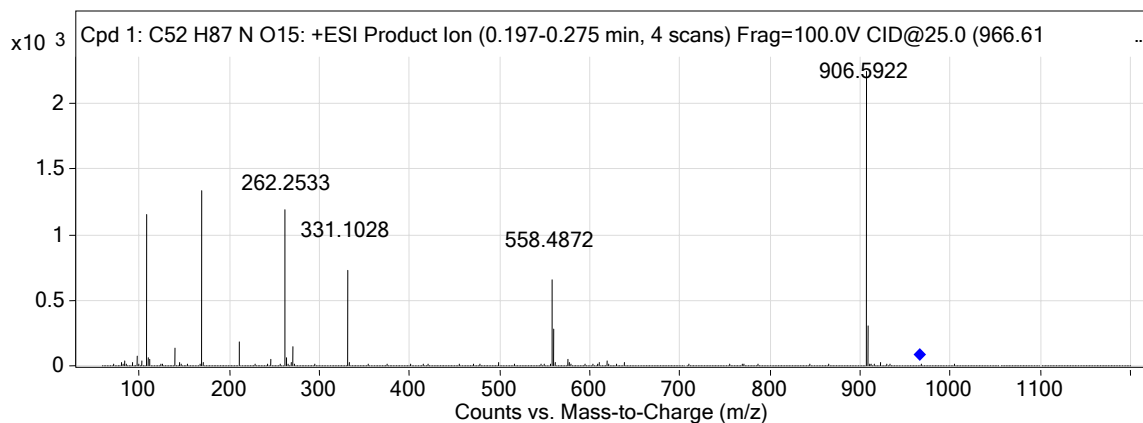


Figure II.11. ESI MS/MS (positive mode) fragmentation analysis of the acetylated sample. **Top:** ESI MS/MS spectrum. **Bottom:** A possible sequence of fragmentations. **In the box:** A fragment structure which accounts for an ion at m/z 331.1028.

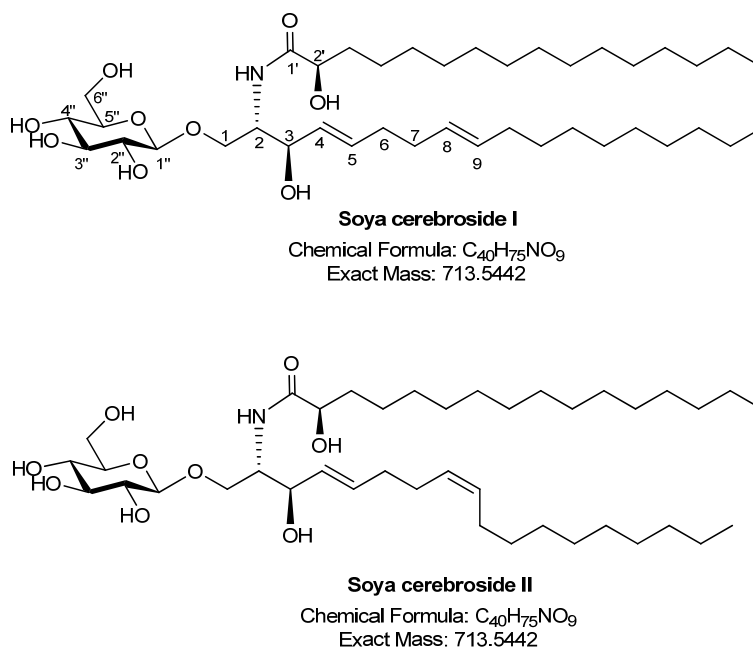


Figure II.12. Structures of soya cerebrosides I and II. Soya cerebroside I is the major isomer purified from soy beans.

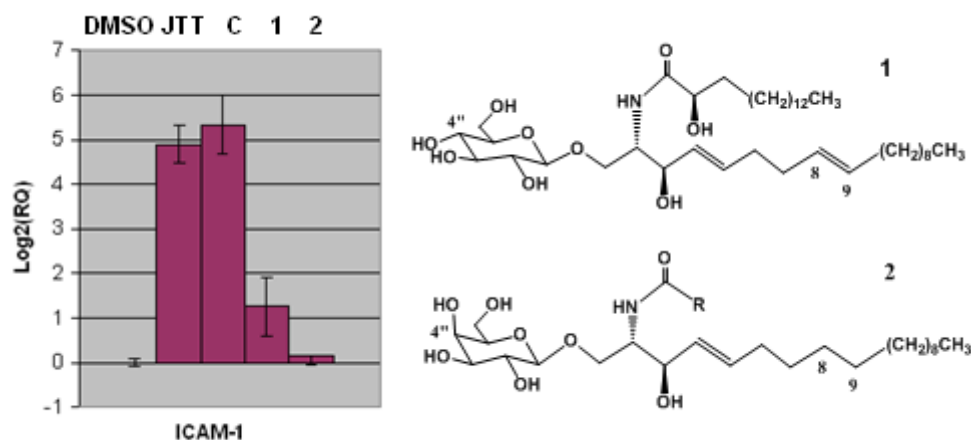


Figure II.13. ICAM-1 qRT-PCR analysis of Fraction C, soya-cerebroside I (1) and β -galactosylceramides (mixture) (2). DMSO (0.1%, vehicle control); JTT (100 μ g/ml, positive control); C: Fraction C (5 μ g/ml); 1: soya-cerebroside I (5 μ g/ml); 2: β -galactosylceramides (5 μ g/ml). Minimum duplicate experiments were performed for each condition.

II.4. Discussion

Biomarker-guided screening of JTT led to the identification of β -glucosylceramides (cerebrosides) as the first group of monocyte-stimulants in this herbal formulation. Although their exact chemical structures remain to be determined, the identification of cerebrosides as a group of active components in JTT offers explanations for many technical challenges we faced throughout this screening.

Amphiphilic lipids, like cerebrosides, are particularly difficult groups of compounds to purify from natural sources. The polar head groups dominate the elution profiles on normal phase chromatography, making it very challenging to differentiate subtle structural differences among these lipids. On the other hand, the large aliphatic chains interact with the reversed phase resins so strongly that it is difficult to attain fine separation of structural isomers, such as configurational isomers of isolated double bonds in the middle of aliphatic chains. As a result, many lipids from natural sources, including cerebrosides, are often characterized as mixtures through mass spectrometric means [62-64].

The identification of cerebrosides may enable us to improve the purification scheme of monocyte-stimulants from JTT. Cerebrosides have been extracted with aqueous methanol or ethanol [65-67], which is much more polar than our extraction condition. Likewise, several different partition conditions, such as ethyl acetate/water 1:1 [67, 68], have been used to enrich this class of compounds. Thus, it may be possible to further optimize the purification yields by examining various literature protocols for cerebrosides.

The minute quantity of these cerebroside in JTT was another source of problems that made our screening challenging. The $^1\text{H-NMR}$ spectrum of Fraction C (~1.5 mg) (Figure II.8.B) suggests that the actual amounts of these cerebroside was probably in the order of several hundred micrograms. Given the fact that fraction C was purified from three kilograms of JTT, it was, in retrospect, an extremely challenging task to purify minuscule quantities of cerebroside from the immensely heterogeneous mixtures of compounds from ten different herbs. The minute quantities of these cerebroside also made it difficult to detect them during purification. Although the cerebroside have an amide bond and two double bonds, the small amounts of these samples as well as the background UV absorption by the other compounds made it hard to observe them with the PDA detector. ELSD detector also failed to detect the cerebroside in JTT probably because of their small amounts.

Here, it is also important to note a technical limitation of ELSD, which is generally considered as a “universal detector” of non-volatile compounds [53-55]. Although ELSD failed to detect the cerebroside from JTT, it was able to detect comparable amounts (a few hundred micrograms) of steroid glycoside (The fraction 1 in Figure II.4.a) [52]. ELSD detects light scattered by molecular aggregates in HPLC eluent, which, upon entering ELSD, is dried by heat and nebulizing nitrogen gas. In retrospect, it is not surprising that ELSD is more sensitive to the compounds that are prone to aggregate, such as steroids. When unknown mixtures of compounds are analyzed, it is important to be aware of this limitation of ELSD.

The identification of the immunostimulatory cerebroside from JTT provides molecular and structural bases to understand the biological activity of JTT. It is now

possible to develop new hypotheses that can account for the distinct biological difference between fraction C and soya-cerebroside I. One possible cause of the difference is the structural differences between JTT cerebroside and soya-cerebroside I. The position of the isolated double bond, which is between C-8 and C-9 in soya-cerebroside I (Figure II.12), may be different in the JTT cerebroside. In addition, the *cis*-configuration of this double bond, as observed in one of the JTT cerebroside may be important for the potency: Soya-cerebroside I has the *trans*-configuration. Our finding sets a stage for structure-activity relationship (SAR) studies to define the structural elements important for the observed monocyte-stimulatory activity.

There also is a possibility that fraction C still contained as-yet uncharacterized but more potent monocyte-stimulants. The ¹H-NMR spectrum of fraction C, however, did not reveal compounds other than monostearin (major) and the JTT cerebroside (minor) (Figure II.8.B). ESI-MS spectrum of Fraction C (Figure II.8.A) also mainly showed ions corresponding to monostearin and JTT cerebroside. Although there were several unidentified ions, most of them are smaller than the monostearin ions and possibly fragments of either monostearin or JTT cerebroside.

Synergism is another possibility that can now be tested with the identified constituents in fraction C. For example, monostearin may play some roles as a formulation agent to improve the solubility of cerebroside, even though it by itself does not possess any monocyte-stimulatory activity. It is now possible to prepare defined mixtures of monostearin and cerebroside and quantitatively evaluate the potential synergism among these compounds.

In addition, as mentioned earlier in this chapter, PGs have been identified as the major components of fraction E (Figure II. 7), exhibiting moderate immunostimulatory activity [52]. Although our current study conclusively determined that PGs were not the monocyte-stimulatory components, there remains a possibility that PGs still play some important roles as formulation agents in JTT. In fact, “PG-rich” fraction E has been shown to form various nanoparticles in a solvent dependent manner, and the immunostimulatory activity correlated with the size of particles [52]. Thus, it is still important to further characterize the possible roles of PGs in JTT.

Identification of β -glucosylceramides from JTT may also have broader medical implications. Possible immunomodulatory roles of β -glucosylceramides have long been suggested in the studies of Gaucher disease, which is caused by the deficiency of glucocerebrosidase (the enzyme that cleaves the β -glucosidic linkage of β -glucosylceramides) [69]. The accumulation of β -glucosylceramide causes the pathological symptoms of Gaucher disease, including enlarged spleen and swelling of lymph nodes. On the other hand, the enzyme replacement therapy (ERT) of Gaucher disease, which causes the depletion of β -glucosylceramide, has been linked to higher incidence of various diseases, including cancer [70, 71]. Our current finding, when combined with such epidemiological associations, underscores the importance of further studies to characterize immunomodulatory properties of β -glucosylceramides. This is an important point especially because β -glucosylceramides have been generally considered as less potent analogs of α -galactosylceramides because of preclinical SAR studies during the development of KRN7000 [31, 72-74]. Although α -galactosylceramides exhibit more potent immunostimulatory activities in experimental animal models, β -glucosylceramides

might be the group of compounds with clinical utility. Perhaps, there is a reason why β -glucosylceramides have been kept as immunostimulants in the oriental herbal medicine for thousands of years.

II.5 Materials and Methods

Materials: All solvents for purification were in the HPLC grade and were purchased from VWR and Fisher Scientific. The Juzen-taiho-to (JTT) formulation was purchased from Honso Pharmaceutical Co. (Nagoya, Japan) as a dry water extract. Unless specified otherwise, all other chemicals and reagents were obtained through Fisher Scientific and used without further purification. Reverse phase Extract-CleanTM SPE C₈ 200 mg/4 mL columns were purchased from Alltech[®]. HPLC analysis and purification were carried on an Agilent 1100 Series, using a ChemStation operating system. HPLC was equipped to an Agilent 1100 photodiode array detector and an Evaporative Laser Light Scattering detector (ELSD) model 800 (Alltech[®]). HPLC columns used in this study were Econosil C₁₈ 10 × 250 mm semi-preparative column (Alltech[®]) and Eclipse-XD8 C₈ 4.6 × 150 mm analytical column (Agilent). NMR spectra were recorded on a Bruker 500 MHz instrument.

Cell culture: THP-1 cells were purchased from American Type Culture Collection (ATCC). Cells were propagated in RPMI-1640 media containing 25mM HEPES and L-Glutamine (HyClone), 10% Fetal Bovine Serum (Fisher), 1% Penicillin Streptomycin and Amphotericin B (VWR) and 0.005 mM β -mercaptoethanol. Cells were maintained in a 37°C humidified 5% CO₂ incubator.

Cell treatment and lysis: THP-1 cells were split on the day before the treatment at the concentration of 1×10^6 cells in 10ml of media or 0.2×10^6 cells in 2 ml media. After 24 hours, THP1 cells were treated with either JTT (100 $\mu\text{g}/\text{ml}$), fractions or DMSO vehicle control for 4 h in a 37°C humidified 5% CO₂ incubator. The fractions (dry) for the treatment were quantified with analytical scale and then dissolved in biological grade DMSO for the treatment. Final DMSO concentration for each treatment did not exceed 0.5%. The 4 h time point was used to detect the early (primary) transcriptional events, which are less susceptible to experimental errors compared to later (secondary) transcriptional responses. After the 4 h incubation, the cell suspension was transferred to a 15 ml falcon tube and centrifuged at 1,300 rpm for 5 minutes. The medium was aspirated out. The cell pellet was lysed with 350 μl of TRK Lysis buffer (containing 1% β -mercaptoethanol). The cell lysate was then loaded to an Omega[®] Homogenizer column (Omega Bio-Tek) and centrifuged at 13,200 rpm for two minutes. The homogenized lysate was either stored at -80°C or immediately processed for RNA purification.

RNA purification and quantification: Total RNA was purified using a total RNA kit (Omega Bio-Tek). 70% ethanol (350 μl) was added to the cell lysate (350 μl) and the mixture was loaded into a HiBind[®] RNA mini column. The mixture was centrifuged at 13,200 rpm for 1 minute and the flow through was discarded. 500 μl of RW1 buffer (first wash buffer of RNA kit) were added to the column and centrifuged at 13,200 rpm for 1 minute. The flow through was discarded. The column was then washed twice with 500 μl of RW2 buffer (second wash buffer), centrifuged for 1 minute at 13,200 rpm and the flow through was discarded. The column was centrifuged for additional 2 minutes in order to

dry up the membrane. Then the HiBind[®] RNA mini column was placed in a new collection tube and 25 μ l of RNase-free water was added. The column was incubated at room temperature for 5 minutes and then centrifuged at 13,200 rpm for 1 minute. The resulting RNA sample was quantified using UV absorbance at 260nm. Samples with the 260nm/280nm ratio \sim 1.8 or higher were used for subsequent studies. Purified RNA samples were used for cDNA synthesis.

Reverse Transcription for qRT-PCR: The RNA yields were between 0.2-1 μ g from 0.2×10^6 cells and 3.5-4 μ g from 1×10^6 cells. For each RT reaction, the following materials were mixed: 1 μ l of 10 mM dNTP mixture, 2 μ l of Random primers (0.3 μ g/ μ l, Invitrogen), and 13 μ l of purified RNA in RNase-free water in order to have total volume of the mixture equal to 16 μ l. The mixture was incubated at 70 $^{\circ}$ C for 3 minutes in a thermocycler and then cooled down to 4 $^{\circ}$ C for 1 minute. After that, the following reagents were added to each RT mixture: 4 μ l of M-MLV RT 5 \times buffer (Promega) and 0.5 μ l of 200 U/ μ l M-MLV Reverse Transcriptase (Promega). The mixture was then incubated at 42 $^{\circ}$ C for 1 hour followed by 95 $^{\circ}$ C for 10 minutes and then 37 $^{\circ}$ C for 20 minutes in order to eliminate any RNA-DNA hybrids. RT reactions from 0.2-1 μ g of RNA were diluted with 30 μ l of RNase free water, whereas RT reactions ranging from 3.5-4.0 μ g were diluted with 130 μ l of DEPC water. Synthesized cDNA was either immediately processed for real-time PCR analysis, or stored at -20 $^{\circ}$ C.

Real-Time PCR: Taqman[®] Gene Expression assays (Applied Biosystems) were carried out on Applied Biosystems 7500 Real-Time PCR system using pre-optimized assays for selected genes and GAPDH (endogenous control). Amplification products were

monitored using FAM-MGB probe. For ICAM-1 and GAPDH the following reagents were mixed: 10 μ l (per reaction) of 2 \times Taqman[®] Universal PCR master mix and 1 μ l (per reaction) of 20X probe. 9 μ l of diluted cDNA were added to the appropriate PCR tubes for total PCR mixture volume of 20 μ l. The PCR experiment is divided into three stages: (1) 2 minutes at 50 °C (one cycle), (2) 10 minutes at 95 °C (one cycle) and (3) 15 seconds at 95 °C followed by an hour at 60 °C (40 cycles). Cycle threshold value (CT) was set at 0.2 and data was collected at the beginning of the linear phase. The $\Delta\Delta$ CT was employed to quantify the selected genes induction. The raw data were first normalized by the endogenous control (GAPDH) for individual samples. Then the relative quantification (RQ) values, i.e. the ratio, were obtained by comparing the normalized data against the DMSO vehicle control. At least duplicate experiments were carried out for each sample.

Extraction and purification of JTT: 400 grams of JTT sample was extracted with 3 L of chloroform/methanol (2:1) mixture. The mixture was stirred for 24 hours at room temperature, in a covered 5 L-round bottom flask. Vacuum paper filtration was the next step in order to remove the entire insoluble fraction. The soluble fraction was dried *in vacuo* of which 34 g was recovered. The recovered fraction was dissolved in 250 mL of 1-butanol. The solution was transferred to a 1 L separatory funnel and 250 mL of Millipore water was added. The mixture were shaken and vented 3 times and the layers were allowed to separate. Both organic and aqueous layers were collected into separate flasks. The 1-butanol fraction layer was dried *in vacuo* and 18 g were recovered. The dried extract was re-dissolved in a minimum amount of methanol and divided to 3 portions of approximately 6 g each, to which silica gel 60 was added. The entire sample

was dried again in vacuo until silica was fully dry. Each one of the portions was fractionated separately on a silica open column. A 4.6 cm i.d × 40 cm column was prepared with 120 g of silica bedding. The column was dry packed and washed with dichloromethane. The sample was eluted with step gradient of 1% MeOH, 10% MeOH, 20% MeOH, and 30% MeOH in CH₂Cl₂. 500 mL fractions were collected. All fractions were dried in vacuo and the 20% fraction gave 700 mg of dried material. The dried 20% fraction was divided to 120 mg portions. Each one of the portions was dissolved in 400 µl of 50% MeOH. To an Alltech Extract-Clean SPE C-8 (containing 200 mg of resin) 200 µl of the 20% fraction was added. The sample was eluted with 50% MeOH, 75% MeOH, and 100% MeOH. Further purification was carried on an Agilent 1100 series HPLC.

HPLC - The reversed phase HPLC purification was carried out using Agilent 1100 series HPLC equipped with photo-diode array detector (PDA) and Evaporative Light Scattering Detector (ELSD). All samples were dissolved in biological grade DMSO and filtered through 0.22 µm PTFE membrane filters (Whatman[®]). The reverse phase purification was carried on an Alltech Econosil C₁₈ 10 mm × 250 mm with operating temperature 26°C. The mobile phase used was 100% MeOH. Isocratic elution was carried out over a period of 20 minutes with a flow rate of 3 mL/min. Injection volume was 80 µl (into a 200 µl loop), which contained 0.7 mg of sample. UV signals were collected at 220 nm, 280 nm, 254 nm, 350 nm. The data were recorded and processed using Agilent ChemStation software. ELSD analysis was performed on an Alltech ELSD 800 detector, in which nitrogen in a drift temperature of 43°C, nebulizer pressure of 4.4 Bar. From the previous purification fractions A-F have been collected.

NMR: NMR spectra of acetylated fraction C (1.2 mg) in CDCl_3 were measured by Brüker Avance 500MHz Spectrometer equipped with a dual [^{13}C , ^1H] CryoProbe. Data were acquired and processed with the Brüker XWIN-NMR software package. ^1H -NMR spectra was collected with a total of 64 scans, H-H COSY with 2 scans, ^{13}C -NMR and DEPT with 7000 scans, HMBC with 60 scans and HSQC with 90 scans.

Acetylation of Fraction C: Fraction C (1mg) was dissolved in pyridine (1ml) and the mixture was treated with acetic anhydride (200 μg) and left overnight. The mixture was then diluted with 1 ml of H_2O and extracted with dichloromethane. Dried sample was then purified with silica gel open column (0.5 mm i.d. \times 30 mm).

II. 6 References

1. Society, A.C., Cancer facts and figures 2009. *American Cancer Society*, 2009.
2. Goldman, J.M., Treatment strategies for CML. *Best Pract. Res. Clin. Haematol.*, 2009. 22(3): p. 303-13.
3. Schmitt, F., HER2+ breast cancer: how to evaluate? *Adv. Ther.*, 2009. 26 (Suppl. 1): p. S1-8.
4. Garnock-Jones, K.P., Keating, G. M., Scott, L. G., Trastuzumab: A review of its use as adjuvant treatment in human epidermal growth factor receptor 2 (HER2)-positive early breast cancer. *Drugs*, 2010. 70(2): p. 215-39.
5. Waller, C.F., Imatinib mesylate. *Recent Results Cancer Res.*, 2010. 184: p. 3-20.
6. Dizon, D.S., Treatment options for advanced endometrial carcinoma. *Gynecol. Oncol.*, 2010. 117(2): p. 373-81.
7. Bookman, M.A., Trials with impact on clinical management: first line. *Int. J. Gynecol. Cancer*, 2009. 19(Suppl. 2): p. S55-62.
8. Marchetti, C., Pisano, C., Facchini, G., Bruni, G. S., Magazzino, F. P., Losito, S., Pignata, S., First-line treatment of advanced ovarian cancer: current research and perspectives. *Expert Rev. Anticancer Ther.*, 2010. 10(1): p. 47-60.
9. Merry, C., Fu, K., Wang, J., Yeh, I. J., Zhang, Y., Targeting the checkpoint kinase Chk1 in cancer therapy. *Cell Cycle*, 2010. 9 (2): p. 279-83.
10. Saad, F., Lipton, A., SRC kinase inhibition: targeting bone metastases and tumor growth in prostate and breast cancer. *Cancer Treat. Rev.*, 2010. 36(2): p. 177084.
11. Tan, A., Xia, N., Gao, F., Mo, Z., Cao, Y., Angiogenesis-inhibitors for metastatic thyroid cancer. *Cochrane Database Syst. Rev.*, 2010. 17(3).
12. Ganjoo, K., Jacobs, C., Antiangiogenesis agents in the treatment of soft tissue sarcomas. *Cancer*, 2010. 16(5): p. 1177-83.
13. Pathania, D., Millard, M., Neamati, N., Opportunities in discovery and delivery of anticancer drugs targeting mitochondria and cancer cell metabolism. *Adv. Drug Deliv. Rev.*, 2009. 61(14): p. 1250-75.
14. Tennant, D.A., Durán, R. V., Gottlieb, E., Targeting metabolic transformation for cancer therapy. *Nat. Rev. Cancer*, 2010. 10(4): p. 267-77.

15. Chaudhuri, D., Suriano, R., Mittelman, A., Tiwari, R. K., Targeting the Immune System in Cancer. *Curr. Pharm. Biotechnol.*, 2009. 10(2): p. 166-84.
16. Parish, C.R., Cancer immunotherapy: The past, the present and the future. *Immunol. Cell. Biol.*, 2003. 81(2): p. 106-13.
17. Ruzsala-Mallon, V., Lin, Y. I., Durr, F. E., Wang, B. S., Low molecular weight immunopotentiators. *Int. J. Immunopharmacol.*, 1988. 10(5): p. 497-510.
18. Borghaei, H., Smith, M. R., Campbell, K. S., Immunotherapy of cancer. *Eur. J. Pharmacol.*, 2009. 625 (1-3): p. 41-54.
19. Kandalaf, L.E., Singh, N., Liao, J. B., Facciabene, A., Berek, J. S., Powell, D. J. Jr., Coukos, G., The emergence of immunomodulation: Combinatorial immunochemotherapy opportunities for the next decade. *Gynecol. Oncol.*, 2010. 116(2): p. 222-33.
20. Schwandner, R., Dziarski, R., Wesche, H., Rothe, M. & Kirschning, C.J., Peptidoglycan- and lipoteichoic acid-induced cell activation is mediated by toll-like receptor 2. *J. Biol. Chem.*, 1999. 274: p. 17406-409.
21. Schroder, N.W., Morath, S., Alexander, C., Hamann, L., Hartung, T., Zahringer, U., Gobel, U.B., Weber, J.R. & Schumann, R.R., Lipoteichoic acid (LTA) of *Streptococcus pneumoniae* and *Staphylococcus aureus* activates immune cells via Toll-like receptor (TLR)-2, lipopolysaccharidebinding protein (LBP), and CD14, whereas TLR-4 and MD-2 are not involved. *J. Biol. Chem.*, 2003. 278: p. 15587-94.
22. Leon, C.G., Tony, R., Jia, J., Sivak, O., Wasan, K. M., Discovery and development of toll-like receptor 4 (TLR4) antagonists: a new paradigm for treating sepsis and other diseases. *Pharm. Res.*, 2008. 25(8): p. 1751-61.
23. Hakomori, S., Tumor-associated carbohydrate antigens defining tumor malignancy: basis for development of anti-cancer vaccines. *Adv. Exp. Med. Biol.*, 2001. 491: p. 369-402.
24. Ragupathi, G., Carbohydrate antigens as targets for active specific immunotherapy. *Cancer Immunol. Immunother.*, 1996. 43: p. 152-57.
25. Buskas, T., Thompson, P. Boons, G. J., Immunotherapy for cancer: synthetic carbohydrate-based vaccines. *Chem. Commun.*, 2009. 36: p. 5335-49.
26. Ochsenbein, A.F., Klenerman, P., Karrer, U., Ludewig, B., Pericin, M., Hengartner, H., Zinkernagel, R. M., Immune surveillance against a solid tumor fails because of immunological ignorance. *Proc. Natl. Acad. Sci. USA*, 1999. 96: p. 2233-38.

27. Zhongwu, G., Qianli, W., Recent development in carbohydrate-based cancer vaccines. *Curr. Opin. Chem. Biol.*, 2009. 13(5-6): p. 608-17.
28. Morris-Stiff, G., Teli, M., Jardine, N., Puntis, M. C., CA19-9 antigen levels can distinguish between benign and malignant pancreatic obiliary disease. *Hepatobiliary Pancreat. Dis. Int.*, 2009. 8(6): p. 620-6.
29. Rustin, G.Z., Marples, M., Nelstrop, A. E., Mahmoodi, M., Meyer, T., Use of CA-125 to define progression of ovarian cancer in patients with persistently elevated levels. *J. Clin. Oncol.*, 2001. 19(20): p. 4054-7.
30. Natori, T., Motoki, K., Akimoto, K., Koezuka, Y., Higa, T., Development of KRN7000, derived from agelasphin produced by Okinawan sponge. *Nippon Yakurigaku Zasshi*, 1997. 110(Supl. 1): p. 63P-68P.
31. Natori, T., Morita, M., Akimoto, K., Koezuka, Y., Agelasphins, novel antitumor and immunostimulatory cerebroside from the marine sponge *Agelas mauritanus*. *Tetrahedron*, 1994. 50(9): p. 2771-84.
32. Franck, R.W., Tsuji, M., alpha-C-Galactosylceramides: Synthesis and immunology. *Acc. Chem. Res.*, 2006. 39(10): p. 692-701.
33. Kobayashi, E., Motoki, K., Uchida, T., Fukushima, H., Koezuka, Y., KRN7000, a novel immunomodulator, and its antitumor activities. *Oncol. Res.*, 1995. 7(10-11): p. 529-34.
34. Nakagawa, R., Serizawa, I., Motoki, K., Sato, M., Ueno, H., Iijima, R., Nakamura, H., Shimosaka, A., Koezuka, Y., Antitumor activity of alpha-galactosylceramide, KRN7000, in mice with the melanoma B16 hepatic metastasis and immunohistological study of tumor infiltrating cells. *Oncol. Res.*, 2000. 12(2): p. 51-8.
35. Fuji, N., Ueda, Y., Fujiwara, H., Toh, T., Yoshimura, T., Yamagishi, H., Antitumor effect of alpha-galactosylceramide (KRN7000) on spontaneous hepatic metastases requires endogenous interleukin 12 in the liver. *Clin. Cancer Res.*, 2000. 6(8): p. 3380-7.
36. Kunii, N., Horiguchi, S., Motohashi, S., Yamamoto, H., Ueno, N., Yamamoto, S., Sakurai, D., Taniguchi, M., Nakayama, T., Okamoto, Y., Combination therapy of in vitro-expanded natural killer T cells and alpha-galactosylceramide-pulsed antigen-presenting cells in patients with recurrent head and neck carcinoma. *Cancer Sci.*, 2009. 100(6): p. 1092-8.
37. Motohashi, S., Nagato, K., Kunii, N., Yamamoto, H., Yamasaki, K., Okita, K., Hanaoka, H., Shimizu, N., Suzuki, M., Yoshino, I., Taniguchi, M., Fujisawa, T., Nakayama, T., A phase I-II study of alpha-galactosylceramide-pulsed IL-2/GM-

- CSF-cultured peripheral blood mononuclear cells in patients with advanced and recurrent non-small cell lung cancer. *J. Immunol.*, 2009. 182(4): p. 2492-501.
38. Yamada, H., Saiki, I., *Juzen-taiho-to (Shi-Quan-Da-Bu-Tang): Scientific Evaluation and Clinical Applications*. 2005, FL.: CRC, Boca Raton.
 39. Maruyama, H., Kawamura, H., Takemoto, N., Komatsu, Y., Maruyama, N., Antitumor effect of Juzen-taiho-to, A Kampo medicine, combined with surgical excision for transplanted Meth-A-fibrosarcoma. *Int. J. Immunother.*, 1993. 9: p. 117-25.
 40. Haranaka, R., Hasegawa, R., Nakagawa, S., Sakurai, A., Satomi, N., Haranaka, K. , Antitumor activity of combination therapy with traditional Chinese medicine and OK432 or MMC. *J. Biol. Response Mod.*, 1988. 7(1): p. 77-90.
 41. Sugiyama, K., Ueda, H., Ichiko, Y., Yokota, M. , Improvement of cisplatin toxicity and lethality by Juzen-taiho-to in mice. *Biol. Pharm. Bull.*, 1995. 18(1): p. 53-8.
 42. Terasawa, K., *The status of traditional Sino-Japanes (Kampon) medicine currently practised in Japan., in Economic and Medicinal Plant Research*, H. Wagner, Farnsworth, N. R., Editor. 1990, Academic Press: San Diego. p. 57-70.
 43. Ohnishi, Y., Fujii, H, Hayakawa, Y, Sakukawa, R, Yamaura, T, Sakamoto, T, Tsukada, K, Fujimaki, M, Nunome, S, Komatsu, Y, Saiki, I., Oral Administration of a Kampo (Japanese Herbal) Medicine Juzen-taiho-to Inhibits Liver Metastasis of Colon 26-L5 Carcinoma Cells. *Jpn. J. Cancer Res.*, 1998. 89(2): p. 206-13.
 44. Saiki, I., A Kampo Medicine "Juzen-taiho-to"- Prevention of Malignant Progression and Metastasis of Tumor Cells and the Mechanism of action. *Biol. Pharm. Bull.*, 2000. 23(6): p. 677-88.
 45. Zheng, Y., Wei, W., Zhu, L., Liu, J., Effects and mechanisms of Paeonifl orin, a bioactive glucoside from paeony root, on adjuvant arthritis in rats. *Inflamm. Res.*, 2007. 56: p. 182-8.
 46. Kim, I.D., Ha, B. J., Paeoniflorin protects RAW 264.7 macrophages from LPS-induced cytotoxicity and genotoxicity. *Toxicol. in vitro*, 2009. 23(6): p. 1014-19.
 47. Liu, D.Z., Xie, K. Q., Ji, X. Q., Ye, Y., Jiang, C. L., Zhu, X. Z., Neuroprotective effect of paeoniflorin on cerebral ischemic rat by activating adenosine A1 receptor in a manner different from its classical agonists. *Br. J. Pharmacol.*, 2005. 146(4): p. 604-11.

48. Takeda, S., Isono, T., Wakui, Y., Matsuzaki, Y., Sasaki, H., Amagaya, S., Maruno, M., Absorption and excretion of paeoniflorin in rats. *J. Pharm. Pharmacol.*, 1995. 47(12A): p. 1036-40.
49. Takeda, S., Isono, T., Wakui, Y., Mizuhara, Y., Amagaya, S., Maruno, M., Hattori, M., In-vivo assessment of extrahepatic metabolism of paeoniflorin in rats: relevance to intestinal floral metabolism. *J. Pharm. Pharmacol.*, 1997. 49(1): p. 35-39.
50. Kawamura, A., Brekman, A., Grigoryev, Y., Hasson, T. H., Takaoka, A., Wolfe, S., Soll, C. E., Rediscovery of natural products using genomic tools. *Bioorg. Med. Chem. Lett.*, 2006. 16(11): p. 2846-9.
51. Kawamura, A., Iacovidou, M., Takaoka, A., Soll, C. E., Blumenstein, M., A polyacetylene compound from herbal medicine regulates genes associated with thrombosis in endothelial cells. *Bioorg. Med. Chem. Lett.*, 2007. 17(24): p. 6879-82.
52. Hasson, T.H., *Isolation and Characterization of Immunomodulatory Compounds from Juzen-Taiho-To: Novel Understanding of Phytosteryl Glucosides Nano-Aggregates and Synergism in Biochemistry*. 2009, The Graduate Center of CUNY: New York. p. 165.
53. Niiho, Y., Nakajima, Y., Yamazaki, T., Okamoto, M., Tsuchihashi, R., Koderu, M., Kinjo, J., Nohara, T., Simultaneous analysis of isoflavones and saponins in Pueraria flowers using HPLC coupled to an evaporative light scattering detector and isolation of a new isoflavone diglucoside. *J. Nat. Med.*, 2010. 64(3): p. 313-20.
54. Almeling, S., Holzgrabe, U., Use of evaporative light scattering detection for the quality control of drug substances: Influence of different liquid chromatographic and evaporative light scattering detector parameters on the appearance of spike peaks. *J. Chromatogr. A*, 2010. 1217(14): p. 2163-70.
55. Lucena, R., Cardenas, S., Valcareel, M., Evaporative light scattering detection: trends in its analytical uses. *Anal. Bioanal. Chem.*, 2007. 388: p. 1663-72.
56. Bouic, P.J., Etsebeth, S., Liebenberg, R. W., Albrecht, C. F., Pegel, K., Van Jaarsveld, P. P., beta-Sitosterol and beta-sitosterol glucoside stimulate human peripheral blood lymphocyte proliferation: implications for their use as an immunomodulatory vitamin combination. *Int. J. Immunopharmacol.*, 1996. 18(12): p. 693-700.
57. Bouic, P.J., Lamprecht, J. H., Plant sterols and sterolins: a review of the their immune-modulating properties. *Altern. Med. Rev.*, 1999. 4(3): p. 170-77.

58. Bock, K., Pedersen, C., Carbon-13 nuclear magnetic resonance spectroscopy of monosacharides. *Adv. Carbohydr. Chem. Biochem.*, 1983. 41: p. 27-66.
59. Stothers, J.B., *Carbon-13 NMR spectroscopy. Organic Chemistry: A series of monographs*. Vol. 24. 1972, New York: Academic Press.
60. Shibuya, H., Kawashima, K., Sakagami, M., Kawanishi, H., Shimomura, M., Kazuyoshi, O., Kitagawa, I., Sphingolipids and Glycerolipids I. Chemical structures and ionophoretic activities of soya-cerebrosides I and II from soybean. *Chem. Pharm. Bull.*, 1990. 38(11): p. 2933-38.
61. Inagaki, M., Harada, Y., Yamada, K., Isobe, R., Higuchi, R., Matsuura, H., Itakura, Y., Isolation and structure determination of cerebrosides from garlic, the bulbs of *Allium Sativum* L. *Chem. Pharm. Bull.*, 1998. 46(7): p. 1153-56.
62. Welti, R., Shah, J., Li, W., Li, M., Chen, J., Burke, J. J., Fauconnier, M. L., Chapman, K., Chye, M. L., Wang, X., Plant lipidomics: discerning biological function by profiling plant complex lipids using mass spectrometry. *Front. Biosci.*, 2007. 12: p. 2494-506.
63. Gu, M., Kerwin, J. L., Watts, J. D., Aebersold, R., Ceramide Profiling of Complex Lipid Mixtures by Electrospray Ionization Mass Spectrometry. *Anal. Biochem.*, 1997. 244(2): p. 347-56.
64. Kerwin, J.L., Tuininga, A. R., Ericsson, L H., Identification of molecular species of glycerophospholipids and sphingomyelin using electrospray mass spectrometry. *J. Lipid Res.*, 1994. 35(6): p. 1102-14.
65. Yang, N., Ren, D., Duan, J., Xu, X., Xie, N., Tian, L., Ceramides and cerebrosides from *Ligusticum chuanxiong*. *Helv. Chim. Acta*, 2009. 92(2): p. 291-7.
66. Zhao, C., Shao, J., Wang, N., Li, X., Wang, J., A new cerebroside from fruits of *Ailanthus altissima* Swingle. *Nat. Prod. Res.*, 2006. 20(13): p. 1187-91.
67. Row, L., Ho, J., Chen, C., Cerebrosides and Tocopherol trimers from the seeds of *Euryale ferox*. *J. Nat. Prod.*, 2007. 70(7): p. 1214-17.
68. Babu, U.V., Bhandari, S. P. S., Garg, H. S., Temnosides A and B, Two new glycosphingolipids from the sea urchin *temnopleurus toreumaticus* of the Indian coast. *J. Nat. Prod.*, 1997. 60(7): p. 732-4.
69. Ilan, Y., Elstein, D., Zimran, A., Glucocerebroside: an evolutionary advantage for patients with Gaucher disease and a new immunomodulatory agent. *Immunol. Cell. Biol.*, 2009. 87(7): p. 514-24.

70. Bertram, H.C., Eldibany, M., Padgett, J., Dragon, L. H., Splenic lymphoma arising in a patient with Gaucher disease. A case report and review of the literature. *Arch. Pathol. Lab. Med.*, 2003. 127(5): p. e242-5.
71. Lo, S.M., Stein, P., Mullaly, S., Bar, M., Jain, D., Pastores, G. M., Mistry, P. K., Expanding spectrum of the association between Type 1 Gaucher disease and cancers: a series of patients with up to 3 sequential cancers of multiple types--correlation with genotype and phenotype. *Am. J. Hematol.*, 2010. 85(5): p. 340-5.
72. Morita, M., Natori, T., Akimoto, K., Osawa, T., Fukushima, H., Koezuka, Y., Syntheses of α -, β -monoglycosylceramides and four diastereomers of an α -galactosylceramide. *Bioorg. Med. Chem. Lett.*, 1995. 5(7): p. 699-704.
73. Natori, T., Koezuka, Y., Higa, T., Agelasphins, novel α -galactosylceramides from the marine sponge *Agelas mauritianus*. *Tetrahedron Lett.*, 1993. 34(35): p. 5591-2.
74. Morita, M., Motoki, K., Akimoto, K., Natori, T., Sakai, T., Sawa, E., Yamaji, K., Koezuka, Y., Kobayashi, E., Fukushima, H., Structure-activity relationship of alpha-galactosylceramides against B16-bearing mice. *J. Med. Chem.*, 1995. 38(12): p. 2176-87.

CHAPTER III:

Uncovering hidden biosynthetic potential of soil Actinomycetes

III.1. Introduction

Soil is where the fierce survival game of microorganisms is always at play. In order to adapt into changing microenvironments, their genetic makeup has to be continually diversified. Only those who gain growth advantage in their biological niches are allowed to survive. Among soil microorganisms are a group of bacteria with a gift of organic chemistry. These bacterial “organic chemists” sacrifice a substantial portion of their genomes for the production of secondary metabolites. Those who produce useful compounds, such as chemical weapons and shields, are able to survive, whereas those who waste their resources to produce useless compounds are bound for extinction. In this way, structures of bacterial secondary metabolites have been refined over billions of years of biological selection. Behind each metabolite is a unique story of the survival of the fittest. Even each functional group on a metabolite may have some story to tell, if anybody cares enough to listen.

Among all known bacterial chemists, actinomycetes are arguably the most prolific producers of secondary metabolites [1-4]. The name “Actinomycetes” has been derived from their apparently fungus-like morphology in Greek; ‘aktis’ (a ray) and ‘mykes’ (fungus) [1]. They are gram-positive bacteria with high GC content (> 55%) in their DNA. Most actinomycetes are free living, saprophytic bacteria in soil, water and colonizing plants [1]. Some well-known antibiotics like streptomycin, neomycin and chlorphenicol have been found from the taxa of Actinomycetes. Thus, Actinomycetes are widely known as the important source of antibiotics. In fact, since the discovery of streptothricin in 1942, roughly 3,000 antibiotics have been found from the genus of actinomycetes; 90% of them are from Streptomycetes [5]. Streptomycetes are the largest

group of Actinomycetes, and predominantly found in soil. Streptomyces have provided a number of clinically important therapeutic agents, including erythromycin and vancomycin (antibiotics) [1], nystatin and amphotericin B (antifungals) [6, 7], rapamycin and FK-506 (immunosuppressants) [8, 9], and migrastatin (anticancer agent) [10] (Figure III.1). Without a question, research on soil bacteria has played a central role in drug discovery and development in the last century.

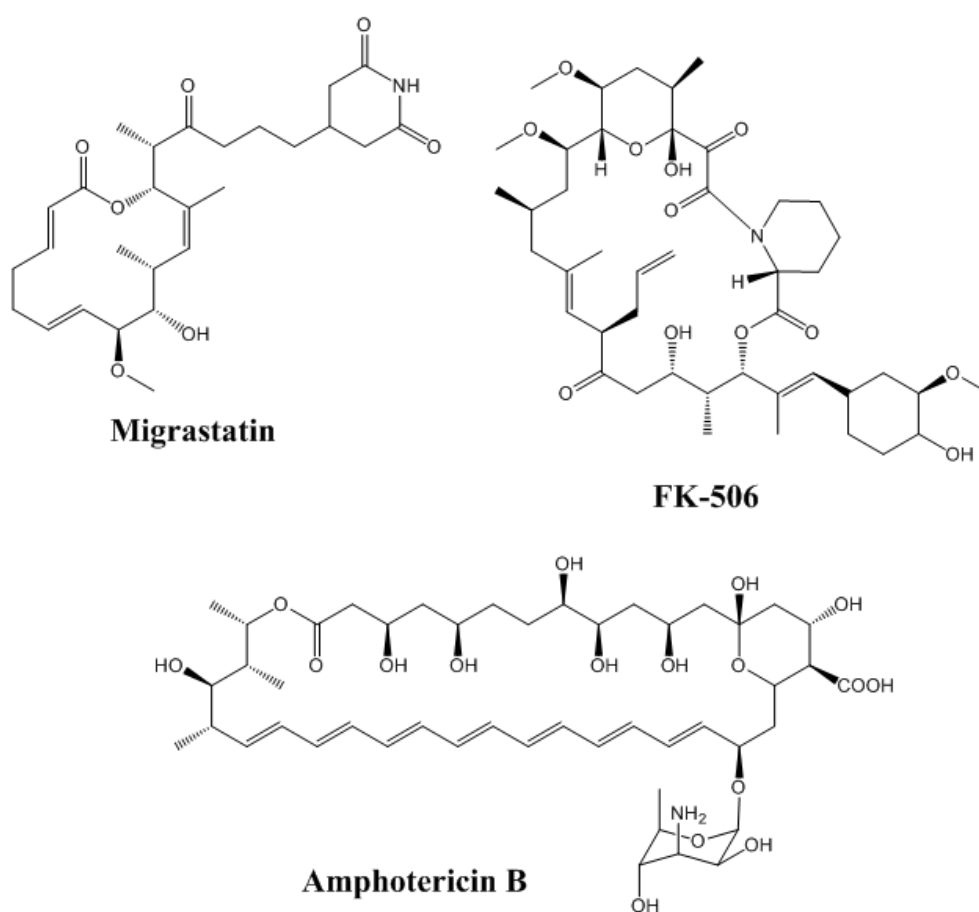


Figure III. 1. Clinically important therapeutic agents isolated from the genus of Streptomyces.

Over the last few decades, however, screening of secondary metabolites from soil bacteria has declined rapidly. Soil bacteria are now widely perceived as an “exhausted” resource of natural products [11]. In fact, old antibiotics are frequently rediscovered from soil bacteria. Although a population of 10^4 Actinomycete strains contains roughly 2,500 producers of antibiotics, it is estimated that 2,250 of them produce streptothricin, 125 streptomycin, and 40 tetracycline (Figure III.2) [12]. In a hope to identify new compounds, many academic investigators moved on to study more exotic natural resources, such as marine invertebrates and deep ocean bacteria [13-16]. The pharmaceutical industry has taken an even more drastic action by closing down most of their natural products operations altogether [17].

While the general trend in the scientific community is not encouraging, there still may be many interesting compounds waiting to be discovered from soil bacteria [11]. How could the enormous bacterial resource with billions of years of history be exhausted by the several decades of human exploration with limited scopes? Perhaps screenings in the past had too much emphasis on identifying new antibiotics. Maybe bacteria just do not produce certain metabolites when they are isolated and cultured in a laboratory. There is also a possibility that some metabolites require specific environmental cues to become biologically active; just like certain enzymes are produced as zymogens in the cell. A recent genome sequencing of *Streptomyces griseus* IFO 13350, which is one of the best characterized producers of streptomycin, shed new light on the biosynthetic potential of soil bacteria [18]. In addition to the gene cluster for streptomycin biosynthesis, this “well-known” soil bacterium turned out to possess many as-yet uncharacterized biosynthetic gene clusters, such as terpenoid cyclases, nonribosomal peptide synthases (NRPS),

polyketide synthases (PKS) and PKS-NRPS hybrids [18]. Clearly, there is still a need to reexamine the biosynthetic potential of soil bacteria.

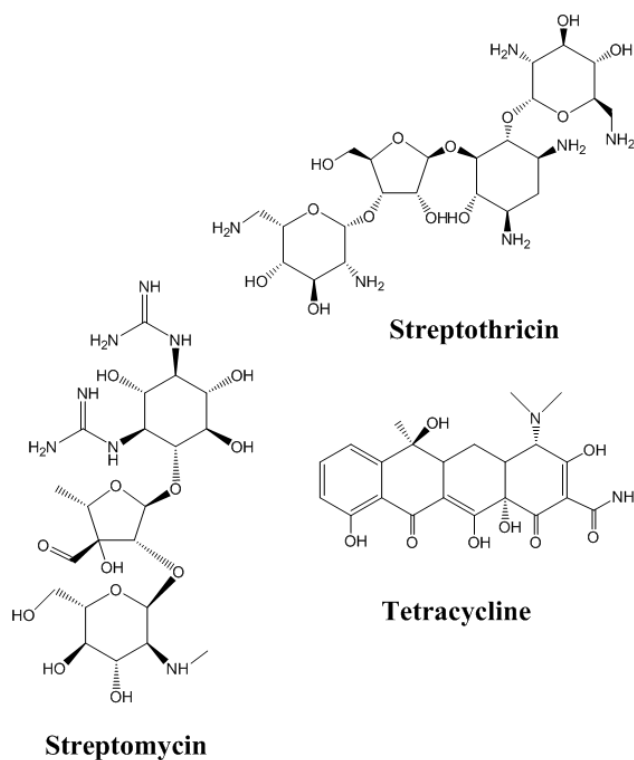


Figure III. 2. Structures of known antibiotics isolated from the taxa of actinomycetes.

Reexamination of the biosynthetic potential of soil bacteria is also important at the time when the powerful tools of metabolic engineering have become available to produce bacterial metabolites through biosynthesis. Biosynthetic genes of Actinomycetes can now be readily characterized, manipulated, and, if needed, heterologously expressed in *Escherichia coli* [19-21]. Thus, without the use of hazardous chemicals and long steps of organic synthesis, bacterial metabolites and their structural analogs can be rapidly produced from simple and inexpensive carbon sources. Even if a metabolite does not exhibit obvious biological activity, its production by metabolic engineering might be

warranted if the structural complexity provides an easy access to new chemical and pharmacological spaces, which cannot be readily explored with diversity oriented synthesis [22, 23]. Alternatively, metabolic engineering may also be justified if a compound possesses unique chemical reactivities, which through synthetic means not easy to reproduce. In this regard, new goals of the screening of bacterial metabolites are the identification of complex structural scaffolds and unique chemical properties.

In order to reexamine the biosynthetic potential of soil bacteria, our group teamed up with Professor Monica Trujillo (Queensborough Community College), an expert of metabolic engineering with many years of industry experience at Kosan Biosciences (now, Bristol-Myers Squibb Company). The group of Prof. Trujillo is responsible for the collection and isolation of culturable soil bacteria, whereas our group is in charge of the purification and structural characterization of unique secondary metabolites. This exploratory collaboration led to the discovery of highly sophisticated organic chemistry that has been quietly carried out for many years by an actinomycete strain in the State of New York.

III. 2. Isolation of metabolite-producing soil bacteria

Soil samples were collected from various parts of New York in the summer of 2006; mainly from Lake Oakland, Bayside. Collected soil samples were air dried, resuspended in sterile water, and plated on Actinomycete Isolation Agar (AIA) plate containing nalidixic acid and cycloheximide to inhibit the growth of fungi. Isolated colonies were further purified on Soy Flour Mannitol (SFM) Agar plate. Collectively, sixteen different strains have been isolated from eight different locations in NY. Pigment

formation on the agar plate was used to identify metabolite-producing strains (Figure III.3). Liquid culture conditions were then optimized for individual strains. Preliminary LC/MS screening indicated that one strain, MTE4a, produced several metabolites that were not present in the background (the culture medium: MTF1) (data not shown). In addition, the culture supernatant of MTE4a exhibited antimicrobial activity against *Staphylococcus aureus* (see Figure III.9). The sequence analysis of 16S rRNA indicated that MTE4a was a strain of *Streptomyces griseus* (personal communication with Prof. Monica Trujillo). Collectively, these preliminary data set a stage to explore the biosynthetic potential of *Streptomyces griseus* MTE4a.

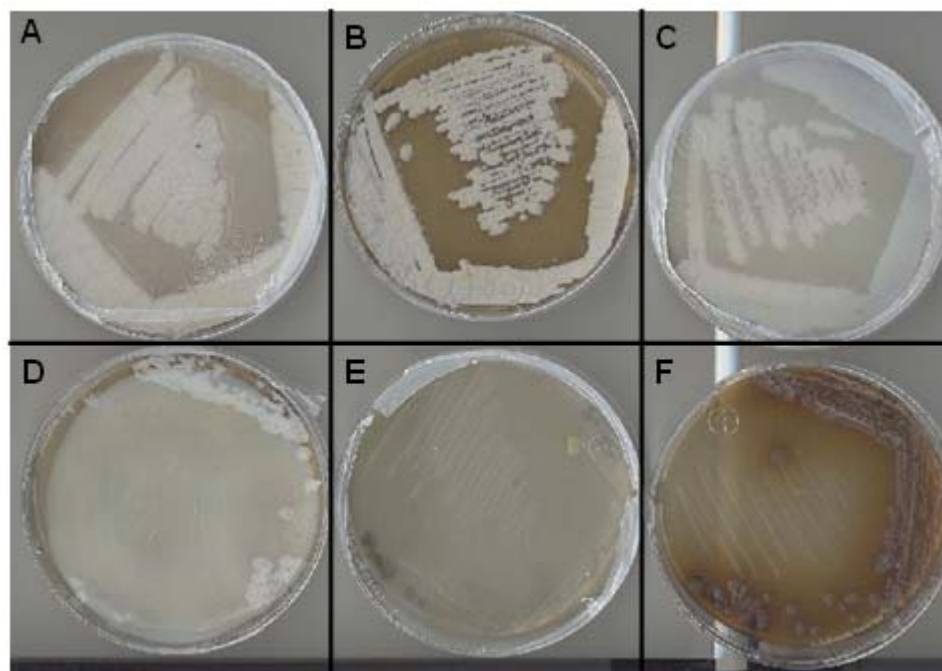


Figure III.3. Metabolites-producing strains isolated from various locations in NY. Pigmentation shown on plates A-F indicates the production of secondary metabolites. Some strains are sporulated (F) with powdery, velvet-like texture and grey/black color, whereas some are non-sporulated (A-E) with rough texture and white or other colors.

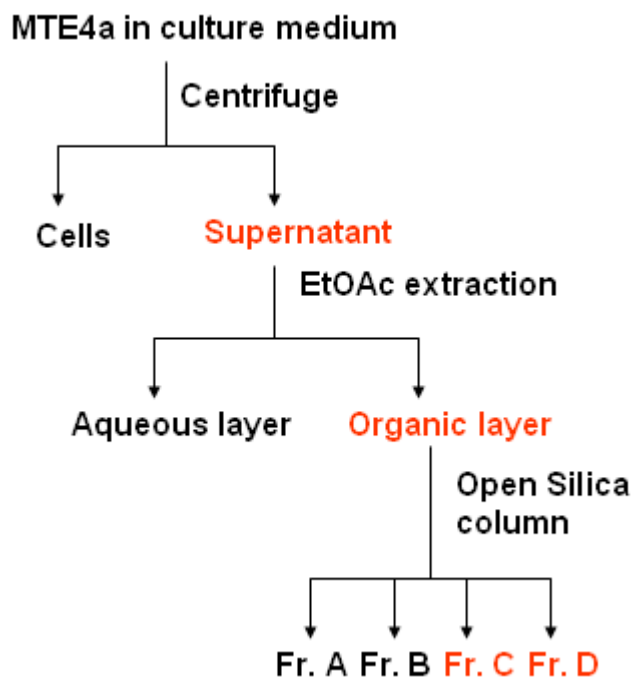
III. 3. Search for unique metabolites produced by *Streptomyces griseus* MTE4a

As noted in the Introduction section, past screenings of soil bacteria may have been circumscribed because of their focus on the discovery of new antibiotics. In order to obtain a broader view of secondary metabolites produced by *Streptomyces griseus* MTE4a, our screening searched for isolable chemical constituents regardless of their antimicrobial activities.

The initial fractionation was carried out with a simple procedure as outlined in Scheme III.1. Briefly, pooled cultures of MTE4a (total 7 liters) were centrifuged to obtain the supernatant, which was then extracted with EtOAc to give a crude extract (3 g). Crude extract was fractionated by silica gel open column chromatography with a step-gradient elution with (A) 100% hexane, (B) hexane/EtOAc (95:5), (C) hexane/EtOAc (90:10) and (D) CH₂Cl₂/MeOH (90:10). Non-polar fractions, A-C, exhibited well resolved TLC spots that were not present in the background (i.e., the EtOAc extract of the culture medium MTF1). On the other hand, fraction D had more complex chemical constituents. Our screening, therefore, initially focused on the characterization of isolable components in fractions A-C.

Purification of chemical constituents in fractions A-C, however, turned out to be much more difficult task than we had originally anticipated. Although it was easy to purify well-resolved TLC spots by silica gel chromatography, the NMR spectra of the purified samples indicated that they were still mixtures of multiple compounds. Further attempts to purify these mixtures with HPLC and preparative TLC resulted in either loss of sample or decomposition (data not shown). We, therefore, were forced to shift our focus on fraction D.

Fraction D was a complex mixture of various polar compounds. Many TLC spots of fraction D overlapped with the background spots (the EtOAc extract of culture medium MTF1). This fraction had a distinct odor, which was absent in the background. Fraction D was separated with a step-gradient elution on silica gel chromatography, in which the solvent polarity was gradually increased from 0% to 10% MeOH in CH₂Cl₂ over 20 fractions (Figure III. 4A). Most TLC spots of obtained fractions overlapped with the background spots. For example, the fraction 10, which overlapped with a major background spot, turned out to be a cyclic dimer of proline-tryptophan, which most likely came from the culture medium: MTF1 contains tryptone (trypsin-digest of caseine protein commonly used in microbiology.) The distinct odor was eluted around fractions 2-10. However, many spots in these fractions overlapped with multiple background spots. Further TLC analyses revealed that the fractions 15-18 contained a compound that was distinctly different from any of the background spots (Figure III.4.B): This spot is clearly visible in the fraction 16 (Figure III.4.A). Thus, fractions 15-18 were combined and further purified with reversed phase HPLC (C₁₈ analytical column, 1 ml/min, 20-80% MeOH_{aq.} over 30 min). The isolated compound (ca. 2 mg) was then subjected to spectroscopic characterization.



Scheme III.1. Fractionation of the supernatant of *S. griseus* MTE4a culture. The supernatant of the MTE4a culture was extracted with EtOAc and then fractionated by silica gel chromatography with a step-gradient elution with (A) 100% hexane, (B) hexane/EtOAc (95:5), (C) hexane/EtOAc (90:10) and (D) CH₂Cl₂/MeOH (90:10). The fractions with antimicrobial activity are highlighted with the red color.

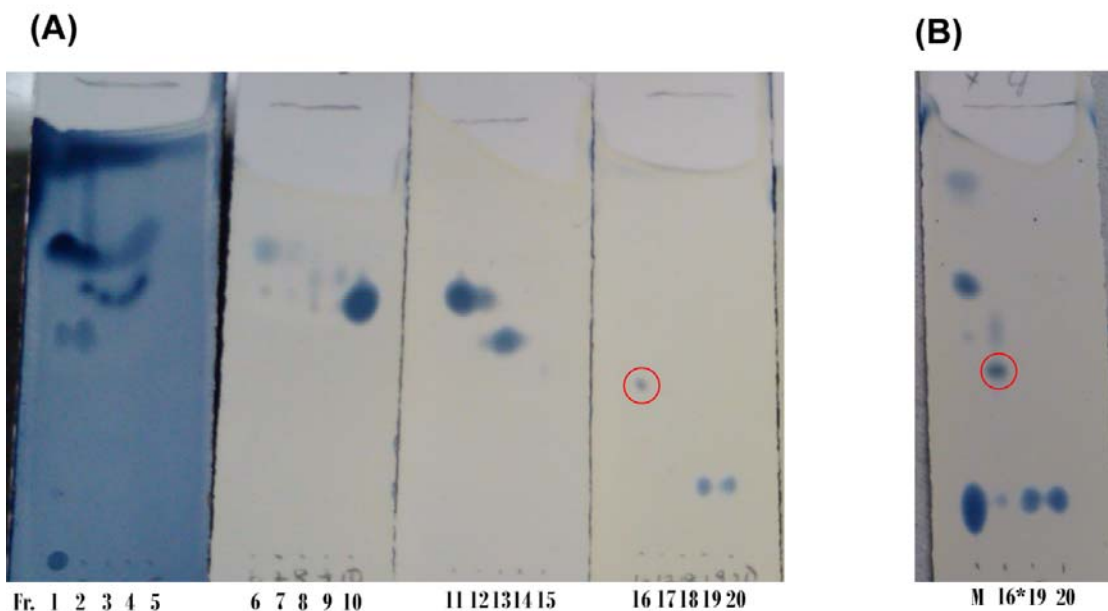


Figure III.4. Separation of chemical constituents in Fraction D. The CH_2Cl_2 solution of Fraction D was loaded on to a silica gel open column (15 cm \times 1 cm i.d.) and eluted with a step-gradient (0-10% MeOH in CH_2Cl_2 over 20 fractions). (A) TLC profile of the subfractions obtained from Fraction D. TLC was developed with 20% MeOH in CH_2Cl_2 . (B) Comparisons of fractions 16*, 19 and 20 to the background spots (M: The EtOAc extract of the culture medium). Fraction 16* is a combined fraction (Fractions 15-18 in Figure III. 3A). TLC was developed four times with 10% MeOH in CH_2Cl_2 . The unique spot from *Streptomyces griseus* MTE4a is highlighted with a red circle.

III.4. Structural elucidation of cyclooctatin B (COB)

The molecular formula of the purified material was deduced to be $\text{C}_{20}\text{H}_{34}\text{O}_4$ based on the positive high resolution ESI-MS: $[\text{M}+\text{H}]^+$ m/z 339.2497, calcd 339.2530; $[\text{M}+\text{H}-\text{H}_2\text{O}]^+$ 321.2425, calcd 321.2424; $[\text{M}+\text{H}-2(\text{H}_2\text{O})]^+$ 303.2318, calcd 303.2319. The ^1H ,

^{13}C , DEPT, and HSQC spectra in chloroform-*d* were then used to obtain twenty carbon pieces (see Appendices G-K), which included two olefinic carbons (δ_{C} 119.6 and 154.0 ppm), four oxygen bearing carbons (δ_{C} 77.2, 75.3, 65.9 and 63.5 ppm), and three methyl carbons (δ_{C} 26.7, 25.1, and 17.1 ppm). HMBC (10 Hz) correlations from the three methyl groups, followed by COSY analysis led to the assembly of the individual carbon pieces into larger fragments except for the methylene at 24.8 ppm (Figure III. 5, left) (see also Appendices L and M). Further analyses of HMBC unequivocally led to the elucidation of a planar structure of diterpene with a fused 5-8-5 ring system as shown on the right of Figure III.5.

Relative stereochemistry of this diterpene was then determined based on the NOESY correlations as summarized on Figure III.6.a. (see also Appendix N). In addition, a distinct U-shape conformation of the central 8-membered ring was indicated by the NOESY cross peaks between 1- H_{β} and 6-H and among 2-H/8- H_{α} /20-H cross peaks (Figure III.6.b, c).

Although higher plants and fungi are known to produce terpenes with the fused 5-8-5 ring framework [24-27], production of such a complex terpenoid by bacteria is rare. In fact, the only other known example is cyclooctatin from *Streptomyces melanosporofaciens* MI614-43F2, which had been isolated from a soil sample collected in Kanagawa, Japan (Figure III.7) [28]. Although our compound and cyclooctatin are structurally very close, including the ring fusion patterns and relative stereochemistry, there is an extra 17-OH group in our compound; thus, our compound was named “cyclooctatin B (COB)” (Figure III.7). The ^{13}C -NMR signals of cyclooctatin and its biosynthetic precursors, which were reported recently [29], are in good agreement with

the ^{13}C -NMR signals of COB except, of course, for the signals at the oxygenated carbons (Table III.1).

The structural difference between cyclooctatin B and cyclooctatin appeared minor at first. It was later found, however, that the presence of 17-OH plays a unique role in an acid catalyzed transformation of COB, which may have important biological implications (*vide infra*).

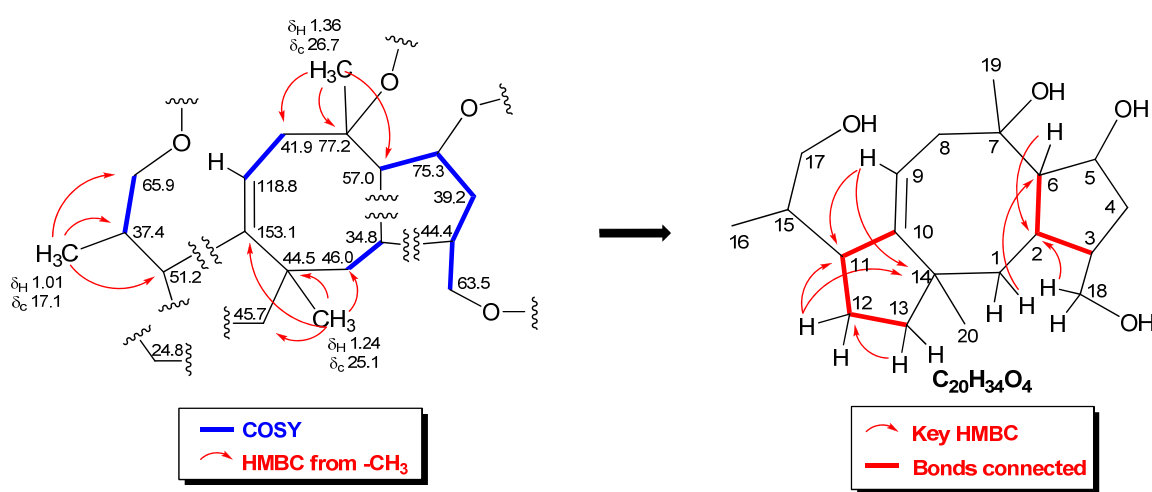


Figure III.5. Elucidation of the planar structure of a diterpene from *Streptomyces griseus* MTE4a. **Left:** Fragment structures around the three methyl groups were first elucidated with HMBC correlations from the methyl protons (red arrows). The fragments were further extended by COSY correlations (bold blue lines). After this initial analysis, 19 out of 20 carbons were assembled into larger fragments. The ^1H and ^{13}C chemical shifts of three methyl groups as well as the ^{13}C chemical shifts of all other carbons are shown. **Right:** Further analyses of HMBC correlations (red arrows) were used to obtain the planar structure of the diterpene. Bold red lines represent the bonds connected at this stage of the HMBC analysis.

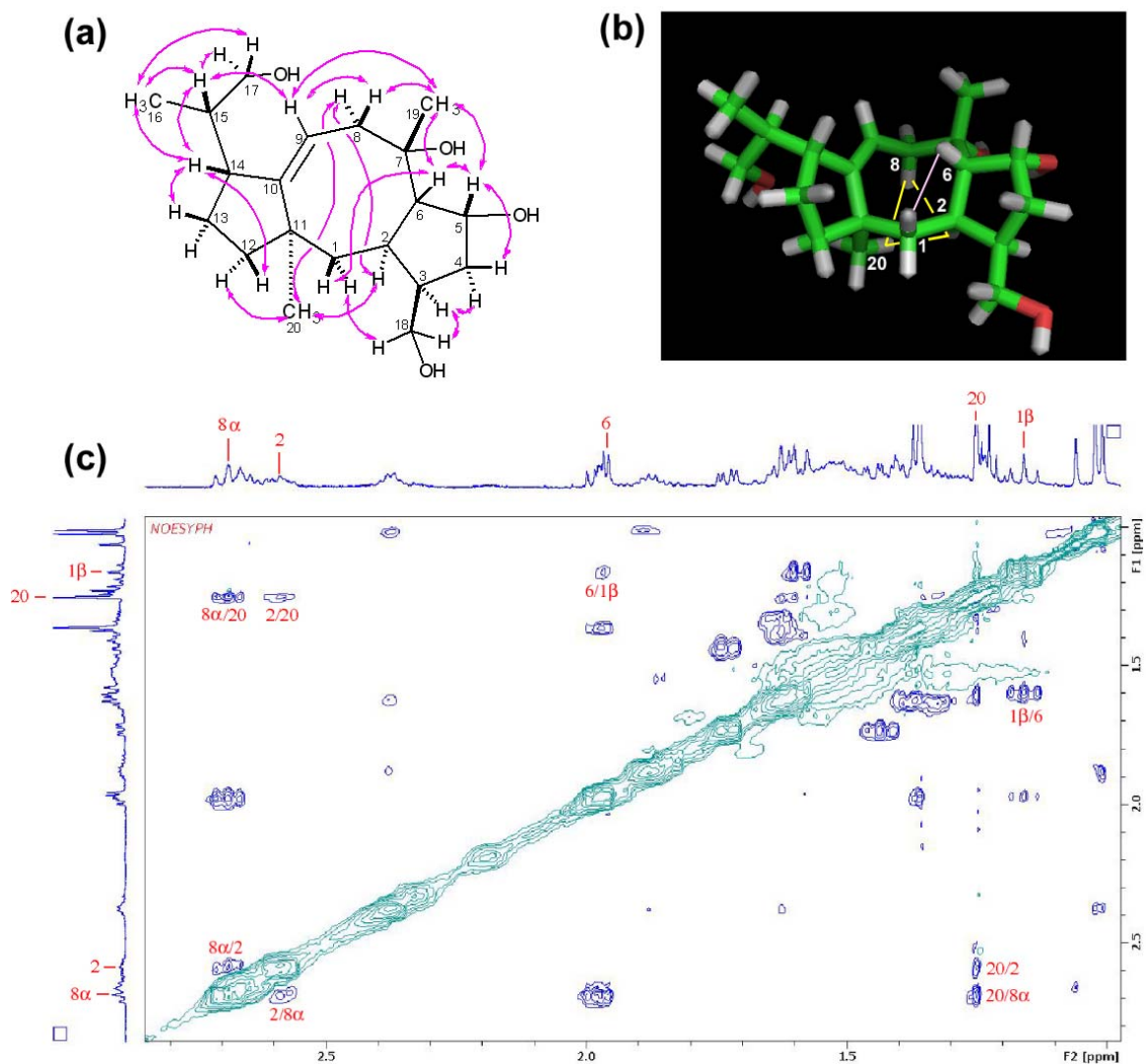


Figure III. 6. Relative stereochemistry and conformation of the diterpene from *Streptomyces griseus* MTE4a. (a) Relative stereochemistry as determined by NOESY correlations. (b) U-shaped conformation of the central 8-membered ring was suggested by the NOESY correlations of 1-H_β/6-H (β-face; pink line) and 2-H/8-H_α/20-H (α-face; yellow triangle). (c) The NOESY crosspeaks of 1-H_β/6-H and 2-H/8-H_α/20-H. Positive NOESY crosspeaks are shown in dark blue.

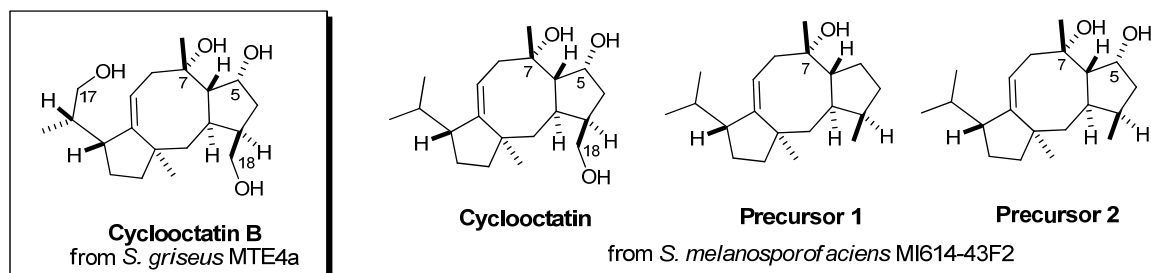


Figure III. 7. Two different strains of Streptomyces produce structurally close diterpenes with a fused 5-8-5 ring system. Two precursors of cyclooctatin have recently been isolated from cytochrome P-450 mutant strains of *S. melanosporofaciens* MI614-43-F2 [29].

Table III.1. The ^{13}C -NMR data of COB, cyclooctatin, and biosynthetic precursors. Signals of oxygenated carbons are highlighted by the yellow background. *Values from Ref [29].

Carbon #	COB (CDCl ₃)	COB (CD ₃ OD)	Cyclooctatin* (CD ₃ OD)	Precursor 1* (CDCl ₃)	Precursor 2* (CDCl ₃)
1	44.5	45.5	45.6	45.8	44.7
2	34.8	35.8	35.8	38.1	36.4
3	44.4	44.9	44.9	40.0	35.6
4	39.2	39.7	39.7	34.7	44.0
5	75.3	75.7	75.7	26.7	75.5
6	57.0	57.9	58.0	52.9	57.0
7	77.2	78.4	78.4	76.2	77.3
8	41.9	42.2	42.2	41.3	41.8
9	118.8	119.6	119.1	117.8	117.9
10	153.1	154.0	154.5	153.1	153.3
11	46.0	45.9	45.9	44.8	44.7
12	45.7	46.6	46.6	45.5	45.6
13	24.8	25.3	24.3	23.5	23.3
14	51.2	52.3	55.1	53.9	53.9
15	37.4	38.8	30.2	29.1	29.0
16	17.1	17.3	17.8	17.5	17.4
17	65.9	65.6	22.5	22.2	22.2
18	63.5	63.4	63.4	15.6	15.4
19	26.7	26.7	26.7	26.6	26.6
20	25.1	25.9	25.2	25.0	24.9

III.5. Acid-sensitivity of COB

During the NMR measurements it was found that COB was gradually converted into another compound in chloroform-*d* (Figure III.8.a,b). Although the sample was kept in the refrigerator (4 °C) whenever it was not used for the NMR measurements, a new set of peaks appeared after a week of storage in chloroform-*d* as indicated by the blue arrows in Figure III.8.b. This was most likely caused by the trace amount of acid that exists in chloroform-*d*. Further examinations of this newly formed compound revealed a carbon signal at ~95.5 ppm on HMBC (This signal is not visible on ¹³C-NMR). This signal showed HMBC correlations with a singlet methyl at 1.16 ppm and a triplet proton at 3.94 ppm (Figure III.8.c). These HMBC crosspeaks are consistent with the formation of a compound with a new tetrahydrofuran (THF) ring, in which 17'-H and 20'-Me are three bonds away from the carbon 10' (C-10') ($\delta_c \sim 100$ ppm as estimated by ChemBioDraw) (Figure III.8.d). Although full structural characterization of this product was not possible due to its small quantity, the observation of this product suggested that COB underwent intramolecular cyclization mediated by 17-OH in a slightly acidic condition.

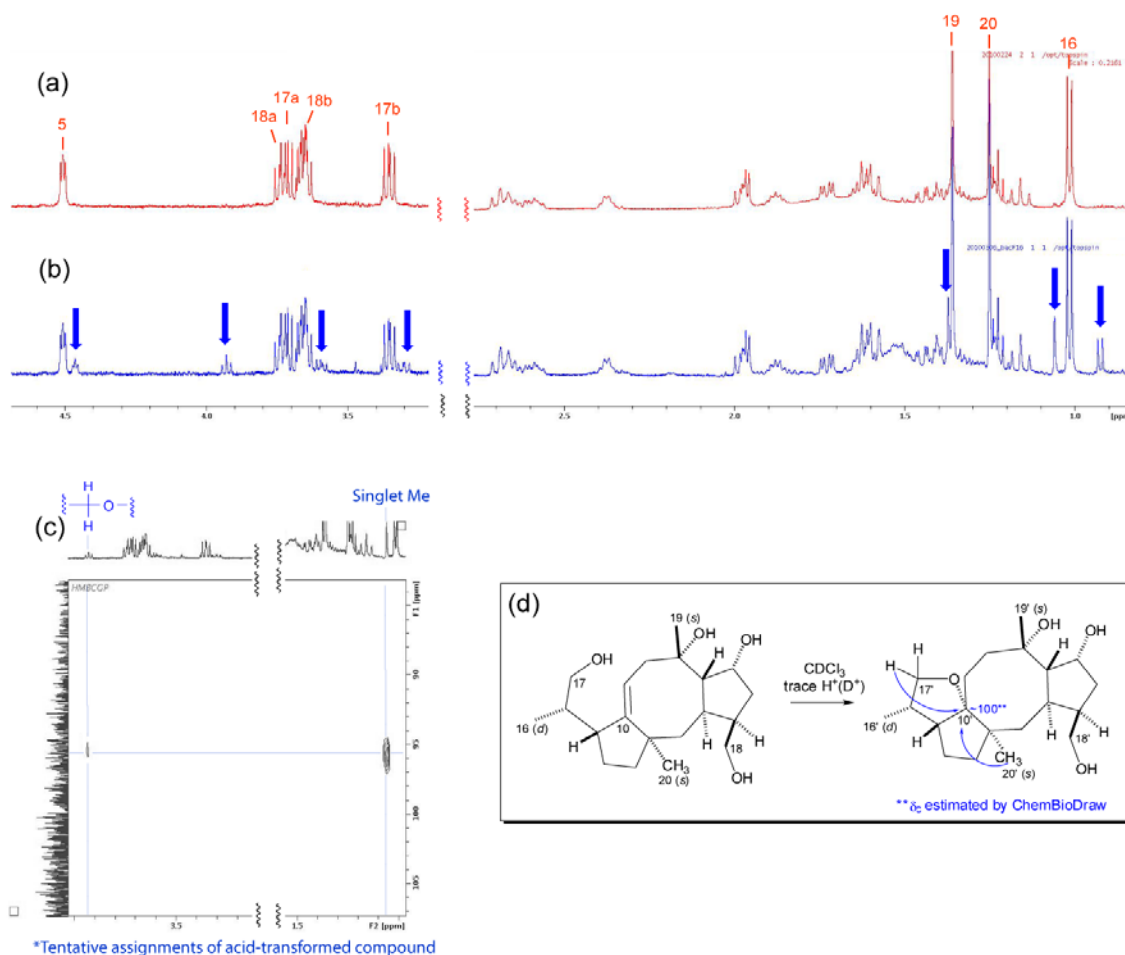


Figure III.8. (a) $^1\text{H-NMR}$ spectrum of COB in $\text{chloroform-}d$ shortly after its purification. (b) $^1\text{H-NMR}$ spectrum of COB after the sample was stored in $\text{chloroform-}d$ for a week. Blue arrows show the conspicuous new peaks emerged during the storage. (c) HMBC crosspeaks of the product formed in $\text{chloroform-}d$. A strong HMBC crosspeak was observed from a methyl (s) at 1.16 ppm to a carbon at ~ 95.5 ppm. In addition, a weak crosspeak was also seen from a proton at 3.94 ppm to the same carbon. (d) A possible reaction occurred in $\text{chloroform-}d$. The $^{13}\text{C-NMR}$ chemical shift for C-10' was estimated on ChemBioDraw.

III.6. Preliminary biological characterization of COB

Preliminary characterization of antimicrobial activity was carried out by the Agar disk method against a lawn culture of *Staphylococcus aureus*. While the culture supernatant of *Streptomyces griseus* MTE4a (positive control) exhibited clear inhibition of *Staphylococcus aureus* growth, COB did not show clear growth inhibitory activity (Figure III. 9). Thus, the result suggests that the strong activity of the *S. griseus* MTE4a culture supernatant is not due to COB. The activity might reside in the odorous fractions obtained during the silica gel chromatography.

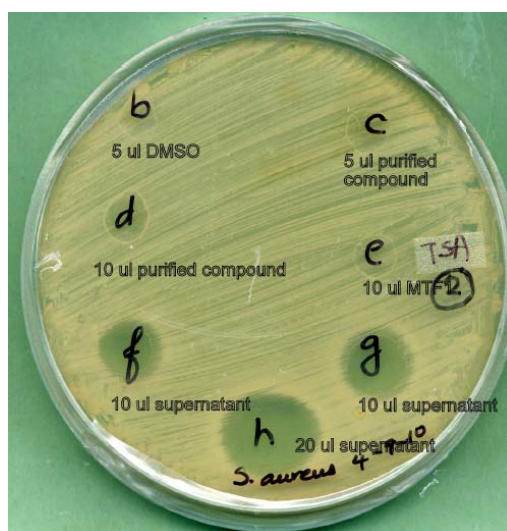


Figure III.9. Antimicrobial activity of COB. The activity indicated by Agar disk method against a lawn culture of *Staphylococcus aureus*. The supernatant of the MTE4a culture was used as positive control and the MTF1 medium as negative control. DMSO was used to dissolve cyclooctatin B (1 mg/ml).

Although the lack of antimicrobial activity was disappointing at first, this negative result made us wonder why this bacterial strain uses its precious resources to make such a

complex molecule in the first place. Why does this diterpene have such an elaborately furnished structure with distinct conformation? What is the implication of acid-sensitivity? These questions led us to a new hypothesis which might change the way bacterial metabolites are screened and characterized (*vide infra*).

III.7. Discussion

In this study we have isolated and determined the structure of a new diterpene, cyclooctatin B (COB), from a culturable soil Actinomycete, *Streptomyces griseus* MTE4a. There are several known terpenes with the fused 5-8-5 ring system such as ophiobolins [30], fusicoccin A [31] and ceroplastol II [32] (Figure III.10). These compounds, however, are sesterterpenes from insect wax and fungi, whereas COB is a diterpene from bacteria. It is also noted that the production of terpenes with such a complex framework is rare in bacteria although actinomycetes have been known to produce some terpenoids [33-36].

COB is a close structural analog of cyclooctatin, a compound known to be produced by *S. melanosporofaciens* MI614-43F2. Recently, the biosynthetic gene cluster of cyclooctatin in *S. melanosporofaciens* MI614-43F2 was cloned and characterized [29]. The study revealed a *de novo* biosynthetic pathway, in which geranylgeranyl diphosphate (GGDP) synthase (CotB1), terpene cyclase (CotB2), and two putative cytochrome P450 oxidases (CotB3 and CotB4) mediate the assembly of cyclooctatin from isopentenyl diphosphate (IPP) and dimethylallyl diphosphate (DMADP) (Figure III.11). The structural similarity between cyclooctatin and COB indicates that the latter is

biosynthesized in a similar manner in *Streptomyces griseus* MTE4a, which, however, has an additional oxidase to put the hydroxyl group on C-17.

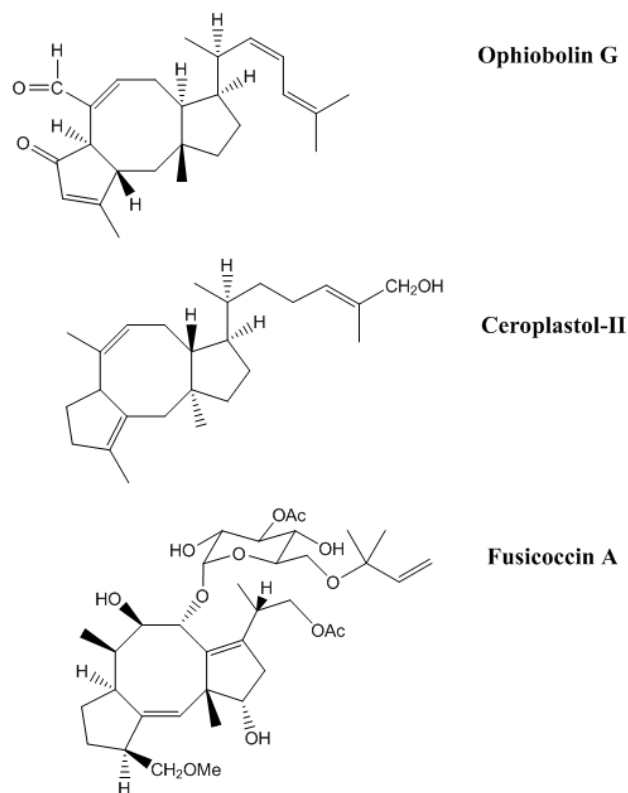


Figure III. 10. Structures of ophiobolin G, fusicoccin A and ceroplastol II isolated from fungi and insects wax.

The biological properties of COB have to be further characterized. For example, it is of our interest to test the anti-inflammatory activity of COB because cyclooctatin, the close structural analog of COB, has been shown to exhibit anti-inflammatory activity through the inhibition of lysophospholipase [37], an enzyme which catalyzes the hydrolysis of the fatty acid ester bonds of lysophospholipids [38, 39]. In addition, side-by-side comparison of COB, cyclooctatin, and their analogs, such as biosynthetic precursors and chemical derivatives, may reveal the structural motifs important for the inhibition of lysophospholipase.

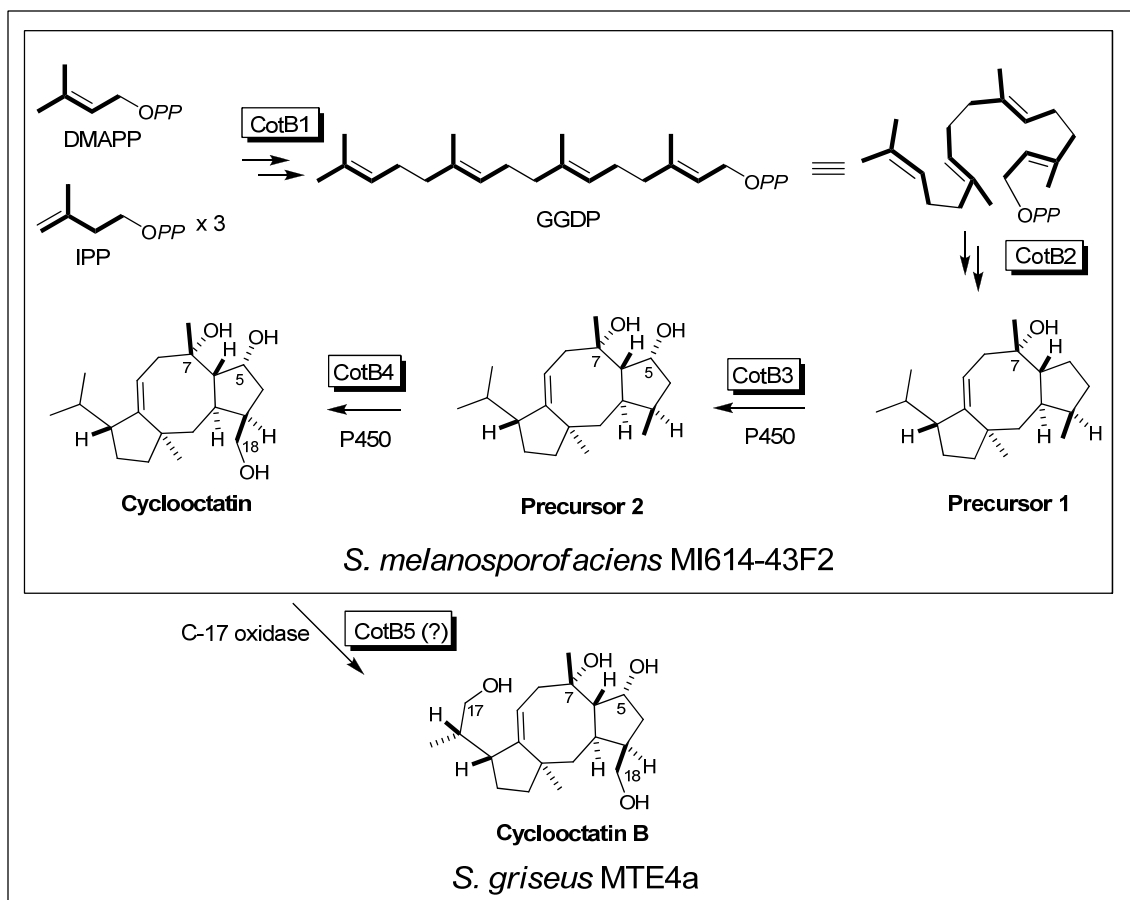


Figure III.11. The biosynthetic pathway of cyclooctatin in *S. melanosporofaciens* MI614-43F2. It is likely that COB is produced through a similar pathway in *S. griseus* MTE4a, which, however, possess an extra oxidase to hydroxylate the C-17 position.

What remains as a mystery is the reason why these bacterial strains expend substantial portions of their genomes for the *de novo* production of cyclooctatins. It is even more puzzling that *S. griseus* MTE4a goes the extra mile to place additional hydroxyl group on the cyclooctatin framework. Another peculiar fact is that, even though COB is acid-sensitive and apparently devoid of antimicrobial activity, *Streptomyces*

griseus MTE4a releases this compound into the soil, which can turn acidic (pH 4-6) when growth competition is high; it is very unlikely that this bacterial strain releases COB just to let it decompose in the soil. These puzzling mysteries could be addressed by one hypothesis; that is, “*COB is acid sensitive by design.*” In this hypothesis, COB is produced as an inert form and meant to be transformed when the microenvironment turns acidic due to high growth competition. In other words, the hypothesis states that cyclooctatins may constitute a new group of pH-sensitive bacterial metabolites.

The unique structure and conformation of COB suggests that the molecule is elaborately crafted to undergo a cascade of organic reactions in acidic soil. While the simple cyclization as seen in chloroform-*d* is one possible reaction (Figure III.8.d), another likely possibility is the formation of tertiary carbocation at C-7, which should be favored in polar environment like moist and acidic soil (Figure III.12.b). Once the C-7 cation is formed, 6-H can be deprotonated intramolecularly by the π -electrons on C-9 because this proton is positioned right above the π -bond: The distance between C-9 and 6-H in COB is approximately 2.7 Å (Figure III.12.a). It is noted that this intramolecular deprotonation is likely to be assisted by 17-OH, which is ideally position to increase the π -electron density on C-9 by pushing the oxygen lone-pair electrons onto C-10. Thus, the formation of ‘Product A’ in Figure III.12.b is anticipated in acidic soil based on the unique structure and conformation of COB. The reaction cascade, however, might not stop here. Because of the newly formed double bond between C-6 and C-7, the 5-OH can be readily eliminated to form an allylic cation. The 18-OH group in this allylic cation can then serve as an intramolecular base to pick up 4-H: The distance between the oxygen of

18-OH and 4-H can be as close as $\sim 2.5\text{\AA}$ (Figure III.12.a). As a result, the formation of 'Product B' can also be anticipated from COB in acidic soil.

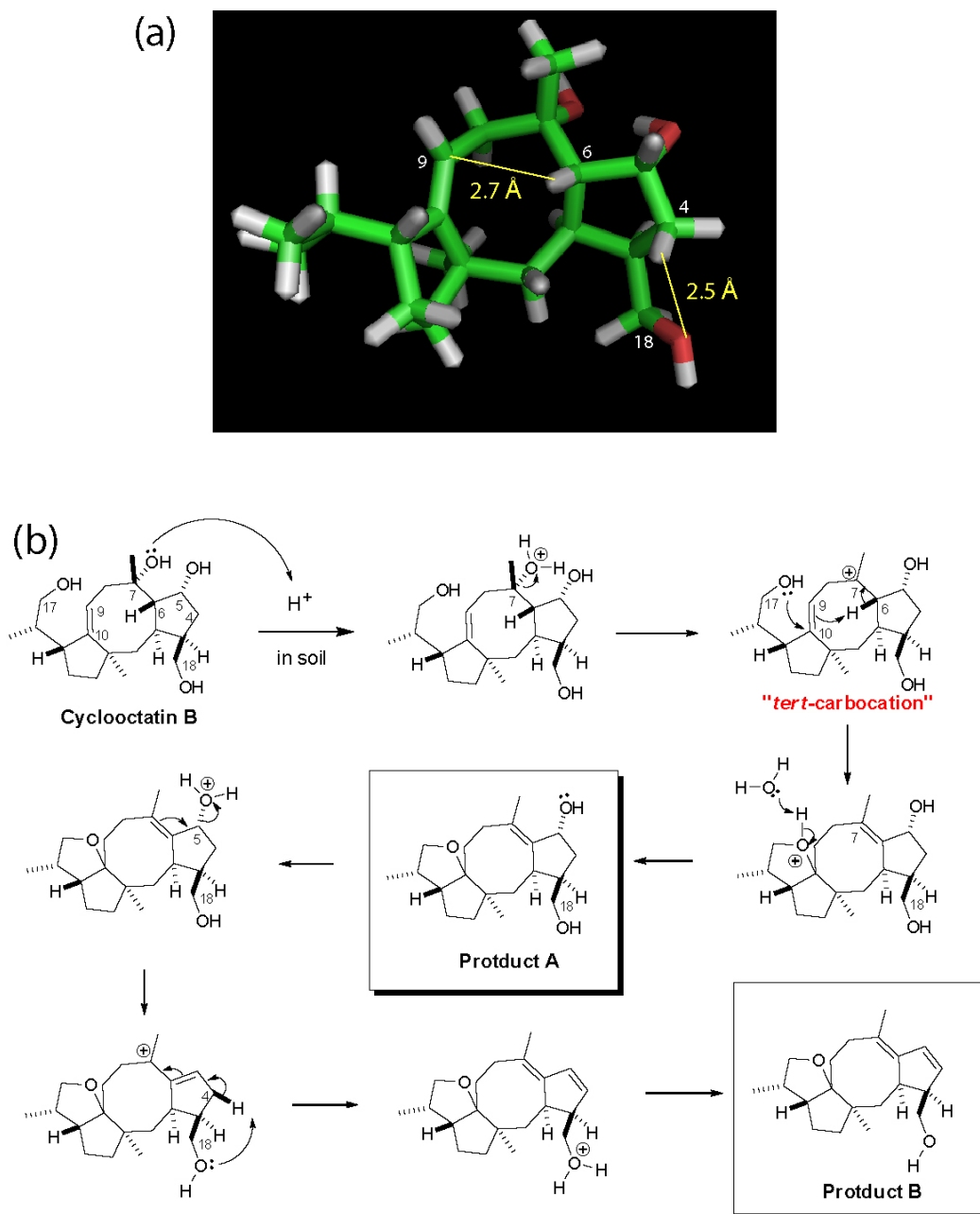


Figure III.12. Possible mechanism of COB transformation in acidic soil.

(a) The sites of intramolecular deprotonation which can be anticipated by the unique structure and conformation of COB. (b) A hypothetical transformation pathway in acidic soil.

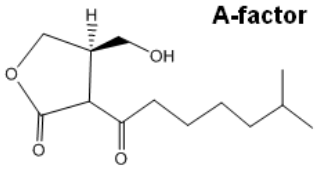
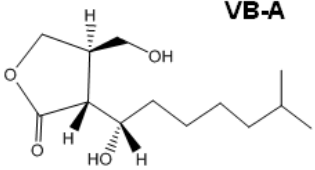
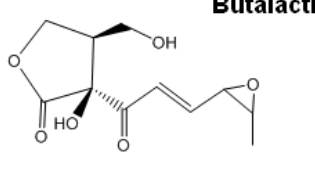
Although the hypothetical transformation pathway described above has to be tested experimentally, it offers a clear chemical reason for the placement of the “extra” 17-OH in COB. As evidenced by the facile THF ring formation from COB in chloroform-*d* (Figure III.8), the 17-OH group is placed in a strategic position to press the oxygen lone pair onto C-10. As a result, C-9 of COB is expected to be more basic than that of cyclooctatin. If an acidic proton approaches C-9, 17-OH would quickly attack C-10 and completes the cyclization-deprotonation cascade. In hydrophobic and aprotic solvents like chloroform-*d*, which disfavors the formation of carbocations, C-9 cannot find intramolecular proton donor and has to wait for an acidic proton to come around from the solvent. In moist and acidic soil, which can facilitate the formation of tertiary carbocation at C-7, C-9 can capture 6-H as soon as the tertiary carbocation forms. It is noted that cyclooctatin can also undergo similar cascade reactions, but the reactions are expected to be slower because of the absence of 17-OH. It is remarkable that *S. griseus* MTE4a has somehow acquired an extra biosynthetic gene to fine-tune the chemical reactivity of the cyclooctatin ring.

Our findings warrant further studies to characterize chemical and biological properties of acid-transformed products from COB. Such studies may establish a new paradigm of “pH-sensing bacterial metabolites,” which have not been explored in the traditional screenings of soil bacteria. Such molecular pH-sensor can possibly be used for various applications, including pharmaceutical and material science. In addition, it is possible that the real biological activity of COB is revealed after acid transformation. Detailed chemical characterizations of acid-treated COB, followed by biological screenings of the resulting products have to be carried out to address these questions.

The discovery of COB suggests the presence of a hitherto uncharacterized cyclooctatin C-17 oxidase in *Streptomyces griseus* MTE4a. Characterization of this gene would open a new opportunity to generate C-17 derivatives of cyclooctatin through metabolic engineering. The resulting cyclooctatin derivatives may serve as new pH-sensitive building blocks to explore chemical and pharmacological spaces, which cannot be readily accessible with the existing methods in organic synthesis.

It is intriguing to speculate the reason why *Streptomyces griseus* MTE4a produces acid-sensitive molecules devoid of antibiotic activity in the environment which can turn acidic at high growth competition. One possible explanation is quorum sensing. Quorum sensing is the cell-cell communication in bacteria achieved by the secretion of chemical signals [40]. This ability to communicate within and between species is critical for bacterial survival and interaction in the different competent microenvironments [40]. During the growth of a culture when a certain cell density can be reached, signaling molecules, such as acyl-homoserine lactones, and α -hydroxyketones [41], are produced for cell-cell communication. It is well-known that *Streptomyces griseus* produces A-factor (2-isocapryloyl-3*R*-hydroxymethyl- γ -butyrolactone) (Table III.2), which regulates morphological differentiation and the production of secondary metabolites [42, 43]. Although A-factor and its structural analogs (Table III.2) are well known for the quorum sensing in *Streptomyces sp.*[44, 45], there remain a possibility that other metabolites with unknown functions, including COB, may play unique roles in the quorum sensing of the producing bacteria.

Table III.2. Structure, biological activities and occurrence of A-factor analogues [45].

Factor	Producer	Biological activity
<p>A-factor</p> 	<i>Streptomyces griseus</i>	Streptomycin Sporulation
<p>VB-A</p> 	<i>S. Virginiae</i>	Virginiamycin
<p>Butalactin</p> 	<i>Streptomyces sp. Y-86, 36923</i>	Antibiotic activity

In conclusion, our screening of secondary metabolites in culturable soil Actinomycetes discovered a novel diterpene, COB. Our preliminary structural and chemical studies indicated that COB may constitute a new class of pH-sensing bacterial metabolites, which may open a new opportunities for various applications, such as pH-sensing materials, insecticides, antimicrobials, and pharmaceuticals. Further studies are underway to characterize the biosynthetic genes responsible for COB production.

III.8. Materials and Methods

Materials: All solvents for purification were in the HPLC grade and were purchased from VWR and Fisher Scientific. Unless specified otherwise, all other chemicals and reagents were obtained through Fisher Scientific and used without further purification. HPLC analysis and purification were carried on an Agilent 1100 Series, using a ChemStation operating system. HPLC was equipped to an Agilent 1100 photodiode array detector and an Evaporative Laser Light Scattering detector (ELSD) model 800. HPLC column used in this study was Eclipse-XD8 C₈ 4.6 × 150 mm analytical column (Agilent). NMR spectra were recorded on a Bruker 500 MHz instrument.

MTF1 media preparation (per liter): the medium is composed of: yeast extract, 1 g; tryptone, 10 g; K₂HPO₄, 0.5 g; glycerol, 8 g; dextrose, 2 g in 1L distilled water (adjusted pH 7.1-7.3).

Difco™ nutrient broth (DNB) (per liter): beef extract, 3g; peptone, 5g.

MTE4a collection and culture: MTE4a was isolated from soil obtained from 1319 Woodland Valley Road, Phoenicia, NY (a state park upstate NY). Two media were used for isolation of Actinomycetes: Glycerol-Yeast extract Agar (GYEA) and Difco Actinomycetes Isolation Agar (AIA). Both media contained the antifungal cyclohexamide (50 mg/L). Purification of the isolated culture was performed using Soy Flour Mannitol (SFM) Agar (Soy Flour 20 g/L; mannitol 20 g/L; agar 20 g/L). After purification, spores were used to inoculate liquid cultures. 50 ml of DNB were inoculated with a loop of spores and shaken at room temperature at 200 rpm for 3 days. Sterile glass beads were added to the flask to disperse the growth of Streptomyces. On the third day 10 ml of the inoculum were added to 125 ml of sterile MTF1 (250 mL flasks). The cultures were grown at room temperature and 200 rpm for seven days and the supernatant was collected.

Purification of COB: 7 L of MTE4a culture was centrifuged for 30 minutes at 6000 rpm at 4°C in order to completely separate the cells from the supernatant. The supernatant (around 6 L) was then extracted with the same amount of EtOAc (use 600 ml per extraction, total 10 extractions). The mixture were shaken and vented 3 times and the layers were allowed to separate. For better separation of the two layers saturated NaCl was used (10-20% per volume). Both organic and aqueous layers were collected into separate flasks. The organic fraction was dried using anhydrous MgSO₄ and the drying agent was removed by vacuum paper filtration. Then the organic fraction was dried from the solvent under reduced pressure and 3 g were recovered. The dried extract was re-dissolved in a minimum amount of dichloromethane to which silica gel 60 was added. The entire sample was dried again in Rotovap until silica was fully dry. A 53 cm × 3.5 cm column was prepared with 30 g of silica bedding. The column was dry packed and washed with hexane. The sample was eluted with 100% hexane (Fraction A), 95:5 hexane:EtOAc (Fraction B), 90:10 hexane:EtOAc (Fraction C) and 90:10 CH₂Cl₂:MeOH (Fraction D). Fraction D was further separated with silica gel chromatography: Fraction D was loaded on to a silica gel open column (15 cm × 1 cm i.d.) and eluted with a step-gradient (0-10% MeOH in CH₂Cl₂) over 20 fractions (approximately 10 ml/fraction). Fractions 15-18, which contained COB, were combined and further purified with RP-HPLC (C₁₈ analytical column, 1 ml/min, 20-80% MeOH_{aq.} over 30 min). HPLC eluent was monitored with photodiode array (PDA) detector and evaporative light scattering detector (ELSD). The major ELSD peak at 22.5 min was collected and dried to give a colorless and clear solid of COB (2 mg).

DNA extraction of MTE4a: DNA extraction from purified cultures was performed using the Wizard Genomic DNA Purification kit. 3ml of MTE4a strain grown in DNB for 48 hours were centrifuged at 13,000 × g for 2 min. The supernatant was discarded and the cells were suspended in 480µl 50Mm EDTA. 120 µl of lysozyme were added and the tube was incubated at 37 °C for 30 minutes. After centrifuging the tube for 2 min at 13,000-16,000 × g the supernatant was discarded and the cells were lysed by adding 600µl of Nuclei Lysis Solution. The mixture was incubated for 5 minutes at 80°C and then cooled to room temperature. RNA was removed by treatment with RNase and then

proteins were precipitated by adding 200µl of protein precipitation Solution. After incubating on ice for 5 minutes the solution was centrifuged at 13,000-16,000 × g for 3 min. DNA was precipitated by transferring the supernatant to a clean tube containing 600µl of room temperature isopropanol. The pellet was washed with 600µl of room temperature 70% ethanol. The pellet obtained after centrifuging at 13,000-16,000 × g for 2 min was air-dried for 10-15 minutes. The DNA pellet was resuspended in 100µl of Rehydration Solution for 1 hour at 65°C or overnight at 4°C.

PCR: PCR was done using KOD polymerase (Novagen) and Actinomycete's specific primers: ActF-CGCGGCCTATCAGCTTGTTG; ActR CCGTACTCCCCAGGCGGGG. Reactions were setup according to manufacture's protocol. PCR program: Initial denaturation at 95°C for 4 min, followed by 35 cycles of 95°C for 30s and 70°C for 1 min. PCR products were separated on 2% agarose gel and stained with SYBR[®] Green I Nucleic Acid Stain from Lonza.

Antimicrobial activity test against *Staphylococcus aureus*: a "lawn" of *Staphylococcus aureus* was prepared by adding and spreading 100 µl of the bacterium on a TSA plate. Then 10 µl of the sample to be tested was spiked on the plate (1mg/ml) and the plate was incubated overnight at 37 °C. The following day the inhibition of *Staphylococcus aureus* growth was checked.

NMR: NMR spectra of COB (2 mg) in CDCl₃ and methanol-*d*₄ were recorded by Brüker Avance 500MHz Spectrometer equipped with a dual [¹³C, ¹H] CryoProbe. Data were acquired and processed with the Brüker XWIN-NMR software package. ¹H-NMR spectra was collected with a total of 64 scans, ¹H-¹H COSY with 2 scans, ¹³C-NMR and DEPT with 7000 scans, HMBC with 60 scans and HSQC with 90 scans.

III. 9. References:

1. Goodfellow, M., Williams, S. T., Mordarski, M., *Actinomycetes in Biotechnology*. 1988, San Diego: Academic Press. 501.
2. Gragg, G.M., Newman, D. J., Snader, K. M., Natural products in drug discovery and development. *J. Nat. Prod.*, 1997. **60**(1): p. 52-60.
3. Harvey, A., Strategies for discovering drugs from previously unexplored natural products. *Drug Disc. Today*, 2000. **5**: p. 294-300.
4. Sonia-Mercado, I.E., Prieto-Davo, A., Jensen, P. R., Fenical, W., Antibiotic terpenoid chloro-dihydroquinones from a new marine actinomycete. *J. Nat. Prod.*, 2005. **68**: p. 904-10.
5. Watve, M.G., Tickoo, R., Jog, M. M., Bhole, B. D., How many antibiotics are produced by the genus *Streptomyces*? *Arch. Microbiol.*, 2001. **176**: p. 386-90.
6. Vanden Bossche, H., Engelen, M., Rochette, F., Antifungal agents of use in animal health--chemical, biochemical and pharmacological aspects. *J.Vet. Pharmacol. Ther.*, 2003. **26**(1): p. 5-29.
7. Torrado, J.J., Espada, R., Ballesteros, M. P., Torrado-Santiago, S., Amphotericin B formulations and drug targeting. *J. Pharm. Sci.*, 2008. **97**(7): p. 2405-25.
8. Vezina, C., Kudelski, A., Sehgal, S. N., Rapamycin (AY-22,289), a new antifungal antibiotic. I. Taxonomy of the producing streptomycete and isolation of the active principle. *J. Antibiot. (Tokyo)*, 1975. **28**(10): p. 721-26.
9. Kim, H.S., Park, Y. I., Isolation and Identification of a Novel Microorganism Producing the Immunosuppressant Tacrolimus. *Journal of Bioscience and Bioengineering*, 2008. **105**(4): p. 418-21.
10. Nakae, K., Yoshimoto, Y., Sawa, T., Homma, Y., Hamada, M., Takeuchi, T., Imoto. M., Migrastatin, a new inhibitor of tumor cell migration from *Streptomyces* sp. MK929-43F1. Taxonomy, fermentation, isolation and biological activities. *J. Antibiot. (Tokyo)*, 2000. **53**(10): p. 1130-6.
11. Van Lanen, S.G., Shen, B., Microbial genomics for the improvement of natural product discovery. *Curr. Opin. Microbiol.*, 2006. **9**: p. 252-60.
12. Baltz, R.H., Antibiotic discovery from actinomycetes: will a renaissance follow the decline and fall? *SIM news*, 2005. **55**: p. 186-196.

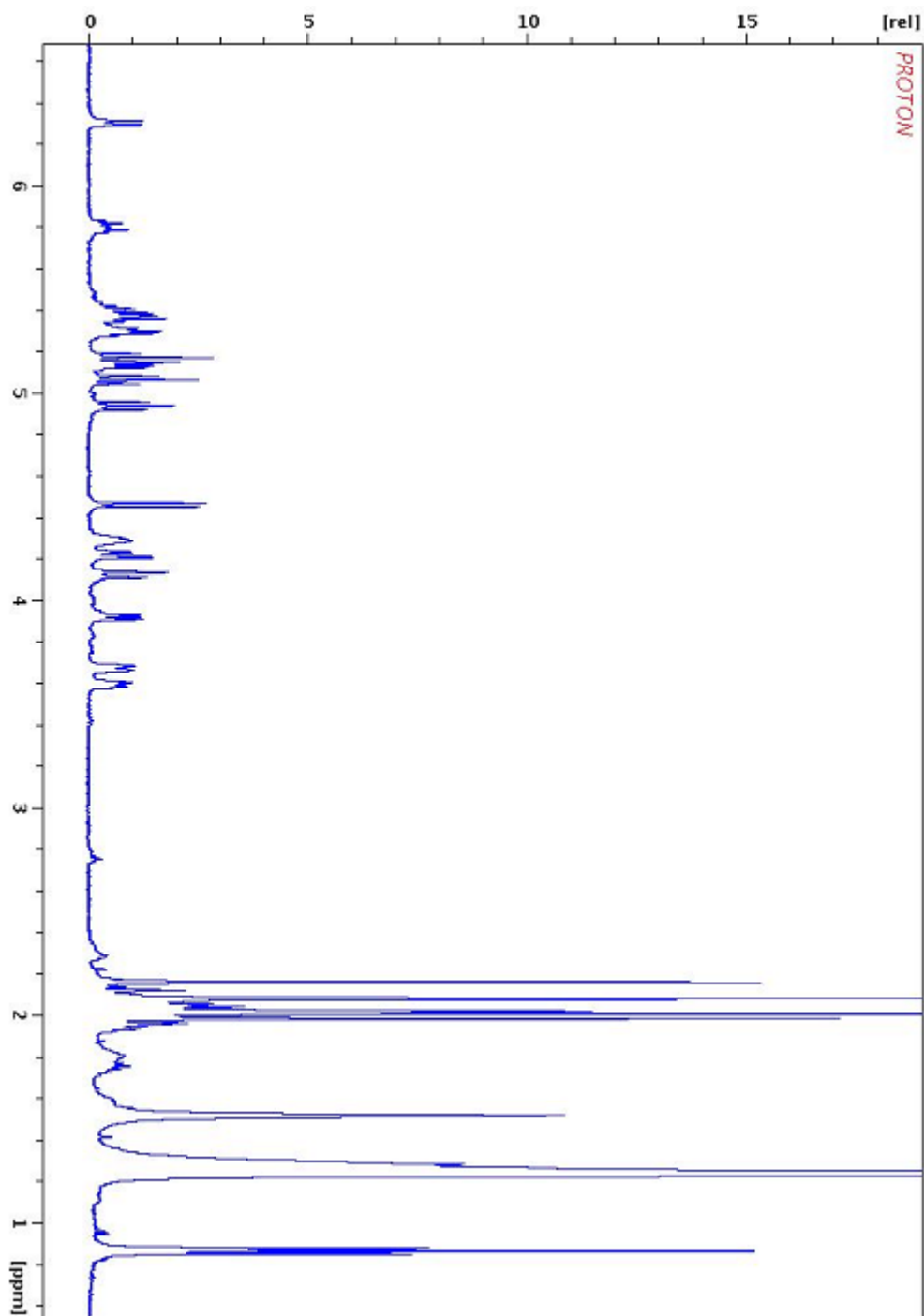
13. Fenical, W., Marine soft corals of the genus *Pseudopterogorgia*: a resource for novel anti-inflammatory diterpenoids. *J. Nat. Prod.*, 1987. **50**(6): p. 1001-8.
14. Jensen, P.R., Mincer, T. J., Williams, P. G., Fenical, W., Marine actinomycete diversity and natural product discovery. *Antonie Van Leeuwenhoek*, 2005. **87**(1): p. 43-8.
15. Fusetani, N., Antifungal substances from marine invertebrates. *Ann. N. Y. Acad. Sci.*, 1988. **544**: p. 113-27.
16. Nakao, Y., Fusetani, N., Enzyme inhibitors of marine invertebrates. *J. Nat. Prod.*, 2007. **70**(4): p. 689-710.
17. Li, J.W., Vederas, J. C., Drug discovery and natural products: end of an era or an endless frontier? *Science*, 2009. **325**(5937): p. 161-5.
18. Ohnishi, Y., Ishikawa, J., Hara, H., Suzuki, H., Ikenoya, M., Ikeda, H., Yamashita, A., Hattori, M., Horinouchi, S., Genome sequence of the Streptomycin-producing microorganism *Streptomyces griseus* IFO 13350. *J. Bacteriol.*, 2008. **190**(11): p. 4050-60.
19. Hopwood, D.A., Antibiotics: opportunities for genetic manipulation. *Philos. Trans. R. Soc. Lond. B. Biol. Sci.*, 1989. **324**(1224): p. 549-62.
20. Khosla, C., Keasling, J. D., Metabolic engineering for drug discovery and development. *Nat. Rev. Drug Discov.*, 2003. **2**(12): p. 1019-25.
21. McDaniel, R., Licari, P., Khosla, C., Process development and metabolic engineering for the overproduction of natural and unnatural polyketides. *Adv. Biochem. Eng. Biotechnol.*, 2001. **73**: p. 31-52.
22. Burke, M.D., Schreiber, S. L., A planning strategy for diversity-oriented synthesis. *Angew. Chem. Int. Ed. Engl.*, 2004. **43**(1): p. 46-58.
23. Tan, D.S., Diversity-oriented synthesis: exploring the intersections between chemistry and biology. *Nat. Chem. Biol.*, 2005. **1**(2): p. 74-84.
24. Cutler, H.G., Crumley, F. G., Cox, R. H., Springer, J. P., Arrendale, R. F., Cole, R. J., Cole, P. D., Ophiobolins G and H: New fungal metabolites from a novel source, *Aspergillus ustus*. *J. Agric. Food Chem.*, 1984. **32**(4): p. 778-82.
25. Sugawara, F., Strobel, G., Strange, R. N., Siedow, J. N., Van Duyne, G. D., Clardy, J., Phytotoxins from the pathogenic fungi *Drechslera maydis* and *Drechslera sorghicola*. *Proc. Natl. Acad. Sci. USA*, 1987. **84**: p. 3081-85.

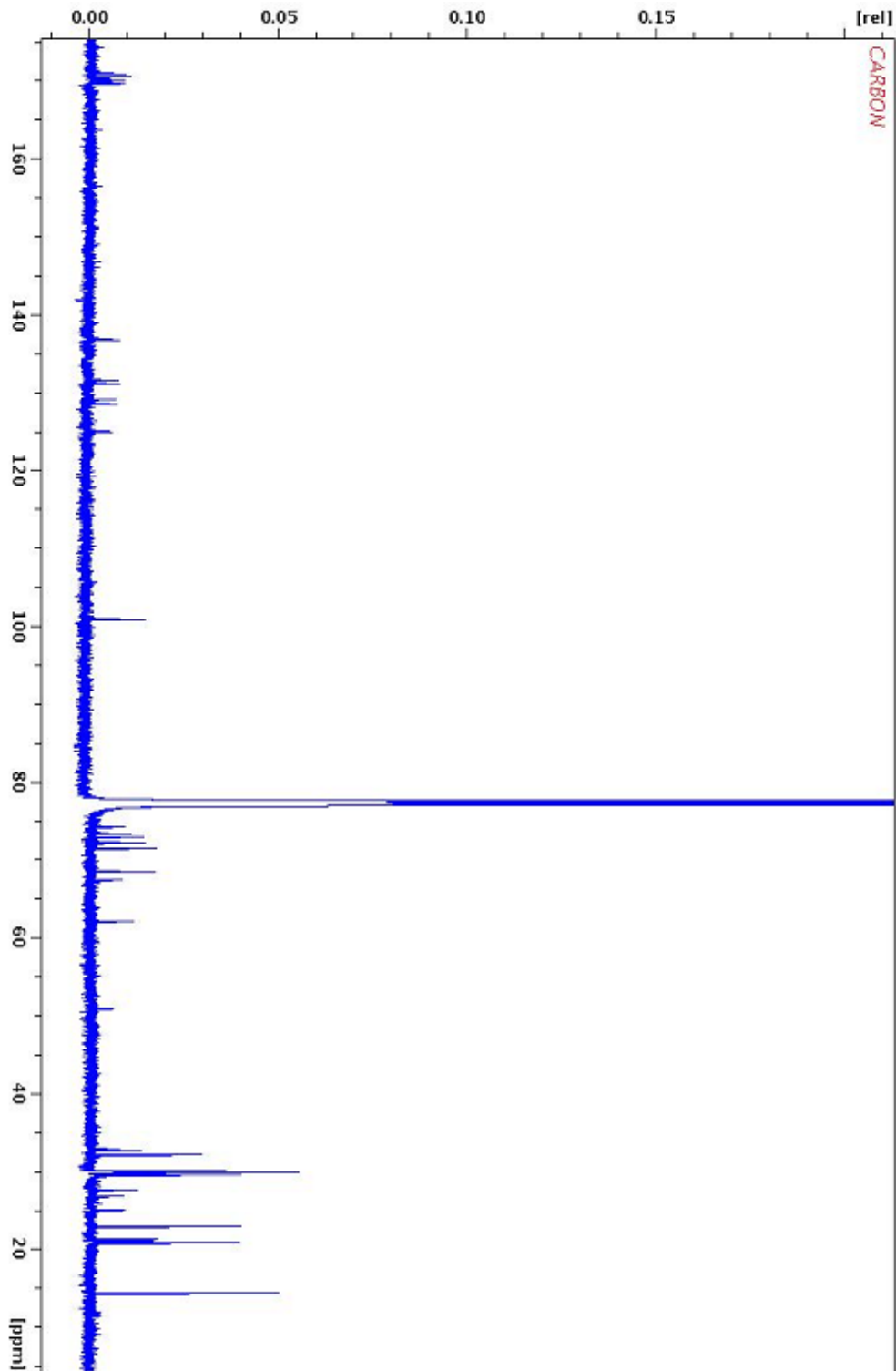
26. Ríos, T., Quijano, L., The structure of ceroplastol II a sesterterpenic alcohol isolated from insects wax. *Tetrahedron Lett.*, 1969. **17**: p. 1317-18.
27. Sassa, T., Tajima, N., Sato, M., Takahashi, A., Kato, N., Fusicoccins P and Q, and 3-epifusicoccins H and Q, new polar fusicoccins from isolate Niigata 2-A of a peach Fusicoccum canker fungus. *Biosci. Biotechnol. Biochem.*, 2002. **66**(11): p. 2356-61.
28. Aoyama, T., Naganawa, H., Muraoka, Y., Aoyagi, T., Takeuchi, T., The structure of cyclooctatin, a new inhibitor of lysophospholipase. *J. Antibiot. (Tokyo)*, 1992. **45**(10): p. 1703-4.
29. Kim, S.Y., Zhao, P., Igarashi, M., Sawa, R., Tomita, T., Nishiyama, M., Kuzuyama, T., Cloning and heterologous expression of the cyclooctatin biosynthetic gene cluster afford a diterpene cyclase and two p450 hydroxylases. *Chem. Biol.*, 2009. **16**(7): p. 736-43.
30. Au, T.K., Chick, W. S., Leung, P. C., The biology of ophiobolins. *Life Sci.*, 2000. **67**(7): p. 733-42.
31. Ballio, A., Brufani, M., Casinovi, C. G., Cerrini, S., Fedeli, W., Pellicciari, R., Santurbano, B., Vaciago, A., The structure of fusicoccin A. *Experientia*, 1968. **24**(6): p. 631-5.
32. Ríos, T., Quijano, L., The structure of ceroplastol II a sesterterpenic alcohol isolated from insects wax. *Tetrahedron Lett.*, 1969. **17**: p. 1317-8.
33. Motohashi, K., Sue, M., Furihata, K., Ito, S., Seto, H., Terpenoids Produced by Actinomycetes: Napyradiomycins from *Streptomyces antimycoticus* NT17. *J. Nat. Prod.*, 2008. **71**(4): p. 595-601.
34. Shirai, M., Okuda, M., Motohashi, K., Imoto, M., Furihata, K., Matsuo, Y., Katsuta, A., Shizuri, Y., Seto, H., Terpenoids produced by actinomycetes: isolation, structural elucidation and biosynthesis of new diterpenes, gifhornenolones A and B from *Verrucospora gifhornensis* YM28-088. *J. Antibiot. (Tokyo)*, 2010. **63**(5): p. 245-50.
35. Olano, C., Mendez, C., Salas, J. A., Antitumor compounds from marine actinomycetes. *Mar. Drugs*, 2009. **7**(2): p. 210-48.
36. Isshiki, K., Tamamura, T., Takahashi, Y., Sawa, T., Naganawa, H., Takeuchi, T., Umezawa, H., The structure of a new antibiotic, terpentecin. *J. Antibiot. (Tokyo)*, 1985. **38**(12): p. 1819-21.
37. Aoyagi, T., Aoyama, T., Kojima, F., Hattori, S., Honma, Y., Hamada, M., Takeuchi, T., Cyclooctatin, a new inhibitor of lysophospholipase, produced by

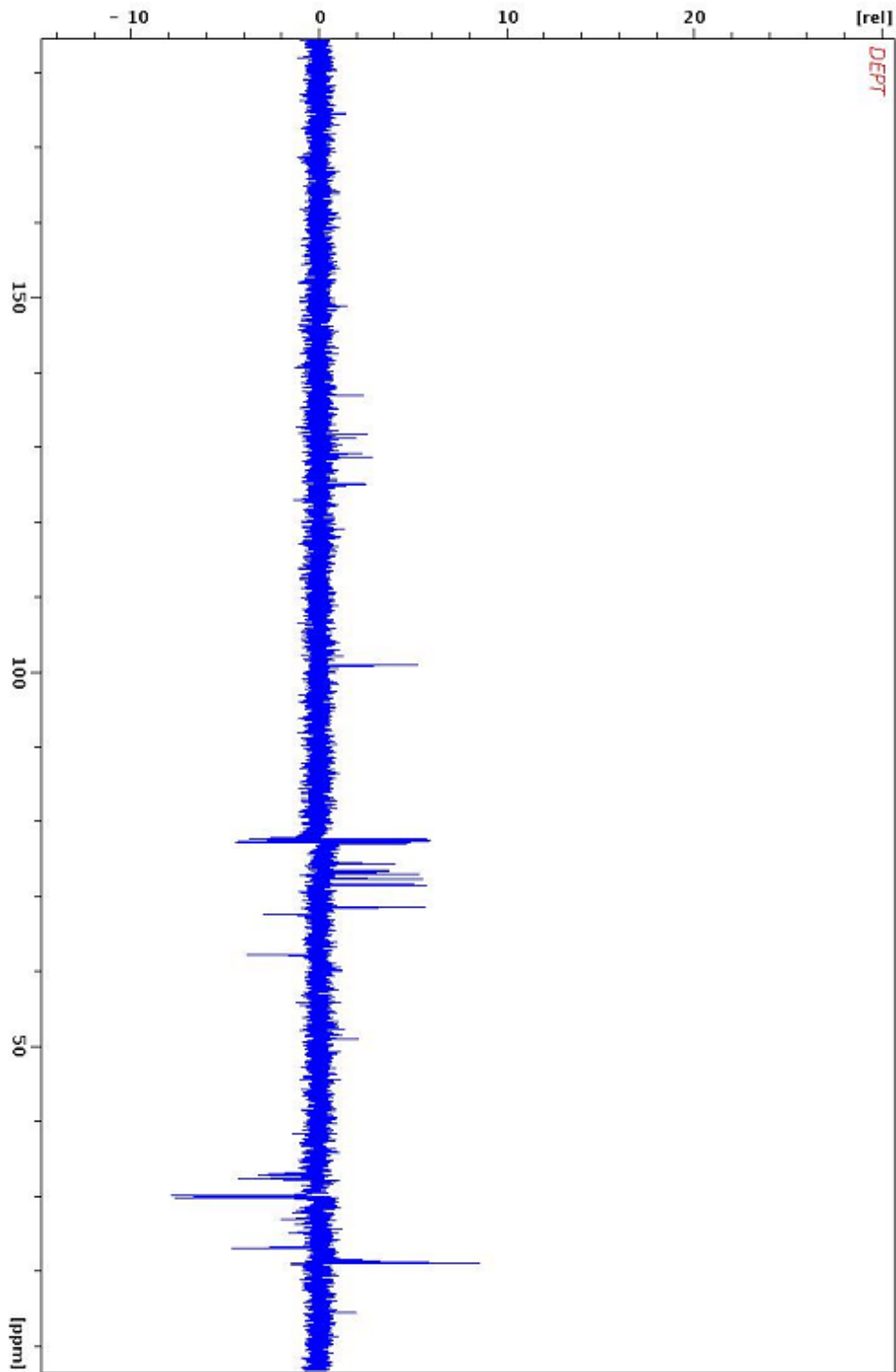
- Streptomyces melanosporofaciens* MI614-43F2. Taxonomy, production, isolation, physico-chemical properties and biological activities. *J. Antibiot. (Tokyo)*, 1992. **45**(10): p. 1587-91.
38. Graler, M.H., Goetzl, E. J., Lysophospholipids and their G protein-coupled receptors in inflammation and immunity. *Biochim. Biophys. Acta*, 2002. **1582**(1-3): p. 168-74.
 39. Chang, D.H., Deng, H., Matthews, P., Krasovsky, J., Ragupathi, G., Spisek, R., Mazumder, A., Vesole, D. H., Jagganath, S., Dhodapkar, M. V., Inflammation-associated lysophospholipids as ligands for CD1d-restricted T cells in human cancer. *Blood*, 2008. **112**(4): p. 1308-16.
 40. Miller, M.B., Bassler, B. L., Quorum sensing in bacteria. *Annu. Rev. Microbiol.*, 2001. **55**: p. 165-99.
 41. Antunes, L.C., Ferreira, R. B., Intercellular communication in bacteria. *Crit. Rev. Microbiol.*, 2009. **35**(2): p. 69-80.
 42. Horinouchi, S., Mining and polishing of the treasure trove in the bacterial genus *Streptomyces*. *Biosci. Biotechnol. Biochem.*, 2007. **71**(2): p. 283-99.
 43. Horinouchi, S., Beppu, T., A-factor and streptomycin biosynthesis in *Streptomyces griseus*. *Antonie Van Leeuwenhoek.*, 1993-1994. **64**(2): p. 177-86.
 44. Horinouchi, S., Beppu, T., Autoregulatory factors and communication in actinomycetes. *Annu. Rev. Microbiol.*, 1992. **46**: p. 377-98.
 45. Beppu, T., Signal transduction and secondary metabolism: prospects for controlling productivity. *Trends Biotechnol.*, 1995. **13**(7): p. 264-9.

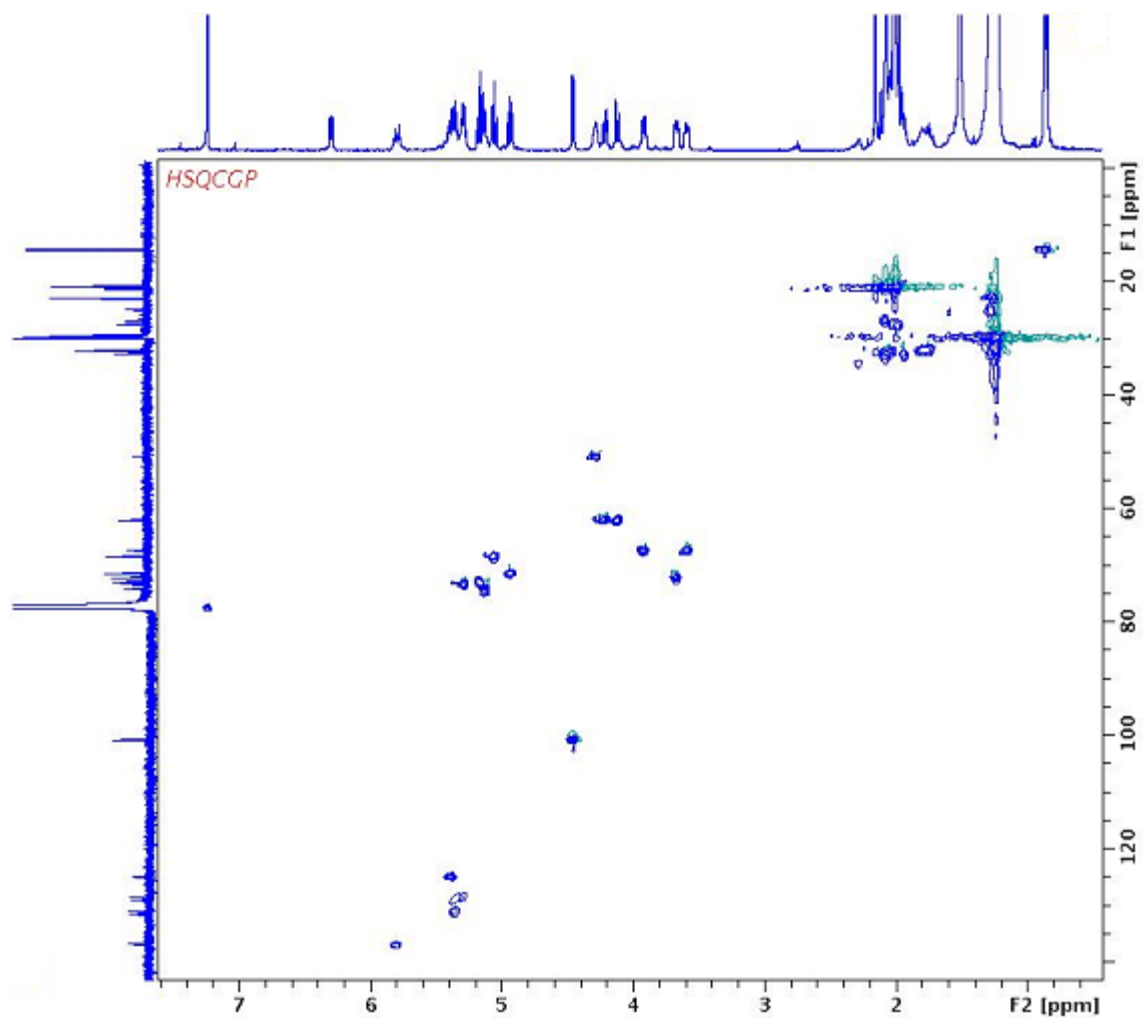
IV. Appendices

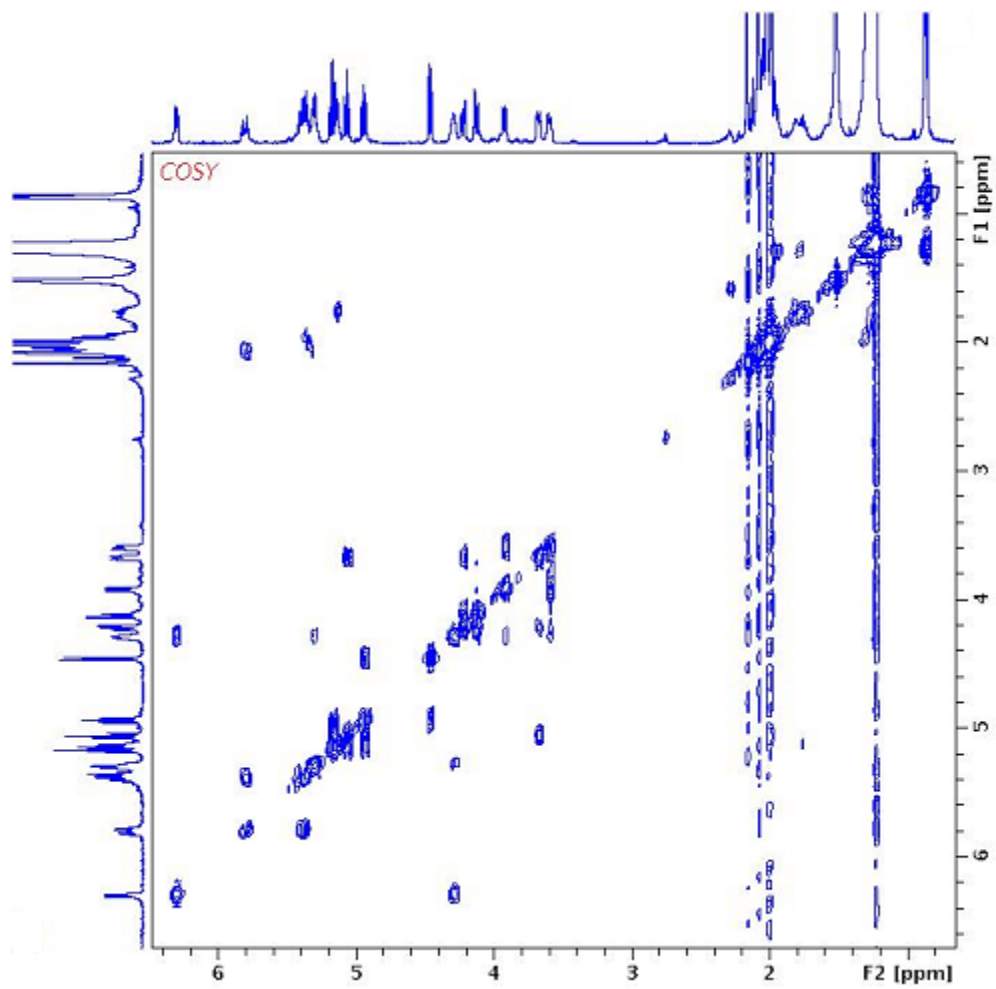
Appendix A: ^1H NMR spectrum of acetylated fraction C (in CDCl_3)

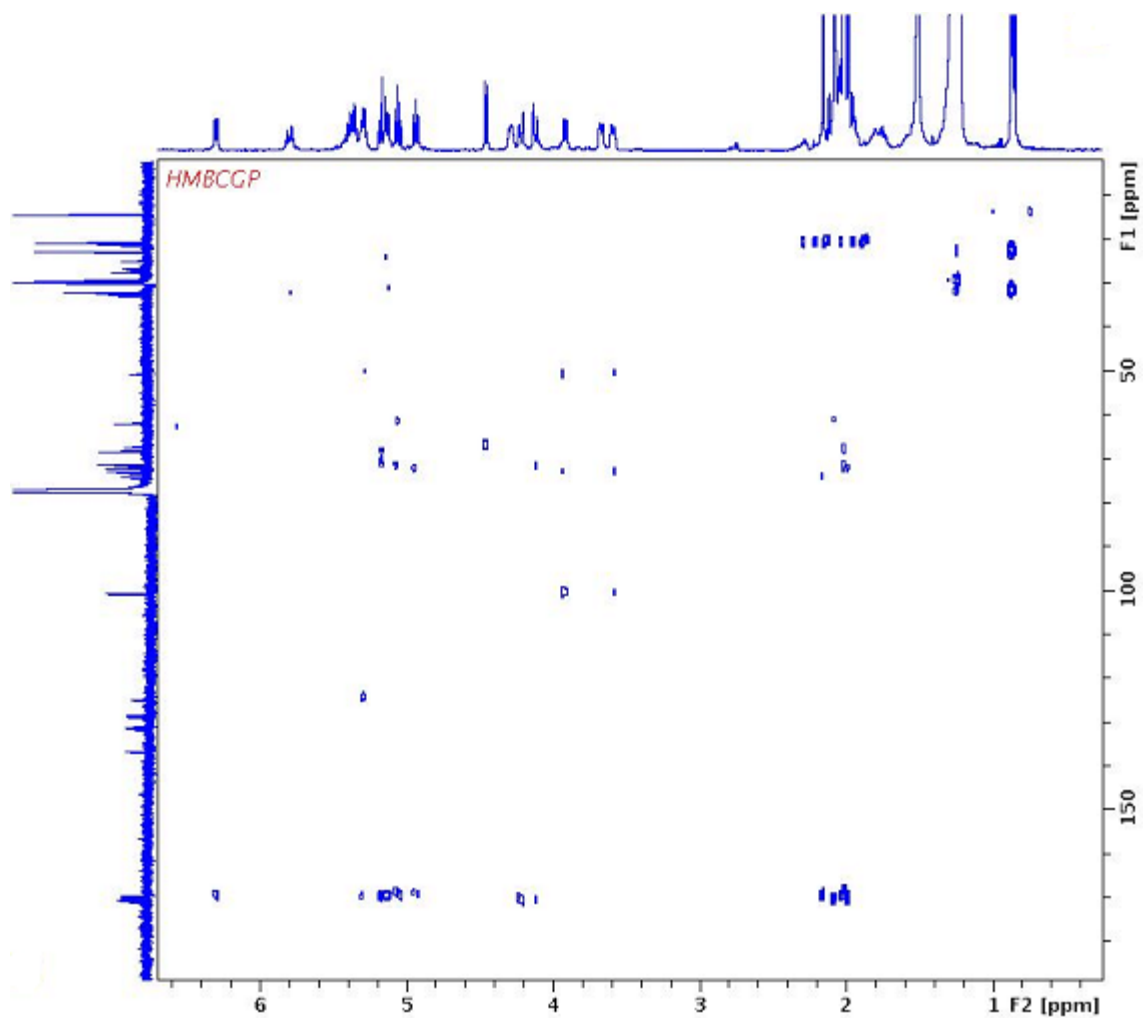


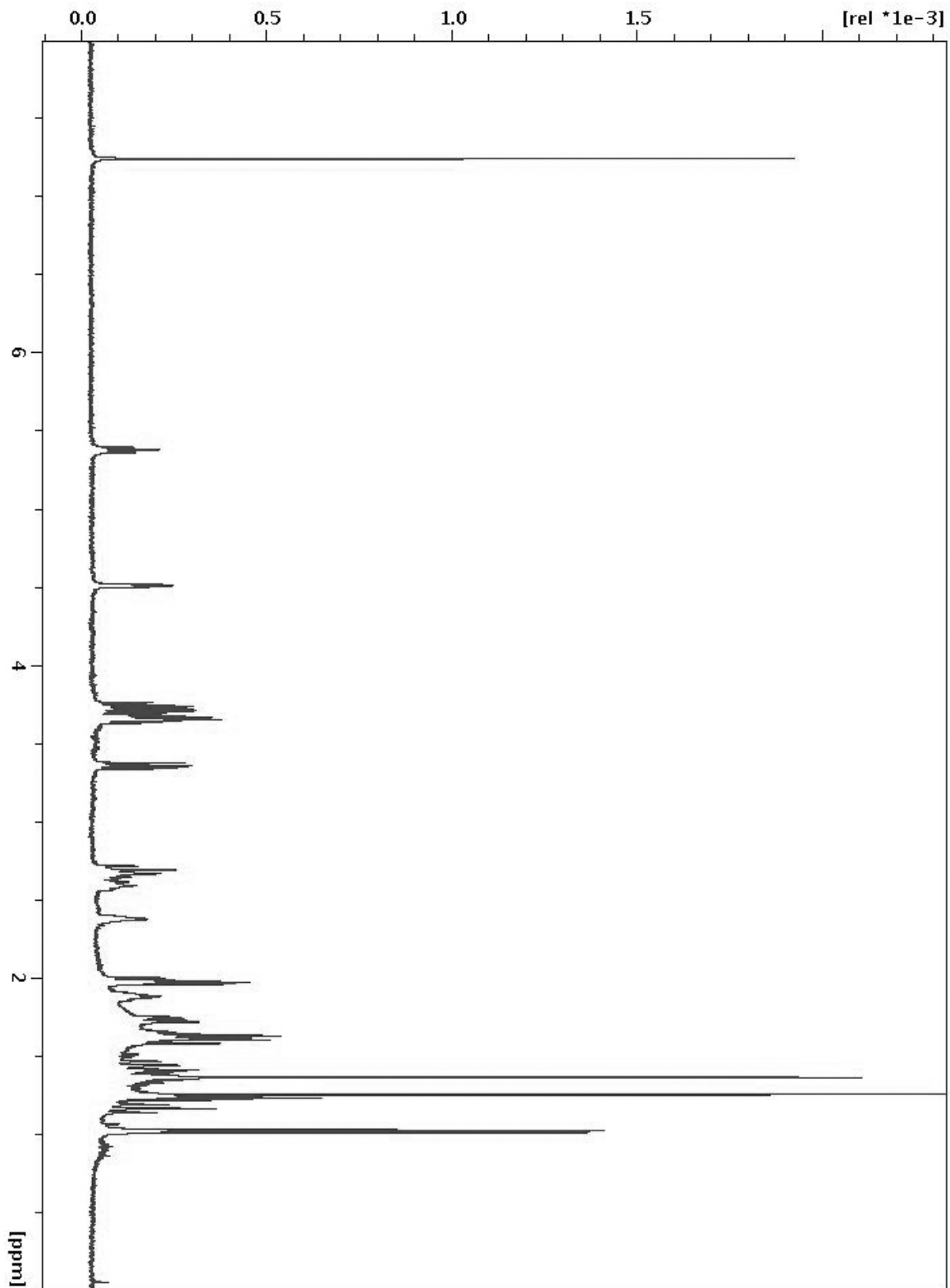
Appendix B: ^{13}C NMR spectrum of acetylated fraction C (in CDCl_3)

Appendix C: DEPT spectrum of acetylated fraction C (in CDCl_3)

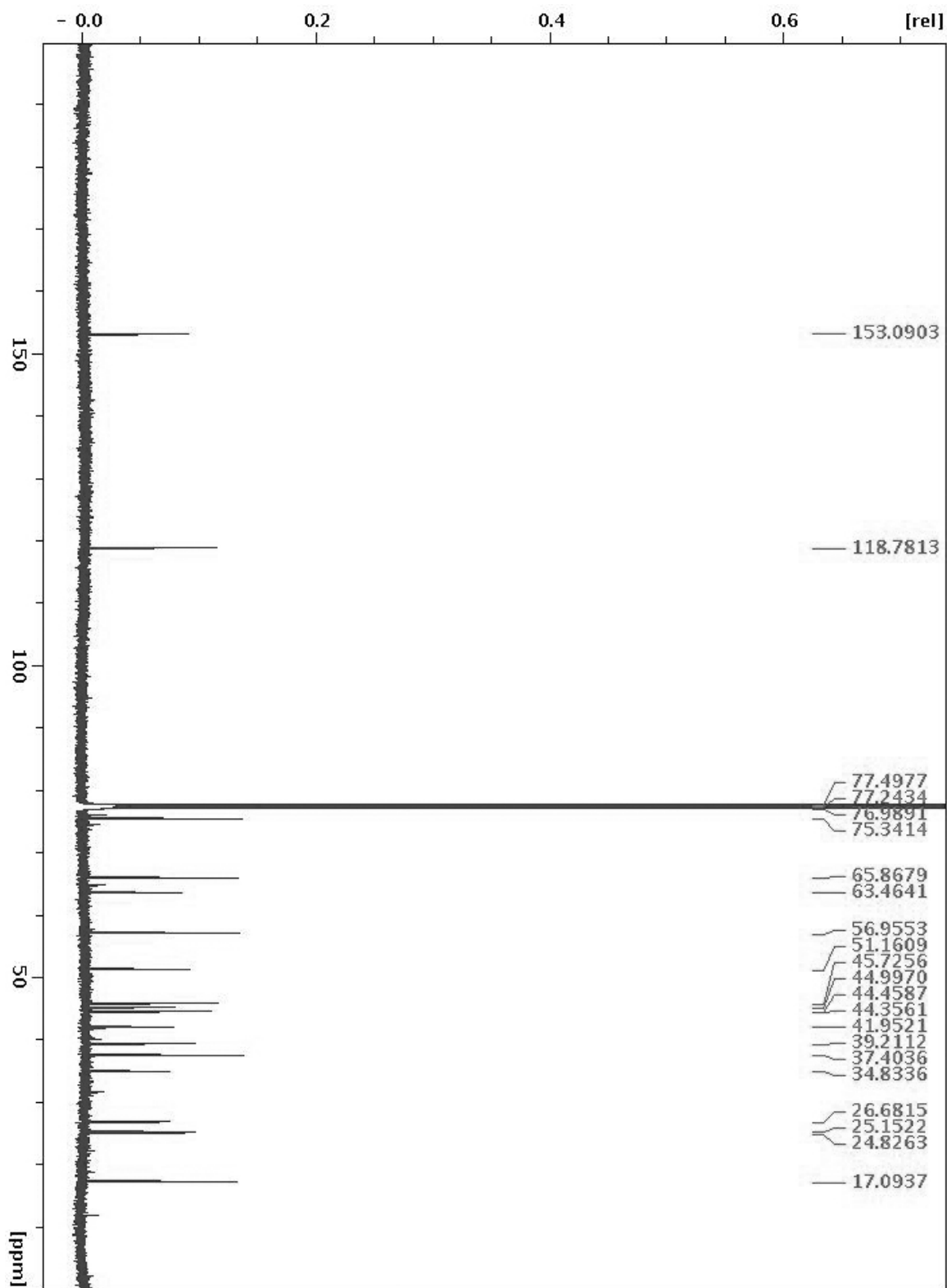
Appendix D: HSQC spectrum of acetylated fraction C (in CDCl₃)

Appendix E: COSY spectrum of acetylated fraction C (in CDCl₃)

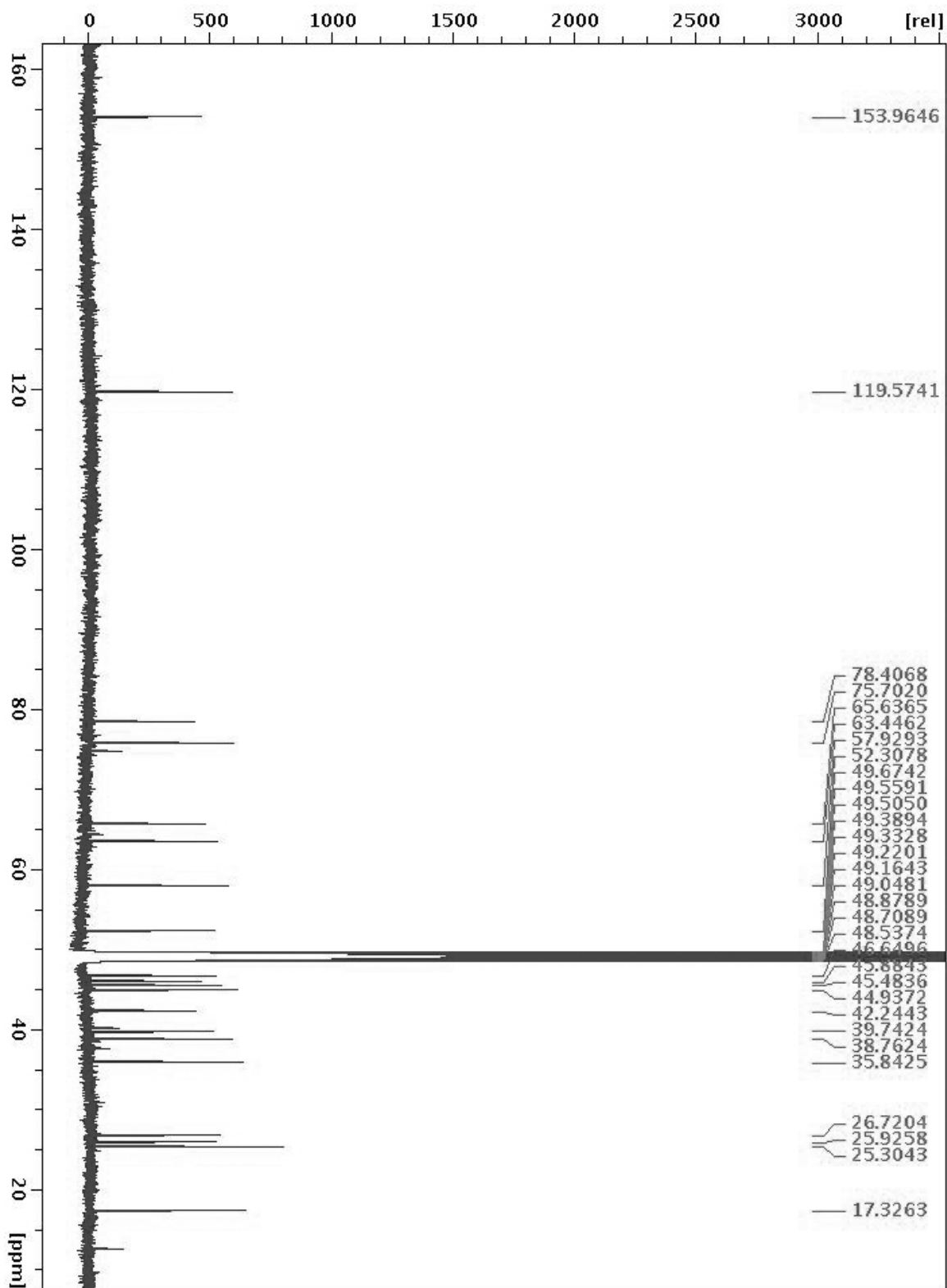
Appendix F: HMBC (4Hz) spectrum of acetylated fraction C (in CDCl₃).

Appendix G: ^1H NMR spectrum of COB in CDCl_3 .

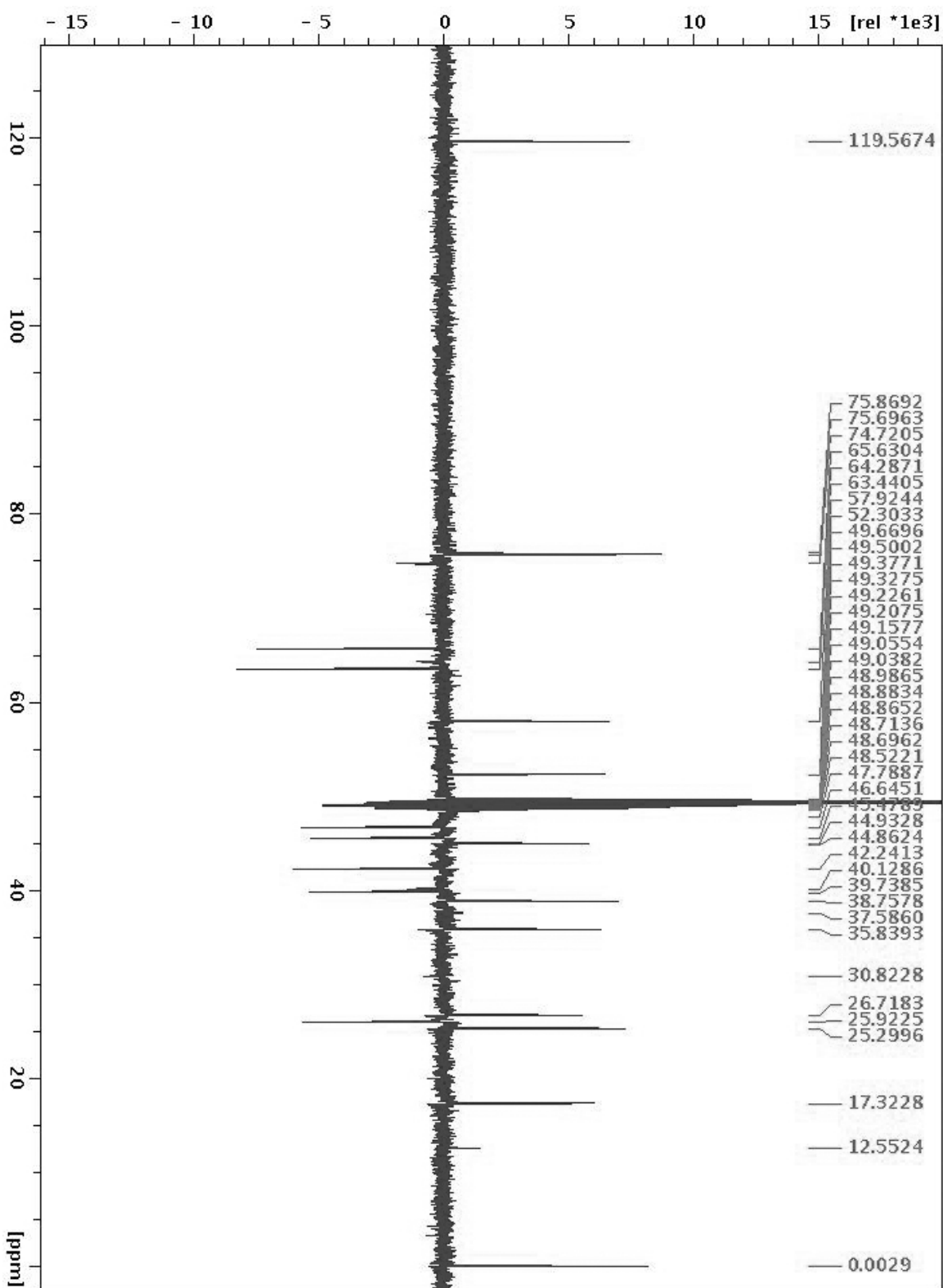
Appendix H: ^{13}C NMR spectrum of COB in CDCl_3 . A small fraction of the sample decomposed during the storage in chloroform-*d* as noted in the main text.



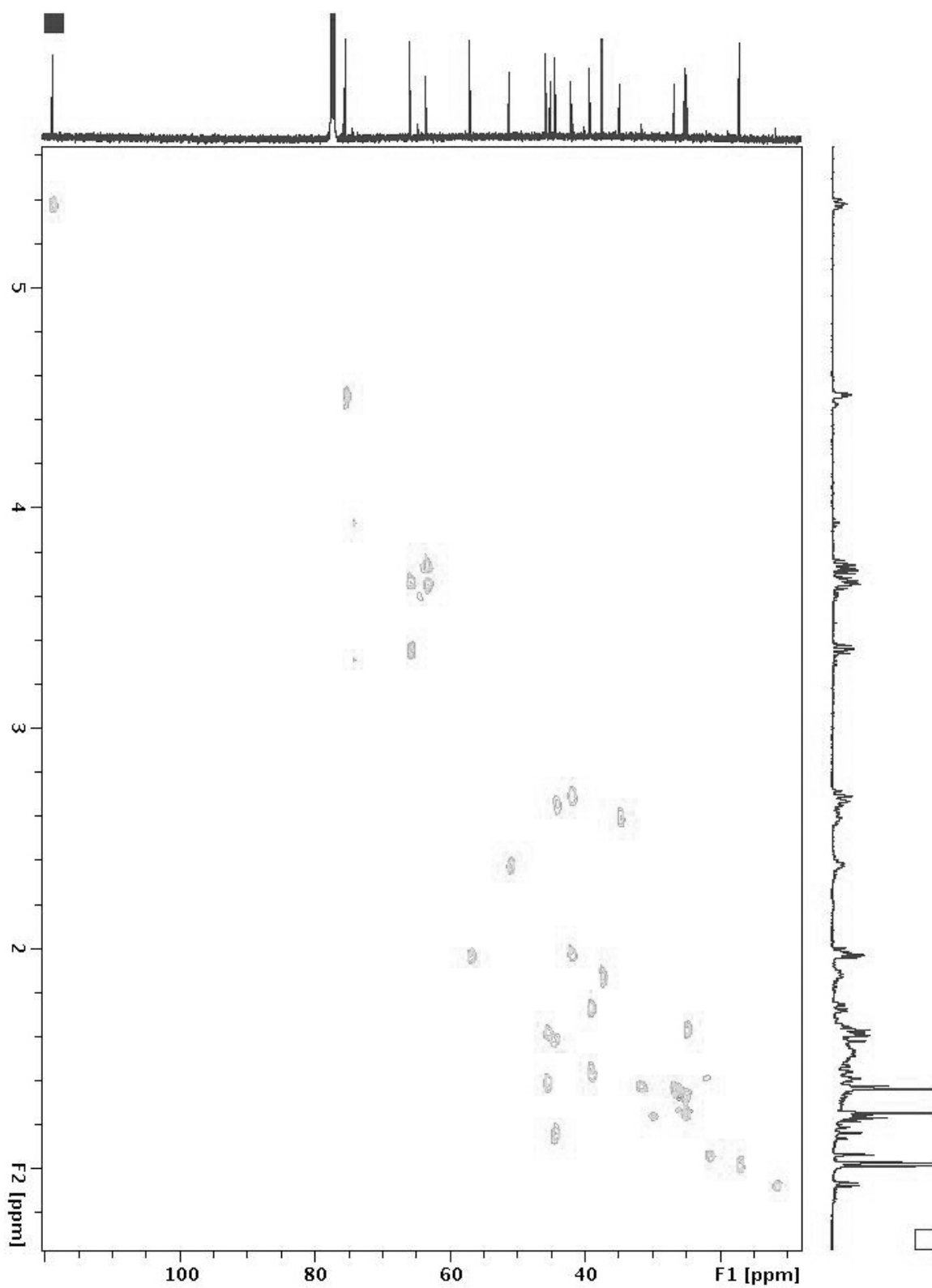
Appendix I: ^{13}C NMR spectrum of COB in methanol- d_4 . This measurement was conducted because one of the carbon singals overlapped with the solvent peak in chloroform- d . A small fraction of the sample decomposed during the storage in chloroform- d as noted in the main text.



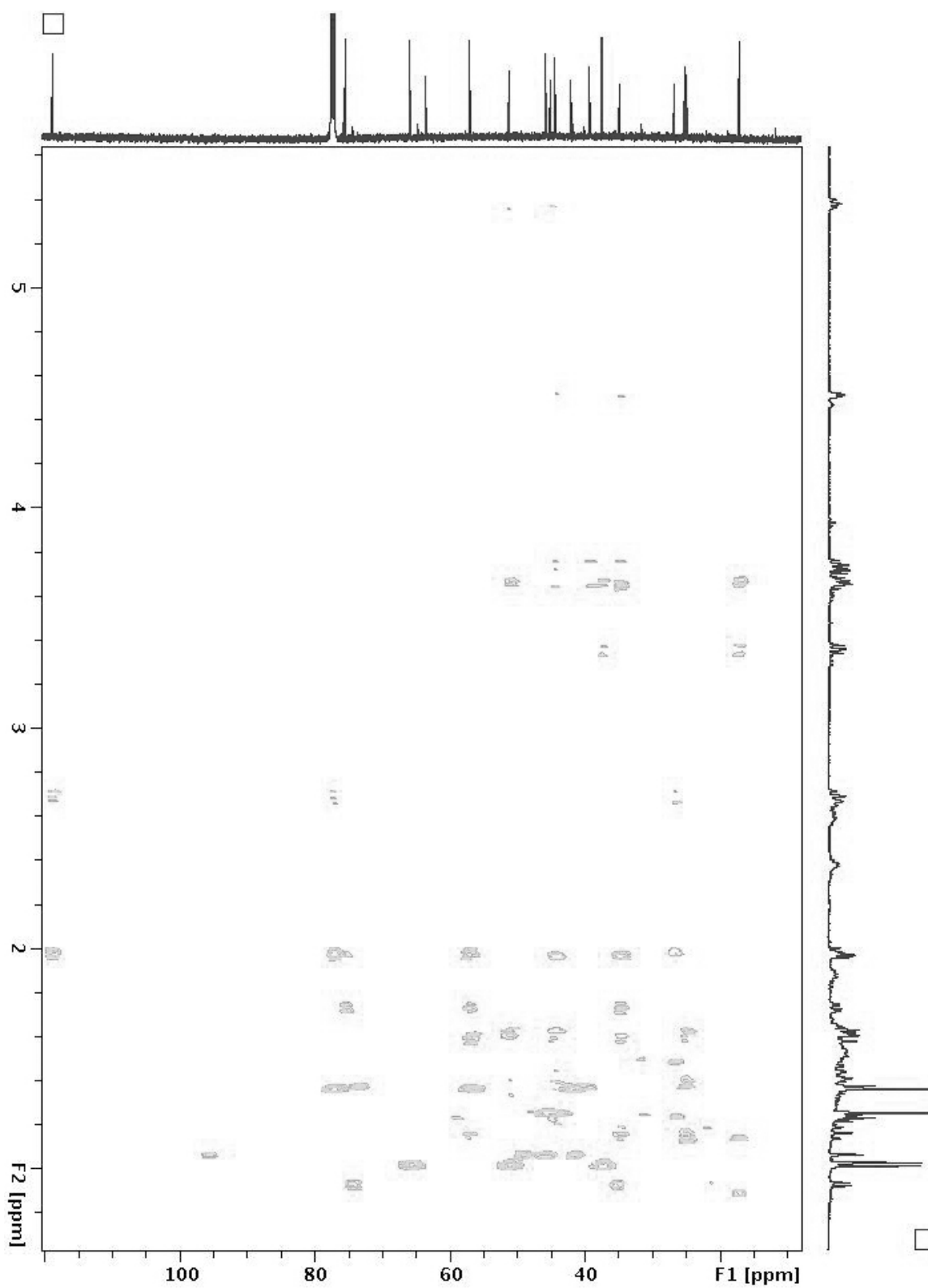
Appendix J: DEPT spectrum of COB in methanol- d_4 . A small fraction of the sample decomposed during the storage in chloroform- d as noted in the main text.



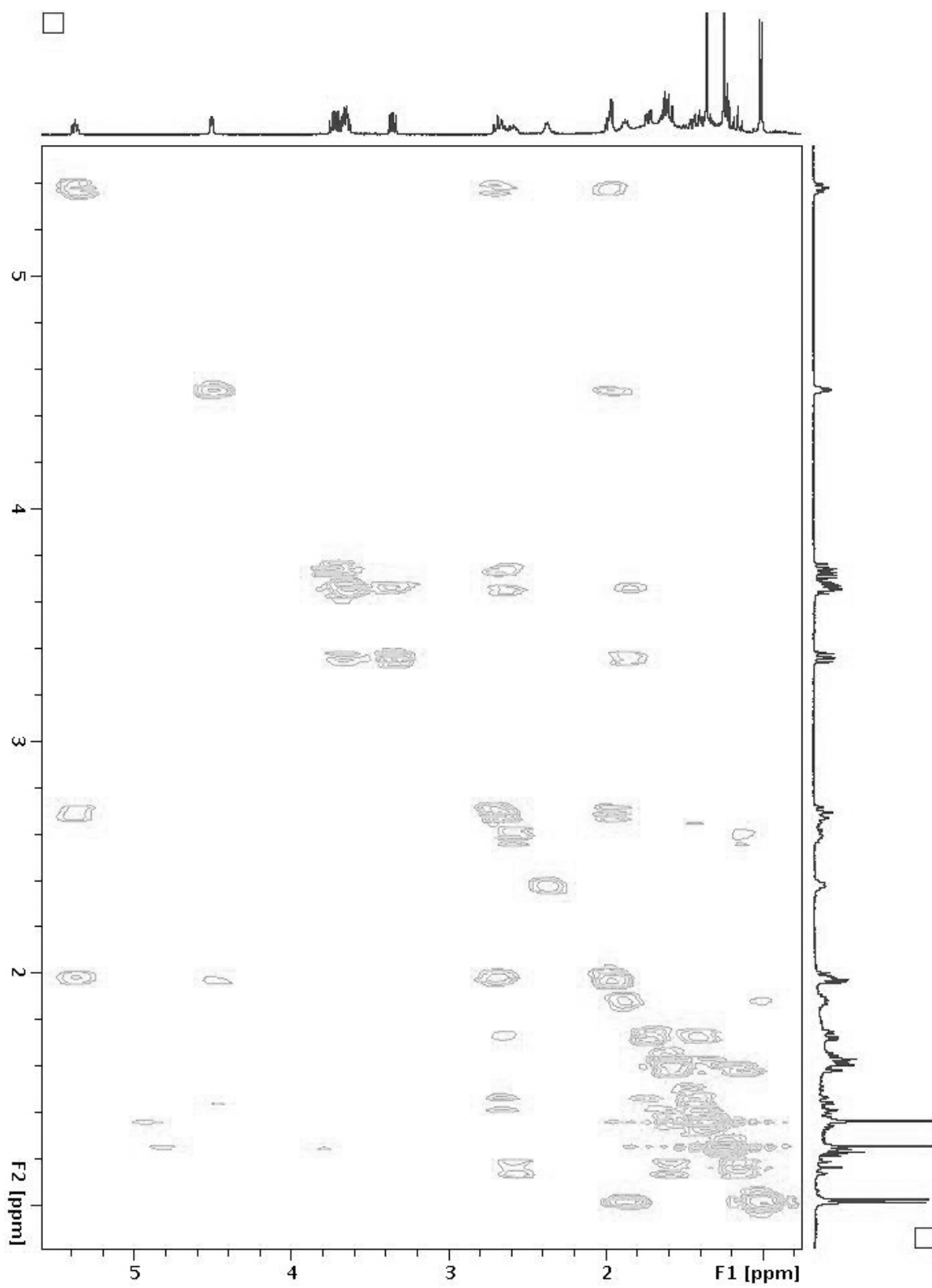
Appendix K: HSQC spectrum of COB in chloroform-*d*. A small fraction of the sample decomposed during the storage in chloroform-*d* as noted in the main text.



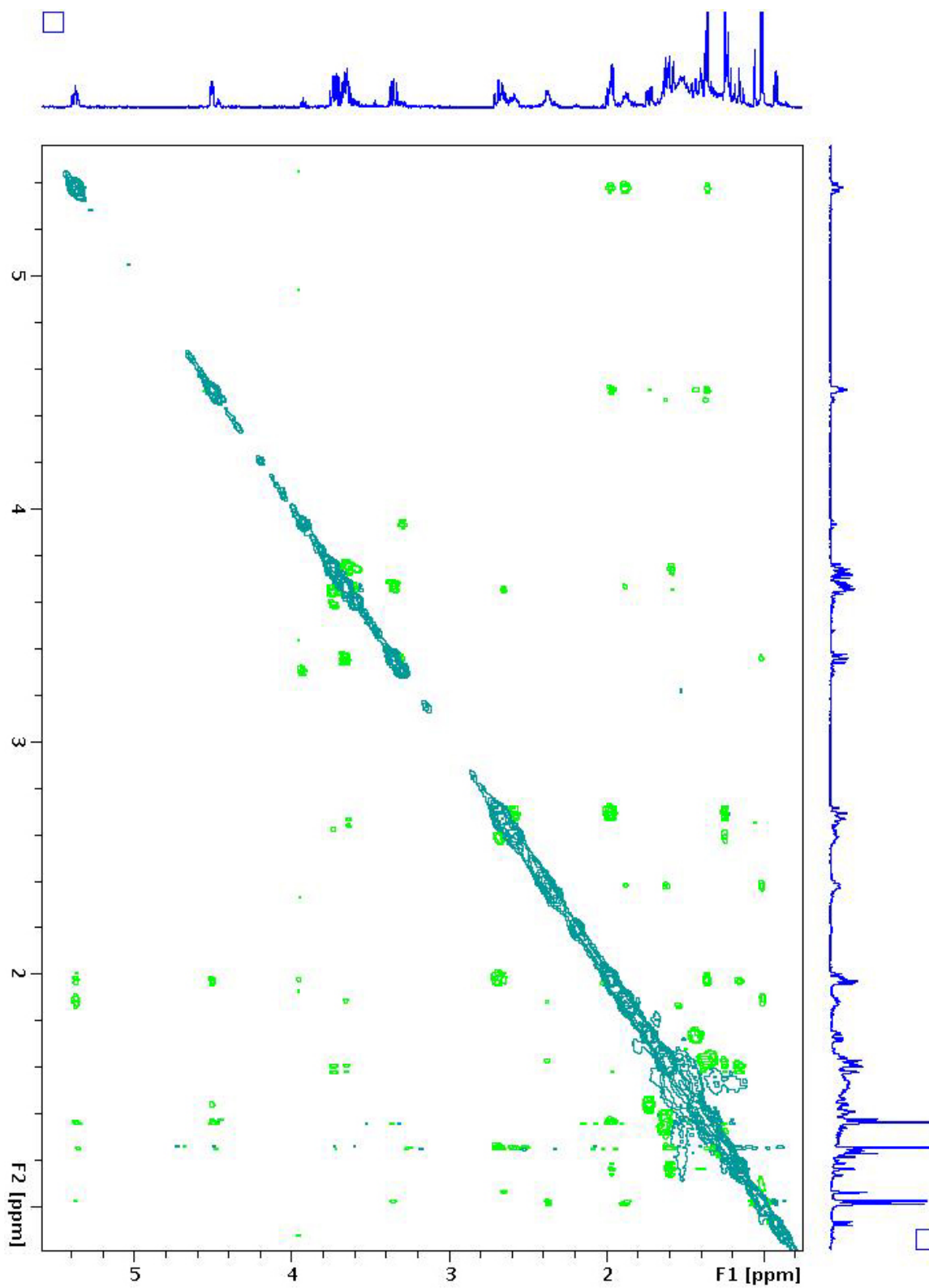
Appendix L: HMBC spectrum of COB in chloroform-*d*. A small fraction of the sample decomposed during the storage in chloroform-*d* as noted in the main text.



Appendix M: COSY spectrum of COB in chloroform-*d*. This spectrum was measured before partial decomposition.



Appendix N: NOESY spectrum of COB in chloroform-*d*. A small fraction of the sample decomposed during the storage in chloroform-*d* as noted in the main text.



V. Bibliography

Chapter I

1. Lloyd-Jones, D., Adams, R. J., Brown, T. M., Carnethon, M., Dai, S., Simone, G. D., Ferguson, T. B., Ford, E., Furie, K., Gillespie, C., Go, A., Greenlund, K., Haase, N., Hailpern, S., Ho, P. M., Howard, V., Kissela, B., Kittner, S., Lackland, D., Lisabeth, L., Marelli, A., McDermott, M. M., Meigs, J., Mozaffarian, D., Mussolino, M., Nichol, G., Roger, V., Rosamond, W., Sacco, R., Sorlie, P., Stafford, R., Thom, T., Wasserthiel-Smoller, S., Nathan, D., Heart Disease and Stroke Statistics 2010 Update. A Report From the American Heart Association. *Circulation*, 2009: p. 1-171.
2. Sørensen, H.T., Lash, T. L., Statins and amyotrophic lateral sclerosis – the level of evidence for an association. *J. Intern. Med.*, 2009. **266**(6): p. 520-6.
3. Palareti, G., Cosmi, B., Bleeding with anticoagulation therapy - who is at risk, and how best to identify such patients. *Thromb. Haemost.*, 2009. **102**(2): p. 268-78.
4. Longstaff, C., Thelwell, C., Understanding the enzymology of fibrinolysis and improving thrombolytic therapy. *FEBS Lett.*, 2005. **579**(15): p. 3303-9.
5. Bramlage, P., Hasford, J., Blood pressure reduction, persistence and costs in the evaluation of antihypertensive drug treatment – a review. *Cardiovascular Diabetol.*, 2009. **8**(18): p. 1-13.
6. Yamada, H., Saiki, I., *Juzen-taiho-to (Shi-Quan-Da-Bu-Tang): Scientific Evaluation and Clinical Applications*. 2005, FL: CRC, Boca Raton. 256.
7. Koyama, T., Role of Kampo (herbal) medicine for management in postmenopausal women in Japan. *J. Jpn. Menopause Soc.*, 1993. **1**: p. 75-9.
8. Kano, T., Ito, C., Kasamatsu, H., Miyawaki, Y., Clinical study of prognosis of 200 deliveries after Kampo-treatment for ovarian dysfunctional infertilities and tocolysis. *Jpn. J. Fertil. Steril.*, 1991. **36**: p. 612-20.
9. Kotani, N., Oyama, T., Sakai, I., Hashimoto, H., Muraoka, M., Ogawa, Y., Matsuki, A., Analgesic Effect of a Herbal Medicine for Treatment of Primary Dysmenorrhea - A Double-blind Study. *Am. J. Chin. Med.*, 1997. **25**(2): p. 205-12.
10. Tanaka, T., Effects of herbal medicines on menopausal symptoms induced by gonadotropin-releasing hormone agonist therapy. *Clin. Exp. Obstet. Gynecol.*, 2001. **28**(1): p. 20-23.
11. Takei, H., Yamamoto, M., Kase, Y., Takeda, S., The Effect of Herbal Medicine Toki-shakuyaku-san on Blood Pressure in an N⁰-Nitro-L-Arginine Methyl Ester-

- Induced Pre-eclampsia Rat Model During Pregnancy and the Postpartum Period. *J. Pharmacol. Sci.*, 2005. **98**(3): p. 255-62.
12. Takei, H., Nakai, Y., Hattori, N., Yamamoto, M., Kurauchi, K., Sasaki, H., Aburada, M., The herbal medicine Toki-shakuyaku-san improves the hypertension and intrauterine growth retardation in preeclampsia rats induced by Nomega-nitro-L-arginine methyl ester. *Phytomedicine*, 2004. **11**(1): p. 43-50.
 13. Ye, J., Duan, H., Yang, X., Yan, W., Zheng, X., Anti-thrombosis effect of paeoniflorin: evaluated in a photochemical reaction thrombosis model in vivo. *Planta Med.*, 2001. **67**(8): p. 766-767.
 14. Wang, B.H., Ou-Yang, J. P., Pharmacological actions of sodium ferulate in cardiovascular system. *Cardiovasc. Drug Rev.*, 2005. **23**(2): p. 161-72.
 15. Li, M., Handa, S., Ikeda, Y., Goto, S., Specific Inhibiting Characteristics of Tetramethylpyrazine, One of the Active Ingredients of the Chinese Herbal Medicine 'Chuanxiong,' on Platelet Thrombus Formation Under High Shear Rates. *Thrombosis Research*, 2001. **104**: p. 15-28.
 16. Zhang, L., Du, J. R., Wang, J., Yu, D. K., Chen, Y. S., He, Y., Wang, C. Y., Z-ligustilide extracted from Radix Angelica Sinensis decreased platelet aggregation induced by ADP Ex Vivo and arterio-venous Shunt Thrombosis in Vivo in rats. *Yakugaku Zasshi*, 2009. **129**(7): p. 855-859.
 17. Yang, H.O., Ko, W. K., Kim, J. Y., Ro, H. S., Paeoniflorin: an antihyperlipidemic agent from Paeonia lactiflora. *Fitoterapia*, 2004. **75**: p. 45-49.
 18. Nizamutdinova, I.T., Jin, Y. C., Kim, J. S., Yean, M. H., Kang, S. S., Kim, Y. S., Lee, J. H., Seo, H. G., Kim, H. J., Chang, K. C., Paeonol and paeoniflorin, the main active principles of Paeonia albiflora, protect the heart from myocardial ischemia/reperfusion injury in rats. *Planta Med.*, 2008. **74**(1): p. 14-18.
 19. Xu, L.N., Ouyang, R., Antithrombotic effect of sodium ferulate in rats. *Zhongguo Yao Li Xue Bao*, 1981. **2**(1): p. 35-7.
 20. Yin, Z.Z., Zhang, L.Y., Xu, L. N., The effect of danggui (Angelica sinensis) and its ingredient ferulic acid on rat platelet aggregation and release of 5-HT. *Yao Xue Xue Bao*, 1980. **15**: p. 321.
 21. Wang, Z., Gao, Y. H., Huang, R. S., Zhu, G. Q., Sodium ferulate is an inhibitor of thromboxane A₂ synthetase. *Zhongguo Yao Li Xue Bao*, 1988. **9**: p. 430-33.
 22. Wang, B., Ouyang, J., Liu, Y., Yang, J., Wei, L., Li, K., Yang, H., Sodium Ferulate Inhibits Atherosclerogenesis in Hyperlipidemia Rabbits. *J. Cardiovasc. Pharmacol.*, 2004. **43**(4): p. 549-54.

23. Xu, H., Shi, D. Z., Guan, C. Y., Clinical application and pharmacological actions of ligustrazine. *Chin. J. Integr. Tradit. West. Med.*, 2003. **23**(5): p. 376-9.
24. Sheu, J.R., Kan, Y. C., Hung, W. C., Ko, W. C., Yen, M. H., Mechanisms Involved in the Antiplatelet Activity of Tetramethylpyrazine in Human Platelets. *Thrombosis Research*, 1997. **88**: p. 259-70.
25. Takeda, S., Isono, T., Wakui, Y., Matsuzaki, Y., Sasaki, H., Amagaya, S., Maruno, M., Absorption and excretion of paeoniflorin in rats. *J. Pharm. Pharmacol.*, 1995. **47**(12A): p. 1036-40.
26. Takeda, S., Isono, T., Wakui, Y., Mizuhara, Y., Amagaya, S., Maruno, M., Hattori, M., In-vivo assessment of extrahepatic metabolism of paeoniflorin in rats: relevance to intestinal floral metabolism. *J. Pharm. Pharmacol.*, 1997. **49**(1): p. 35-39.
27. Xu, R., Li, Y., Huang, X., Recent advances in pharmacokinetics of ligustrazine. *J. Anhui. TCM. Coll.*, 2002. **21**(1): p. 58-61.
28. Goto, H., Satoh, N., Hayashi, Y., Hikiami, H., Nagata, Y., Obi, R., Shimada, Y., A Chinese Herbal Medicine, Tokishakuyakusan, Reduces the Worsening of Impairments and Independence After Stroke: A 1-year Randomized, Controlled Trial. *Evid Based Complement Alternat Med.*, 2009: p. 1-6.
29. Akase, T., Akase, T., Onodera, S., Jobo, T., Matsusita, R., Kaneko, M., Tashiro, S., A Comparative Study of the Usefulness of Toki-shakuyaku-san and An Oral Iron Preparation in the Treatment of Hypochromic Anemia in Cases of Uterine Myoma. *Yakuyaku Zasshi*, 2003. **123**(9): p. 817-24.
30. Kawamura, A., Brekman, A., Grigoryev, Y., Hasson, T. H., Takaoka, A., Wolfe, S., Soll, C. E., Rediscovery of natural products using genomic tools. *Bioorg. Med. Chem. Lett.*, 2006. **16**(11): p. 2846-9.
31. Wright, C.F., Hall, A. , Matthews, F. E., Brayne, C., Biomarkers, Dementia, and Public Health. *Ann. N. Y. Acad. Sci.*, 2009. **1180**: p. 11-19.
32. Yerushalmi, R., Woods, R., Ravdin, P. M., Hayes, M. M., Gelmon, K. A., Ki67 in breast cancer: prognostic and predictive potential. *Lancet Oncol.*, 2010. **11**(2): p. 174-83.
33. Sethupathy, P., Collins, F. S., MicroRNA target site polymorphisms and human disease. *Trends Genet.*, 2008. **24**(10): p. 489-97.
34. Hwang, H.J., Quinn, T., Zhang, J., Identification of glycoproteins in human cerebrospinal fluid. *Methods Mol. Biol.*, 2009. **566**: p. 263-76.
35. Rutella, S., Bonanno, G., De Cristofaro, R., Targeting indoleamine 2,3-dioxygenase (IDO) to counteract tumour-induced immune dysfunction: from

- biochemistry to clinical development. *Endocr. Metab. Immune Disord. Drug Targets*, 2009. **9**(2): p. 151-77.
36. Lockhart, D.J., Winzeler, E.A., Genomics, gene expression and DNA arrays. *Nature*, 2000. **405**: p. 827-36.
 37. Brown, P.O., Botstein, D., Exploring the new world of the genome with DNA microarrays. *Nat. Genet.*, 1999. **21**: p. 33-7.
 38. Watanabe, C.M., Wolfram, S., Ader, P., Rimbach, G., Packer, L., Maguire, J.J., Schultz, P.G., Gohil, K., The in vivo neuromodulatory effects of the herbal medicine ginkgo biloba. *Proc. Natl. Acad. Sci. USA*, 2001. **98**(12): p. 6577-80.
 39. Yang, S.H., Kim, J.S., Oh, T.J., Kim, M.S., Lee, S.W., Woo, S.K., Cho, H.S., Choi, Y.H., Kim, Y.H., Rha, S.Y., Chung, H.C., An, S.W., Genome-scale analysis of resveratrol-induced gene expression profile in human ovarian cancer cells using a cDNA microarray. *Int. J. Oncol.*, 2003. **22**(4): p. 741-50.
 40. Gohil, K., Moy, R.K., Farzin, S., Maguire, J.J., Packer, L., mRNA expression profile of a human cancer cell line in response to Ginkgo biloba extract: induction of antioxidant response and the Golgi system. *Free Radic. Res.*, 2000. **33**(6): p. 831-49.
 41. Sambrook, J., and Russell, D., *Molecular cloning, A laboratory manual*. 2001, Cold Spring Harbor, New York: Cold Spring Harbor Laboratory Press
 42. Kruithof, E.K.B., M. S.; Bunn, C. L., Biological and clinical aspects of plasminogen activator inhibitor type 2. *Blood*, 1995. **86**(11): p. 4007-24.
 43. Medcalf, R.L.S., S. J., The undecided serpin. The ins and outs of plasminogen activator inhibitor type 2. *FEBS J.*, 2005. **272**(19): p. 4858-67.
 44. Astedt, B., Lindoff, C., Lecander, I., Significance of the plasminogen activator inhibitor of placental type (PAI-2) in pregnancy. *Semin. Thromb. Hemost.*, 1998. **24**(5): p. 431-5.
 45. Kano, Y., Komatsu, K., Saito, K., Bando, H., Sakurai, T., A new polyacetylene compound from *Atractylodes* rhizome. *Chem. Pharm. Bull.*, 1989. **37**(1): p. 193-94.
 46. Sakurai, T., Yamada, H., Saito, K., Kano, Y., Enzyme inhibitory activities of acetylene and sesquiterpene compounds in *atractylodes* rhizome. *Biol. Pharm. Bull.*, 1993. **16**(2): p. 142-5.
 47. Sakurai, T., Sugawara, H., Saito, K., Kano, Y., Effects of the acetylene compound from *Atractylodes* rhizome on experimental gastric ulcers induced by active oxygen species. *Biol. Pharm. Bull.*, 1994. **17**(10): p. 1364-8.

48. Kawamura, A., Berova, N., Nakanishi, K., Voigt, B. and Adam, G., Configurational assignment of brassinosteroid sidechain by exciton coupled circular dichroic spectroscopy. *Tetrahedron*, 1997. **53**: p. 11961-70.
49. Kawamura, A., Berova, N., Nakanishi, K., Use of circular dichroism for assigning stereochemistry of sphingosine and other long chain bases. *Methods Enzymol.*, 2000. **312**: p. 217-27.
50. Kawamura, A., Berova, N., Dirsch, V., Mangoni, A., Nakanishi, K., Schwartz, G., Bielawska, A., Hannun, Y., Kitagawa, I., Picomole scale stereochemical analysis of sphingosines and dihydrosphingosines. *Bioorg. Med. Chem.*, 1996. **4**(7): p. 1035-43.
51. Davankov, V.A., Analytical chiral separation methods. *Pure & Appl. Chem.*, 1997. **69**(7): p. 1469-74.
52. Humphries, J., Gossage, J. A., Modarai, B., Burnand, K. G., Sisson, T. H., Murdoch, C., Smith, A., Monocyte urokinase-type plasminogen activator up-regulation reduces thrombus size in a model of venous thrombosis. *J. Vasc. Surg.*, 2009. **50**(5): p. 1127-34.
53. Estelles, A., Gilabert, J., Espana, F., Aznar, J., Galbis, M., Fibrinolytic parameters in normotensive pregnancy with intrauterine fetal growth retardation and in severe preeclampsia. *Am. J. Obstet. Gynecol.*, 1991. **165**: p. 138-42.
54. Gilabert, J., Estelles, A., Ayuso, M. J., Espana, F., Chirivella, M., Grancha, S., Mico, J. M., Aznar, J., Evaluation of plasminogen activators and plasminogen activator inhibitors in plasma and amniotic fluid in pregnancies complicated with intrauterine fetal growth retardation. *Gynecol. Obstet. Invest.*, 1994. **38**(3): p. 157-62.
55. Grancha, S., Estelles, A., Gilabert, J., Chirivella, M., Espana, F., Aznar, J., Decreased expression of PAI-2 mRNA and protein in pregnancies complicated with intrauterine fetal growth retardation. *Thromb. Haemost.*, 1996. **76**(5): p. 761-7.
56. Knox, S.M., Whitelock, J. M., Perlecan: how does one molecule do so many things? *Cell. Mol. Life Sci.*, 2006. **63**: p. 2435-45.
57. Zhang, W., Chuang, Y. J., Swanson, R., Li, J., Seo, K., Leung, L., Lau, L. F., Olson, S. T., Antiangiogenic antithrombin down-regulates the expression of the proangiogenic heparan sulfate proteoglycan, perlecan, in endothelial cells. *Blood*, 2004. **103**: p. 1185-91.
58. Engelberg, H., Endogenous heparin activity deficiency: the 'missing link' in atherogenesis? *Atherosclerosis*, 2001. **159**: p. 253-60.

59. Pillarisetti, S., Lipoprotein modulation of sub-endothelial heparan sulfate proteoglycans (perlecan) and atherogenicity. *Trends Cardiovasc Med.*, 2000. **10**: p. 60-65.
60. Tran-Lundmark, K., Tran, P. K., Paulsson-Berne, G., Friden, V., Soininen, R., Tryggvason, K., Wight, T. N., Kinsella, M. G., Boren, J., Hedin, U., Heparan Sulfate in Perlecan Promotes Mouse Atherosclerosis: Roles in Lipid Permeability, Lipid Retention, and Smooth Muscle Cell Proliferation. *Circ. Res.*, 2008. **103**: p. 43-52.
61. Iezzi, A., Ferri, C., Mezzetti, A., Cipollone, F., COX-2: Friend or Foe? *Curr. Pharm. Des.*, 2007. **13**: p. 1715-21.
62. FitzGerald, G.A., Nonsteroidal anti-inflammatory drugs, coxibs, and cardio-renal physiology: a mechanism-based approach. *Am. J. Cardiol.*, 2002. **89**: p. 1D-2D.
63. Grosser, T., Fries, S., FitzGerald, G. A., Biological basis for the cardiovascular consequences of COX-2 inhibition: therapeutic challenges and opportunities. *J. Clin. Invest.*, 2006. **116**: p. 4-15.
64. Lucerna, M., Pomyje, J., Mechtcheriakova, D., Kadl, A., Gruber, F., Bilban, M., Sobanov, Y., Schabbauer, G., Breuss, J., Wagner, O., Bischoff, M., Clauss, M., Binder, B. R., Hofer, E., Sustained Expression of Early Growth Response Protein-1 Blocks Angiogenesis and Tumor Growth. *Cancer Res.*, 2006. **66**(13): p. 6708-13.
65. Day, S.M., Reeve, J. L., Pedersen, B., Farris, D. M., Myers, D. D., Im, M., Wakefield, T. W., Mackman, N., Fay, W. P., Macrovascular thrombosis is driven by tissue factor derived primarily from the blood vessel wall. *Blood*, 2005. **105**: p. 192-8.
66. Shin, I.S., Kim, J. M., Kim, K. L., Jang, S.Y., Jeon, E. S., Choi, S. H., Kim, D. K., Suh, W., Kim, Y. W., Early Growth Response Factor-1 Is Associated With Intraluminal Thrombus Formation in Human Abdominal Aortic Aneurysm. *J. Am. Coll. Cardiol.*, 2009. **53**(9): p. 792-9.
67. Chicca, A., Pellati, F., Adinolfi, B., Matthias, A., Massarelli, I., Benvenuti, S., Martinotti, E., Bianucci, A. M., Bone, K., Lehmann, R., Nieri, P., Cytotoxic activity of polyacetylenes and polyenes isolated from roots of *Echinacea pallida*. *British Journal of Pharmacology*, 2008. **153**: p. 879-85.
68. Huang, H. Q., Zhang, X., Shen, Y. H., Su, J., Liu, X. H., Tian, J. M., Lin, S., Shan, L., Zhang, W. D., Polyacetylenes from *Bupleurum longiradiatum*. *J. Nat. Prod.*, 2009. **72**: p. 2153-57.
69. Lechner, D., Stavri, M., Oluwatuyi, M., Pereda-Miranda, R., Gibbons, S., The anti-staphylococcal activity of *Angelica dahurica* (Bai Zhi). *Phytochemistry*, 2004. **65**: p. 331-5.

70. Chien, S.C., Young, P. H., Hsu, Y. J., Chen, C. H., Tien, Y. J., Shiu, S. Y., Li, T. H., Yang, C. W., Marimuthu, P., Tsai, L. F., Yang, W. C., Anti-diabetic properties of three common *Bidens pilosa* variants in Taiwan. *Phytochemistry*, 2009. **70**: p. 1246-54.
71. Tobinaga, S., Sharma, M. K., Aalbersberg, W. G., Watanabe, K., Iguchi, K., Narui, K., Sasatsu, M., Waki, S., Isolation and identification of a potent antimalarial and antibacterial polyacetylene from *Bidens pilosa*. *Planta Med.*, 2009. **75**(6): p. 624-8.
72. Wu, L.W., Chiang, Y. M., Chuang, H. C., Wang, S. Y., Yang, G. W., Chen, Y. H., Lai, L. Y., Shyur, L. F., Polyacetylenes Function as Anti-angiogenic Agents. *Pharm. Res.*, 2004. **21**(11): p. 2112-19.
73. Malich, G., Marcovic, B., Winder, C., The sensitivity and specificity of MTS tetrazolium assay for detecting the in vitro cytotoxicity of 20 chemicals using human cell lines. *Toxicology*, 1997. **124**: p. 179-92.
74. Styles, P., Soffe, N. F., Scott, C. A., Cragg, D. A., Row, F., White, D. J., White, P. C. J., A high-resolution NMR probe in which the coil and the preamplifier are cooled with liquid nitrogen. *J. Magn. Reson.*, 1984. **60**: p. 397-404.

Chapter II

1. Society, A.C., Cancer facts and figures 2009. *American Cancer Society*, 2009.
2. Goldman, J.M., Treatment strategies for CML. *Best Pract. Res. Clin. Haematol.*, 2009. **22**(3): p. 303-13.
3. Schmitt, F., HER2+ breast cancer: how to evaluate? *Adv. Ther.*, 2009. **26** (Suppl. 1): p. S1-8.
4. Garnock-Jones, K.P., Keating, G. M., Scott, L. G., Trastuzumab: A review of its use as adjuvant treatment in human epidermal growth factor receptor 2 (HER2)-positive early breast cancer. *Drugs*, 2010. **70**(2): p. 215-39.
5. Waller, C.F., Imatinib mesylate. *Recent Results Cancer Res.*, 2010. **184**: p. 3-20.
6. Dizon, D.S., Treatment options for advanced endometrial carcinoma. *Gynecol. Oncol.*, 2010. **117**(2): p. 373-81.
7. Bookman, M.A., Trials with impact on clinical management: first line. *Int. J. Gynecol. Cancer*, 2009. **19**(Suppl. 2): p. S55-62.

8. Marchetti, C., Pisano, C., Facchini, G., Bruni, G. S., Magazzino, F. P., Losito, S., Pignata, S., First-line treatment of advanced ovarian cancer: current research and perspectives. *Expert Rev. Anticancer Ther.*, 2010. 10(1): p. 47-60.
9. Merry, C., Fu, K., Wang, J., Yeh, I. J., Zhang, Y., Targeting the checkpoint kinase Chk1 in cancer therapy. *Cell Cycle*, 2010. 9 (2): p. 279-83.
10. Saad, F., Lipton, A., SRC kinase inhibition: targeting bone metastases and tumor growth in prostate and breast cancer. *Cancer Treat. Rev.*, 2010. 36(2): p. 177084.
11. Tan, A., Xia, N., Gao, F., Mo, Z., Cao, Y., Angiogenesis-inhibitors for metastatic thyroid cancer. *Cochrane Database Syst. Rev.*, 2010. 17(3).
12. Ganjoo, K., Jacobs, C., Antiangiogenesis agents in the treatment of soft tissue sarcomas. *Cancer*, 2010. 16(5): p. 1177-83.
13. Pathania, D., Millard, M., Neamati, N., Opportunities in discovery and delivery of anticancer drugs targeting mitochondria and cancer cell metabolism. *Adv. Drug Deliv. Rev.*, 2009. 61(14): p. 1250-75.
14. Tennant, D.A., Durán, R. V., Gottlieb, E., Targeting metabolic transformation for cancer therapy. *Nat. Rev. Cancer*, 2010. 10(4): p. 267-77.
15. Chaudhuri, D., Suriano, R., Mittelman, A., Tiwari, R. K., Targeting the Immune System in Cancer. *Curr. Pharm. Biotechnol.*, 2009. 10(2): p. 166-84.
16. Parish, C.R., Cancer immunotherapy: The past, the present and the future. *Immunol. Cell. Biol.*, 2003. 81(2): p. 106-13.
17. Ruszala-Mallon, V., Lin, Y. I., Durr, F. E., Wang, B. S., Low molecular weight immunopotentiators. *Int. J. Immunopharmacol.*, 1988. 10(5): p. 497-510.
18. Borghaei, H., Smith, M. R., Campbell, K. S., Immunotherapy of cancer. *Eur. J. Pharmacol.*, 2009. 625 (1-3): p. 41-54.
19. Kandalaft, L.E., Singh, N., Liao, J. B., Facciabene, A., Berek, J. S., Powell, D. J. Jr., Coukos, G., The emergence of immunomodulation: Combinatorial immunochemotherapy opportunities for the next decade. *Gynecol. Oncol.*, 2010. 116(2): p. 222-33.
20. Schwandner, R., Dziarski, R., Wesche, H., Rothe, M. & Kirschning, C.J., Peptidoglycan- and lipoteichoic acid-induced cell activation is mediated by toll-like receptor 2. *J. Biol. Chem.*, 1999. 274: p. 17406-409.
21. Schroder, N.W., Morath, S., Alexander, C., Hamann, L., Hartung, T., Zahringer, U., Gobel, U.B., Weber, J.R. & Schumann, R.R., Lipoteichoic acid (LTA) of *Streptococcus pneumoniae* and *Staphylococcus aureus* activates immune cells via

- Toll-like receptor (TLR)-2, lipopolysaccharide-binding protein (LBP), and CD14, whereas TLR-4 and MD-2 are not involved. *J. Biol. Chem.*, 2003. 278: p. 15587-94.
22. Leon, C.G., Tony, R., Jia, J., Sivak, O., Wasan, K. M., Discovery and development of toll-like receptor 4 (TLR4) antagonists: a new paradigm for treating sepsis and other diseases. *Pharm. Res.*, 2008. 25(8): p. 1751-61.
 23. Hakomori, S., Tumor-associated carbohydrate antigens defining tumor malignancy: basis for development of anti-cancer vaccines. *Adv. Exp. Med. Biol.*, 2001. 491: p. 369-402.
 24. Ragupathi, G., Carbohydrate antigens as targets for active specific immunotherapy. *Cancer Immunol. Immunother.*, 1996. 43: p. 152-57.
 25. Buskas, T., Thompson, P. Boons, G. J., Immunotherapy for cancer: synthetic carbohydrate-based vaccines. *Chem. Commun.*, 2009. 36: p. 5335-49.
 26. Ochsenbein, A.F., Klenerman, P., Karrer, U., Ludewig, B., Pericin, M., Hengartner, H., Zinkernagel, R. M., Immune surveillance against a solid tumor fails because of immunological ignorance. *Proc. Natl. Acad. Sci. USA*, 1999. 96: p. 2233-38.
 27. Zhongwu, G., Qianli, W., Recent development in carbohydrate-based cancer vaccines. *Curr. Opin. Chem. Biol.*, 2009. 13(5-6): p. 608-17.
 28. Morris-Stiff, G., Teli, M., Jardine, N., Puntis, M. C., CA19-9 antigen levels can distinguish between benign and malignant pancreatic obiliary disease. *Hepatobiliary Pancreat. Dis. Int.*, 2009. 8(6): p. 620-6.
 29. Rustin, G.Z., Marples, M., Nelstrop, A. E., Mahmoodi, M., Meyer, T., Use of CA-125 to define progression of ovarian cancer in patients with persistently elevated levels. *J. Clin. Oncol.*, 2001. 19(20): p. 4054-7.
 30. Natori, T., Motoki, K., Akimoto, K., Koezuka, Y., Higa, T., Development of KRN7000, derived from agelasphin produced by Okinawan sponge. *Nippon Yakurigaku Zasshi*, 1997. 110(Supl. 1): p. 63P-68P.
 31. Natori, T., Morita, M., Akimoto, K., Koezuka, Y., Agelasphins, novel antitumor and immunostimulatory cerebroside from the marine sponge *Agelas mauritanus*. *Tetrahedron*, 1994. 50(9): p. 2771-84.
 32. Franck, R.W., Tsuji, M., alpha-C-Galactosylceramides: Synthesis and immunology. *Acc. Chem. Res.*, 2006. 39(10): p. 692-701.

33. Kobayashi, E., Motoki, K., Uchida, T., Fukushima, H., Koezuka, Y., KRN7000, a novel immunomodulator, and its antitumor activities. *Oncol. Res.*, 1995. 7(10-11): p. 529-34.
34. Nakagawa, R., Serizawa, I., Motoki, K., Sato, M., Ueno, H., Iijima, R., Nakamura, H., Shimosaka, A., Koezuka, Y., Antitumor activity of alpha-galactosylceramide, KRN7000, in mice with the melanoma B16 hepatic metastasis and immunohistological study of tumor infiltrating cells. *Oncol. Res.*, 2000. 12(2): p. 51-8.
35. Fuji, N., Ueda, Y., Fujiwara, H., Toh, T., Yoshimura, T., Yamagishi, H., Antitumor effect of alpha-galactosylceramide (KRN7000) on spontaneous hepatic metastases requires endogenous interleukin 12 in the liver. *Clin. Cancer Res.*, 2000. 6(8): p. 3380-7.
36. Kunii, N., Horiguchi, S., Motohashi, S., Yamamoto, H., Ueno, N., Yamamoto, S., Sakurai, D., Taniguchi, M., Nakayama, T., Okamoto, Y., Combination therapy of in vitro-expanded natural killer T cells and alpha-galactosylceramide-pulsed antigen-presenting cells in patients with recurrent head and neck carcinoma. *Cancer Sci.*, 2009. 100(6): p. 1092-8.
37. Motohashi, S., Nagato, K., Kunii, N., Yamamoto, H., Yamasaki, K., Okita, K., Hanaoka, H., Shimizu, N., Suzuki, M., Yoshino, I., Taniguchi, M., Fujisawa, T., Nakayama, T., A phase I-II study of alpha-galactosylceramide-pulsed IL-2/GM-CSF-cultured peripheral blood mononuclear cells in patients with advanced and recurrent non-small cell lung cancer. *J. Immunol.*, 2009. 182(4): p. 2492-501.
38. Yamada, H., Saiki, I., *Juzen-taiho-to (Shi-Quan-Da-Bu-Tang): Scientific Evaluation and Clinical Applications*. 2005, FL.: CRC, Boca Raton.
39. Maruyama, H., Kawamura, H., Takemoto, N., Komatsu, Y., Maruyama, N., Antitumor effect of Juzen-taiho-to, A Kampo medicine, combined with surgical excision for transplanted Meth-A-fibrosarcoma. *Int. J. Immunother.*, 1993. 9: p. 117-25.
40. Haranaka, R., Hasegawa, R., Nakagawa, S., Sakurai, A., Satomi, N., Haranaka, K., Antitumor activity of combination therapy with traditional Chinese medicine and OK432 or MMC. *J. Biol. Response Mod.*, 1988. 7(1): p. 77-90.
41. Sugiyama, K., Ueda, H., Ichiko, Y., Yokota, M., Improvement of cisplatin toxicity and lethality by Juzen-taiho-to in mice. *Biol. Pharm. Bull.*, 1995. 18(1): p. 53-8.
42. Terasawa, K., *The status of traditional Sino-Japanes (Kampon) medicine currently practised in Japan.*, in *Economic and Medicinal Plant Research*, H. Wagner, Farnsworth, N. R., Editor. 1990, Academic Press: San Diego. p. 57-70.

43. Ohnishi, Y., Fujii, H, Hayakawa, Y, Sakukawa, R, Yamaura, T, Sakamoto, T, Tsukada, K, Fujimaki, M, Nunome, S, Komatsu, Y, Saiki, I., Oral Administration of a Kampo (Japanese Herbal) Medicine Juzen-taiho-to Inhibits Liver Metastasis of Colon 26-L5 Carcinoma Cells. *Jpn. J. Cancer Res.*, 1998. 89(2): p. 206-13.
44. Saiki, I., A Kampo Medicine "Juzen-taiho-to"- Prevention of Malignant Progression and Metastasis of Tumor Cells and the Mechanism of action. *Biol. Pharm. Bull.*, 2000. 23(6): p. 677-88.
45. Zheng, Y., Wei, W., Zhu, L., Liu, J., Effects and mechanisms of Paeonifl orin, a bioactive glucoside from paeony root, on adjuvant arthritis in rats. *Inflamm. Res.*, 2007. 56: p. 182-8.
46. Kim, I.D., Ha, B. J., Paeoniflorin protects RAW 264.7 macrophages from LPS-induced cytotoxicity and genotoxicity. *Toxicol. in vitro*, 2009. 23(6): p. 1014-19.
47. Liu, D.Z., Xie, K. Q., Ji, X. Q., Ye, Y., Jiang, C. L., Zhu, X. Z., Neuroprotective effect of paeoniflorin on cerebral ischemic rat by activating adenosine A1 receptor in a manner different from its classical agonists. *Br. J. Pharmacol.*, 2005. 146(4): p. 604-11.
48. Takeda, S., Isono, T., Wakui, Y., Matsuzaki, Y., Sasaki, H., Amagaya, S., Maruno, M., Absorption and excretion of paeoniflorin in rats. *J. Pharm. Pharmacol.*, 1995. 47(12A): p. 1036-40.
49. Takeda, S., Isono, T., Wakui, Y., Mizuhara, Y., Amagaya, S., Maruno, M., Hattori, M., In-vivo assessment of extrahepatic metabolism of paeoniflorin in rats: relevance to intestinal floral metabolism. *J. Pharm. Pharmacol.*, 1997. 49(1): p. 35-39.
50. Kawamura, A., Brekman, A., Grigoryev, Y., Hasson, T. H., Takaoka, A., Wolfe, S., Soll, C. E., Rediscovery of natural products using genomic tools. *Bioorg. Med. Chem. Lett.*, 2006. 16(11): p. 2846-9.
51. Kawamura, A., Iacovidou, M., Takaoka, A., Soll, C. E., Blumenstein, M., A polyacetylene compound from herbal medicine regulates genes associated with thrombosis in endothelial cells. *Bioorg. Med. Chem. Lett.*, 2007. 17(24): p. 6879-82.
52. Hasson, T.H., *Isolation and Characterization of Immunomodulatory Compounds from Juzen-Taiho-To: Novel Understanding of Phytosteryl Glucosides Nano-Aggregates and Synergism* in Biochemistry. 2009, The Graduate Center of CUNY: New York. p. 165.

53. Niiho, Y., Nakajima, Y., Yamazaki, T., Okamoto, M., Tsuchihashi, R., Kodera, M., Kinjo, J., Nohara, T., Simultaneous analysis of isoflavones and saponins in Pueraria flowers using HPLC coupled to an evaporative light scattering detector and isolation of a new isoflavone diglucoside. *J. Nat. Med.*, 2010. 64(3): p. 313-20.
54. Almeling, S., Holzgrabe, U., Use of evaporative light scattering detection for the quality control of drug substances: Influence of different liquid chromatographic and evaporative light scattering detector parameters on the appearance of spike peaks. *J. Chromatogr. A*, 2010. 1217(14): p. 2163-70.
55. Lucena, R., Cardenas, S., Valcareel, M., Evaporative light scattering detection: trends in its analytical uses. *Anal. Bioanal. Chem.*, 2007. 388: p. 1663-72.
56. Bouic, P.J., Etsebeth, S., Liebenberg, R. W., Albrecht, C. F., Pegel, K., Van Jaarsveld, P. P., beta-Sitosterol and beta-sitosterol glucoside stimulate human peripheral blood lymphocyte proliferation: implications for their use as an immunomodulatory vitamin combination. *Int. J. Immunopharmacol.*, 1996. 18(12): p. 693-700.
57. Bouic, P.J., Lamprecht, J. H., Plant sterols and sterolins: a review of the their immune-modulating properties. *Altern. Med. Rev.*, 1999. 4(3): p. 170-77.
58. Bock, K., Pedersen, C., Carbon-13 nuclear magnetic resonance spectroscopy of monosaccharides. *Adv. Carbohydr. Chem. Biochem.*, 1983. 41: p. 27-66.
59. Stothers, J.B., *Carbon-13 NMR spectroscopy. Organic Chemistry: A series of monographs*. Vol. 24. 1972, New York: Academic Press.
60. Shibuya, H., Kawashima, K., Sakagami, M., Kawanishi, H., Shimomura, M., Kazuyoshi, O., Kitagawa, I., Sphingolipids and Glycerolipids I. Chemical structures and ionophoretic activities of soya-cerebrosides I and II from soybean. *Chem. Pharm. Bull.*, 1990. 38(11): p. 2933-38.
61. Inagaki, M., Harada, Y., Yamada, K., Isobe, R., Higuchi, R., Matsuura, H., Itakura, Y. , Isolation and structure determination of cerebrosides from garlic, the bulbs of *Allium Sativum* L. *Chem. Pharm. Bull.*, 1998. 46(7): p. 1153-56.
62. Welti, R., Shah, J., Li, W., Li, M., Chen, J., Burke, J. J., Fauconnier, M. L., Chapman, K., Chye, M. L., Wang, X., Plant lipidomics: discerning biological function by profiling plant complex lipids using mass spectrometry. *Front. Biosci.*, 2007. 12: p. 2494-506.
63. Gu, M., Kerwin, J. L., Watts, J. D., Aebersold, R., Ceramide Profiling of Complex Lipid Mixtures by Electrospray Ionization Mass Spectrometry. *Anal. Biochem.*, 1997. 244(2): p. 347-56.

64. Kerwin, J.L., Tuininga, A. R., Ericsson, L H., Identification of molecular species of glycerophospholipids and sphingomyelin using electrospray mass spectrometry. *J. Lipid Res.*, 1994. 35(6): p. 1102-14.
65. Yang, N., Ren, D., Duan, J., Xu, X., Xie, N., Tian, L., Ceramides and cerebroside from *Ligusticum chuanxiong*. *Helv. Chim. Acta*, 2009. 92(2): p. 291-7.
66. Zhao, C., Shao, J., Wang, N., Li, X., Wang, J., A new cerebroside from fruits of *Ailanthus altissima* Swingle. *Nat. Prod. Res.*, 2006. 20(13): p. 1187-91.
67. Row, L., Ho, J., Chen, C., Cerebroside and Tocopherol trimers from the seeds of *Euryale ferox*. *J. Nat. Prod.*, 2007. 70(7): p. 1214-17.
68. Babu, U.V., Bhandari, S. P. S., Garg, H. S., Temnosides A and B, Two new glycosphingolipids from the sea urchin *temnopleurus toreumaticus* of the Indian coast. *J. Nat. Prod.*, 1997. 60(7): p. 732-4.
69. Ilan, Y., Elstein, D., Zimran, A., Glucocerebroside: an evolutionary advantage for patients with Gaucher disease and a new immunomodulatory agent. *Immunol. Cell. Biol.*, 2009. 87(7): p. 514-24.
70. Bertram, H.C., Eldibany, M., Padgett, J., Dragon, L. H., Splenic lymphoma arising in a patient with Gaucher disease. A case report and review of the literature. *Arch. Pathol. Lab. Med.*, 2003. 127(5): p. e242-5.
71. Lo, S.M., Stein, P., Mullaly, S., Bar, M., Jain, D., Pastores, G. M., Mistry, P. K., Expanding spectrum of the association between Type 1 Gaucher disease and cancers: a series of patients with up to 3 sequential cancers of multiple types--correlation with genotype and phenotype. *Am. J. Hematol.*, 2010. 85(5): p. 340-5.
72. Morita, M., Natori, T., Akimoto, K., Osawa, T., Fukushima, H., Koezuka, Y., Syntheses of α -, β -monoglycosylceramides and four diastereomers of an α -galactosylceramide. *Bioorg. Med. Chem. Lett.*, 1995. 5(7): p. 699-704.
73. Natori, T., Koezuka, Y., Higa, T., Agelasphins, novel α -galactosylceramides from the marine sponge *Agelas mauritanus*. *Tetrahedron Lett.*, 1993. 34(35): p. 5591-2.
74. Morita, M., Motoki, K., Akimoto, K., Natori, T., Sakai, T., Sawa, E., Yamaji, K., Koezuka, Y., Kobayashi, E., Fukushima, H., Structure-activity relationship of alpha-galactosylceramides against B16-bearing mice. *J. Med. Chem.*, 1995. 38(12): p. 2176-87.

Chapter III

1. Goodfellow, M., Williams, S. T., Mordarski, M., *Actinomycetes in Biotechnology*. 1988, San Diego: Academic Press. 501.
2. Gragg, G.M., Newman, D. J., Snader, K. M., Natural products in drug discovery and development. *J. Nat. Prod.*, 1997. **60**(1): p. 52-60.
3. Harvey, A., Strategies for discovering drugs from previously unexplored natural products. *Drug Disc. Today*, 2000. **5**: p. 294-300.
4. Sonia-Mercado, I.E., Prieto-Davo, A., Jensen, P. R., Fenical, W., Antibiotic terpenoid chloro-dihydroquinones from a new marine actinomycete. *J. Nat. Prod.*, 2005. **68**: p. 904-10.
5. Watve, M.G., Tickoo, R., Jog, M. M., Bhole, B. D., How many antibiotics are produced by the genus *Streptomyces*? *Arch. Microbiol.*, 2001. **176**: p. 386-90.
6. Vanden Bossche, H., Engelen, M., Rochette, F., Antifungal agents of use in animal health--chemical, biochemical and pharmacological aspects. *J.Vet. Pharmacol. Ther.*, 2003. **26**(1): p. 5-29.
7. Torrado, J.J., Espada, R., Ballesteros, M. P., Torrado-Santiago, S., Amphotericin B formulations and drug targeting. *J. Pharm. Sci.*, 2008. **97**(7): p. 2405-25.
8. Vezina, C., Kudelski, A., Sehgal, S. N., Rapamycin (AY-22,289), a new antifungal antibiotic. I. Taxonomy of the producing streptomycete and isolation of the active principle. *J. Antibiot. (Tokyo)*, 1975. **28**(10): p. 721-26.
9. Kim, H.S., Park, Y. I., Isolation and Identification of a Novel Microorganism Producing the Immunosuppressant Tacrolimus. *Journal of Bioscience and Bioengineering*, 2008. **105**(4): p. 418-21.
10. Nakae, K., Yoshimoto, Y., Sawa, T., Homma, Y., Hamada, M., Takeuchi, T., Imoto, M., Migrastatin, a new inhibitor of tumor cell migration from *Streptomyces* sp. MK929-43F1. Taxonomy, fermentation, isolation and biological activities. *J. Antibiot. (Tokyo)*, 2000. **53**(10): p. 1130-6.
11. Van Lanen, S.G., Shen, B., Microbial genomics for the improvement of natural product discovery. *Curr. Opin. Microbiol.*, 2006. **9**: p. 252-60.
12. Baltz, R.H., Antibiotic discovery from actinomycetes: will a renaissance follow the decline and fall? *SIM news*, 2005. **55**: p. 186-196.
13. Fenical, W., Marine soft corals of the genus *Pseudopterogorgia*: a resource for novel anti-inflammatory diterpenoids. *J. Nat. Prod.*, 1987. **50**(6): p. 1001-8.

14. Jensen, P.R., Mincer, T. J., Williams, P. G., Fenical, W., Marine actinomycete diversity and natural product discovery. *Antonie Van Leeuwenhoek*, 2005. **87**(1): p. 43-8.
15. Fusetani, N., Antifungal substances from marine invertebrates. *Ann. N. Y. Acad. Sci.*, 1988. **544**: p. 113-27.
16. Nakao, Y., Fusetani, N., Enzyme inhibitors of marine invertebrates. *J. Nat. Prod.*, 2007. **70**(4): p. 689-710.
17. Li, J.W., Vederas, J. C., Drug discovery and natural products: end of an era or an endless frontier? *Science*, 2009. **325**(5937): p. 161-5.
18. Ohnishi, Y., Ishikawa, J., Hara, H., Suzuki, H., Ikenoya, M., Ikeda, H., Yamashita, A., Hattori, M., Horinouchi, S., Genome sequence of the Streptomycin-producing microorganism *Streptomyces griseus* IFO 13350. *J. Bacteriol.*, 2008. **190**(11): p. 4050-60.
19. Hopwood, D.A., Antibiotics: opportunities for genetic manipulation. *Philos. Trans. R. Soc. Lond. B. Biol. Sci.*, 1989. **324**(1224): p. 549-62.
20. Khosla, C., Keasling, J. D., Metabolic engineering for drug discovery and development. *Nat. Rev. Drug Discov.*, 2003. **2**(12): p. 1019-25.
21. McDaniel, R., Licari, P., Khosla, C., Process development and metabolic engineering for the overproduction of natural and unnatural polyketides. *Adv. Biochem. Eng. Biotechnol.*, 2001. **73**: p. 31-52.
22. Burke, M.D., Schreiber, S. L., A planning strategy for diversity-oriented synthesis. *Angew. Chem. Int. Ed. Engl.*, 2004. **43**(1): p. 46-58.
23. Tan, D.S., Diversity-oriented synthesis: exploring the intersections between chemistry and biology. *Nat. Chem. Biol.*, 2005. **1**(2): p. 74-84.
24. Cutler, H.G., Crumley, F. G., Cox, R. H., Springer, J. P., Arrendale, R. F., Cole, R. J., Cole, P. D., Ophiobolins G and H: New fungal metabolites from a novel source, *Aspergillus ustus*. *J. Agric. Food Chem.*, 1984. **32**(4): p. 778-82.
25. Sugawara, F., Strobel, G., Strange, R. N., Siedow, J. N., Van Duyne, G. D., Clardy, J., Phytotoxins from the pathogenic fungi *Drechslera maydis* and *Drechslera sorghicola*. *Proc. Natl. Acad. Sci. USA*, 1987. **84**: p. 3081-85.
26. Ríos, T., Quijano, L., The structure of ceroplastol II a sesterterpenic alcohol isolated from insects wax. *Tetrahedron Lett.*, 1969. **17**: p. 1317-18.

27. Sassa, T., Tajima, N., Sato, M., Takahashi, A., Kato, N., Fusicoccins P and Q, and 3-epifusicoccins H and Q, new polar fusicoccins from isolate Niigata 2-A of a peach Fusicoccum canker fungus. *Biosci. Biotechnol. Biochem.*, 2002. **66**(11): p. 2356-61.
28. Aoyama, T., Naganawa, H., Muraoka, Y., Aoyagi, T., Takeuchi, T., The structure of cyclooctatin, a new inhibitor of lysophospholipase. *J. Antibiot. (Tokyo)*, 1992. **45**(10): p. 1703-4.
29. Kim, S.Y., Zhao, P., Igarashi, M., Sawa, R., Tomita, T., Nishiyama, M., Kuzuyama, T., Cloning and heterologous expression of the cyclooctatin biosynthetic gene cluster afford a diterpene cyclase and two p450 hydroxylases. *Chem. Biol.*, 2009. **16**(7): p. 736-43.
30. Au, T.K., Chick, W. S., Leung, P. C., The biology of ophiobolins. *Life Sci.*, 2000. **67**(7): p. 733-42.
31. Ballio, A., Brufani, M., Casinovi, C. G., Cerrini, S., Fedeli, W., Pellicciari, R., Santurbano, B., Vaciago, A., The structure of fusicoccin A. *Experientia*, 1968. **24**(6): p. 631-5.
32. Ríos, T., Quijano, L., The structure of ceroplastol II a sesterterpenic alcohol isolated from insects wax. *Tetrahedron Lett.*, 1969. **17**: p. 1317-8.
33. Motohashi, K., Sue, M., Furihata, K., Ito, S., Seto, H., Terpenoids Produced by Actinomycetes: Napyradiomycins from *Streptomyces antimycoticus* NT17. *J. Nat. Prod.*, 2008. **71**(4): p. 595-601.
34. Shirai, M., Okuda, M., Motohashi, K., Imoto, M., Furihata, K., Matsuo, Y., Katsuta, A., Shizuri, Y., Seto, H., Terpenoids produced by actinomycetes: isolation, structural elucidation and biosynthesis of new diterpenes, gifhornenolones A and B from *Verrucosipora gifhornensis* YM28-088. *J. Antibiot. (Tokyo)*, 2010. **63**(5): p. 245-50.
35. Olano, C., Mendez, C., Salas, J. A., Antitumor compounds from marine actinomycetes. *Mar. Drugs*, 2009. **7**(2): p. 210-48.
36. Isshiki, K., Tamamura, T., Takahashi, Y., Sawa, T., Naganawa, H., Takeuchi, T., Umezawa, H., The structure of a new antibiotic, terpentecin. *J. Antibiot. (Tokyo)*, 1985. **38**(12): p. 1819-21.
37. Aoyagi, T., Aoyama, T., Kojima, F., Hattori, S., Honma, Y., Hamada, M., Takeuchi, T., Cyclooctatin, a new inhibitor of lysophospholipase, produced by *Streptomyces melanosporofaciens* MI614-43F2. Taxonomy, production, isolation, physico-chemical properties and biological activities. *J. Antibiot. (Tokyo)*, 1992. **45**(10): p. 1587-91.

38. Graler, M.H., Goetzl, E. J., Lysophospholipids and their G protein-coupled receptors in inflammation and immunity. *Biochim. Biophys. Acta*, 2002. **1582**(1-3): p. 168-74.
39. Chang, D.H., Deng, H., Matthews, P., Krasovsky, J., Ragupathi, G., Spisek, R., Mazumder, A., Vesole, D. H., Jagganath, S., Dhodapkar, M. V., Inflammation-associated lysophospholipids as ligands for CD1d-restricted T cells in human cancer. *Blood*, 2008. **112**(4): p. 1308-16.
40. Miller, M.B., Bassler, B. L., Quorum sensing in bacteria. *Annu. Rev. Microbiol.*, 2001. **55**: p. 165-99.
41. Antunes, L.C., Ferreira, R. B., Intercellular communication in bacteria. *Crit. Rev. Microbiol.*, 2009. **35**(2): p. 69-80.
42. Horinouchi, S., Mining and polishing of the treasure trove in the bacterial genus *Streptomyces*. *Biosci. Biotechnol. Biochem.*, 2007. **71**(2): p. 283-99.
43. Horinouchi, S., Beppu, T., A-factor and streptomycin biosynthesis in *Streptomyces griseus*. *Antonie Van Leeuwenhoek.*, 1993-1994. **64**(2): p. 177-86.
44. Horinouchi, S., Beppu, T., Autoregulatory factors and communication in actinomycetes. *Annu. Rev. Microbiol.*, 1992. **46**: p. 377-98.
45. Beppu, T., Signal transduction and secondary metabolism: prospects for controlling productivity. *Trends Biotechnol.*, 1995. **13**(7): p. 264-9.